UNIVERSIDADE ESTADUAL DE SANTA CRUZ - UESC

NARA LINA OLIVEIRA

PARTIÇÃO DE RECURSOS DE CORAIS CONSTRUTORES DE RECIFES NO BANCO DOS ABROLHOS, BAHIA, BRASIL

RESOURCE PARTITIONING BY REEF BUILDING CORALS IN THE ABROLHOS BANK, BAHIA, BRAZIL

ILHÉUS - BAHIA
2018

NARA LINA OLIVEIRA

RESOURCE PARTITIONING BY REEF BUILDING CORALS IN THE ABROLHOS BANK, BAHIA, BRAZIL

A thesis submitted in partial fulfillment of the requirements for the degree of Doctor of Philosophy at Universidade Estadual de Santa Cruz.

Concentration Area: Ecology and Biodiversity Conservation

Supervisor: Prof. Dr. Rodrigo Leão de Moura
Co-supervisors: Dr. Carlos Eduardo de Rezende
Dr. Paulo Sérgio Salomon

ILHÉUS – BAHIA
2018

O48 Oliveira, Nara Lina
Resource partitioning by reef building corals in the Abrolhos bank, Bahia, Brazil / Nara Lina Oliveira. – Ilhéus, BA: UESC, 2018.
xv,150f. : il.

Supervisor: Rodrigo Leão de Moura
thesis(Doctor's degree) – Universidade Estadual de Santa Cruz. Postgraduate Program in Ecology and Biodiversity Conservation.
Included references and appendix.

1. Ecologia dos recifes de coral. 2. Nutrição. 3. Cadeias alimentares (Ecologia). 4. Nitrogênio. 5. Suscetibilidade genética. 6. Carbono. 7. Simbiose. 8. Isótopos. 9. Parques e reservas marinhas. 10. Grupos funcionais. 11. Abrolhos, Arquipélago dos (BA). 12. Branqueamento. I. Título.

CDD 577.789

NARA LINA OLIVEIRA

RESOURCE PARTITIONING BY REEF BUILDING CORALS IN THE ABROLHOS BANK, BAHIA, BRAZIL

Ilhéus, june 2018

_____

Rodrigo Leão de Moura – Dr.
Universidade Estadual de Santa Cruz
Universidade Federal do Rio de Janeiro
(Supervisor)

_____

Carlos Eduardo de Rezende – Dr.
Universidade Estadual do Norte Fluminense Darcy Ribeiro
(Co-supervisor)

_____

Paulo Sérgio Salomon – Dr.
Universidade Federal do Rio de Janeiro
(Co-supervisor)

David Baker- Dr.
Hong Kong University
(Examination Committee)

Leonardo Tavares Salgado – Dr.
Instituto de Pesquisas Jardim Botânico do Rio de Janeiro
(Examination Committee)

Jason Landrum – Dr.
Lenfest Ocean Program - Pew Charitable Trusts
(Examination Committee)

Arthur Wilma Silva-Lima – Dr.
Universidade Federal do Rio de Janeiro
(Examination Committee)

AKNOWLEDGEMENTS

This thesis is the result of collaborations between four Universities (UESC, UFRJ, UENF, HKU) with the support of many people I can finally turn public my gratitude. First, I want to thank Professor Rodrigo Moura for his supervision and for articulating the essential partnerships to make the Project feasible, and, above all, for his trust to accept the challenge to answer questions at the frontier of knowledge in the field of coral reef ecology. I also thank Rodrigo and Rede Abrolhos for the financial support given to accomplish the fieldwork in Abrolhos.

I thank my co-supervisors Paulo Salomon and Carlos E. de Rezende (Carlão) for opening the doors of their laboratories, agreeing to share their knowledge and lab partners, giving detailed protocols and follow-ups, and for providing highly qualified people for laboratory analysis and help in the field. For all the follow-up in important stages, from the initial field proposal to the final review of manuscript. I thank Carlão for his attention and financial support I received every time I went to Campos, UENF.

I am grateful to all partners and friends at UENF, Marina Suzuki, for her support and guidance with the chlorophyll analysis. Thanks to Thiago Rangel for all his expertise and help in the field. Thanks to Marcos Franco and Marcelo Almeida for the excellent analytical support with stable isotope analysis through all the stages. To Bráulio Oliveira and Diogo Almeida, who prepared and analyzed samples.

I express my gratitude to the team of Moura's lab, and Salomon's lab. Amazing people, smiling faces and best vibes. I appreciate the help of Michele Amario, Tatiana Viana, Rafael Menezes and Giovana Salomon. Special thanks for the strong help in the field from Felipe Ribeiro, Renato Tenan, and Michele Amario. To Laís Araújo for helping with the map of the study area. To Ludmila Falsarella, Érika Garcez, Camila Victória, Kamala Aymara, Ivanete Veloso, Pedro Mendes, Malu Abieri, and Mariana Neves who welcomed me in their homes in Rio de Janeiro as many times as I needed them. In Campos, I thank the lodging of Beatriz Araújo, Emilane Lima, Vanessa Trindade and Miguel Saver and the "couch surf" Angela.

My sincere thanks to Professor Pedro Mello and his student Gabriel Bittencourt from the Phytoplankton laboratory at UESC, for the valuable teachings and guidance with the identification of the zooplankton groups. It was a gift to be introduced to all those sweet baby plankton I had never thought of. Thanks to Professor Gil Reuss with his support with maps whenever I needed and to Ana Amélia for allowing me to use the Geological Oceanography laboratory during all this time. To Pavel, for the consultancy availability regarding the statistical analyzes with R.

I would like to thank the collaboration in research with Dr. David Baker and his entire team (Inga Conti-Jerpe, Phil Thompson, Taihun Kim, Jane Wong, Archana Anand, Arthur Chung, Vriko Yu, Naomi Geeraert, Shelby McIlroy and Jon Cybulski) at the University of Hong Kong (HKU). I appreciate the time and expertise Inga shared with me, guiding me through the

analyzes with the Stable Isotope Bayesian Analysis In R and the invitation to participate in a bleaching experiment which she coordinated. Still in Hong Kong, I was grateful to meet and have the support of all the fine folks at SWIMS (Paolo Guttuso, Peeraporn Punchai, Rebeka Butler, Anna Jöst, Priscila Granado, Laura Augusto, Pedro Jimenez, Kevin Geoghegan, Camilla Campanati, Kayi Chan and Shannon Hanson). Special thanks to my compatriot Aline, who helped me with important decision on statistics.

Along these fours and half years, I had the pleasure to share my life with important people. I feel honored for sharing the vicissitudes of the spiritual life with Rodrigo Oliveira. I thank the blessings that we reap, to the peace we have cultivated in our body and minds and to the moments and learnings that we had together.

DEEP GRATITUDE to my mother, Regina Ferreira, and my father, Edmundo Oliveira, who I late recognized gave me all I needed in LIFE to develop my abilities and overcome my own mind limitations. They provided me with their generosity, pizza and much love! To Indi Oliveira and Yuri Oliveira for the brotherhood, inspiration and love! To my nephew Martin Lamas, a little blessed boy who smiled since he was born and brought me so much LOVE and hope on Earth. Martin was a gift in my thoughts at various times, filled my heart with joy, and clearly showed me the notion of time.

I appreciate the work and progress of the Graduate Program in Ecology and Biodiversity Conservation. I am grateful for being a student at a University that represents the State of Bahia, my home, Universidade Estadual de Santa Cruz - UESC. I am thankful for the infra structured provided. Thanks to all the people involved in this program in the last 4 years. Special thanks to the secretaries Iky Anne and Amábile for the small and great favors and support during these years. All the best to these hardworking girls.

To CAPES, for the 36-month scholarship in Brazil and for the 5-month Sandwich Scholarship in Hong Kong, contributing to my professional training and scientific findings here presented.

Finally, I would like to thank the cities of Ilhéus, Caravelas, Rio de Janeiro and Hong Kong with all their perfections and imperfections. And mostly to Gaia, for providing the awe, beauty and magnificence of coral reefs.

“To share your weakness is to make yourself vulnerable; to make yourself vulnerable is to show your strength.”

Criss Jami

PARTIÇÃO DE RECURSOS DE CORAIS CONSTRUTORES DE RECIFES NO BANCO DOS ABROLHOS, BAHIA, BRASIL

RESUMO

A partição de recursos em corais construtores de recifes reflete estratégias adaptativas evolutivas entre um animal hospedeiro heterotrófico e simbiontes fotossintetizantes. Os corais simbióticos desenvolveram um amplo repertório de vias tróficas e mecanismos para assimilar, reter, reciclar e transferir nutrientes em resposta às pressões seletivas do ambiente. Desta forma, as relações tróficas entre simbiontes e hospedeiro são pontos-chave para a sobrevivência de corais de ambientes rasos. No entanto, ainda existe uma lacuna na compreensão da ecologia trófica de diferentes grupos funcionais de corais e da suscetibilidade relativa desses organismos quando submetidos a crescentes impactos antropogênicos. Dado o cenário atual de mortalidade e branqueamento em massa de corais associado às mudanças climáticas (aumento da temperatura do oceano) e outros impactos locais (sedimentação, poluição e sobrepesca), a compreensão das respostas metabólicas e fisiológicas em diferentes ambientes é essencial para apoiar ações de conservação nos ecossistemas dos recifes. A tese teve como objetivo investigar a plasticidade fisiológica e metabólica, a importância relativa da autotrofia e heterotrofia, e a amplitude do nicho isotópico de duas espécies de corais (*Mussismilia braziliensis* e *Favia gravida)*. Foram coletados dados de recifes costeiros e distantes da costa explorando os efeitos destes ambientes sobre a dinâmica trófica destas espécies. Com uma abordagem interdisciplinar, os parâmetros fisiológicos e metabólicos dos organismos foram avaliados empregando-se citometria de fluxo para quantificar densidades de *Symbiodinium*, espectrometria de massa para determinar a amplitude e variabilidade associada aos isótopos estáveis de nitrogênio (δ^{15}N) e carbono (δ^{13}C), tecnologia de imagem de fluxo (FlowCAM) para acessar medidas de biovolume do *Symbiodinium* e espectrofotometria aplicadas à análise de pigmentos. Os resultados evidenciam que os corais *M. braziliensis* e *F. gravida* possuem plasticidade trófica, amplitude de nicho e demandas nutricionais contrastantes. O coral cérebro endêmico da Bahia, *M. braziliensis*, apresentou nicho isotópico mais estreito, menor plasticidade trófica entre recifes, com maior contribuição da autotrofia e maior acoplamento entre os parâmetros metabólicos e fisiológicos em relação ao "weedy" coral *F. gravida*. Os dados sugerem que *M. braziliensis* beneficiou-se da autotrofia em recifes protegidos distantes da costa uma vez que reduções significativas nos parâmetros fisiológicos da população de simbiontes foram observadas nos recifes próximos da costa. A pesquisa levanta novas hipóteses sobre a dinâmica trófica entre corais de diferentes grupos funcionais e fornece informações relevantes para apoiar a seleção de novas áreas protegidas para a conservação de recifes de corais no Banco dos Abrolhos, Bahia, Brasil.

Palavras-chave: nutrição, cadeia alimentar, nitrogênio, nicho isotópico, suscetibilidade heterotrofia, autotrofia, carbono, simbiontes, isótopos, área marinha protegida, grupos funcionais, Abrolhos

RESOURCE PARTITIONING BY REEF BUILDING CORALS IN THE ABROLHOS BANK, BAHIA, BRAZIL

ABSTRACT

Resource partitioning by reef building corals reflect evolutionary adaptive strategies between an animal heterotrophic host and their photosymbionts. Symbiotic corals have developed a wide repertoire of trophic pathways and mechanisms to assimilate, retain, recycle and transfer nutrients in response to environmental selective pressures. Thus, trophic relationships between symbionts and host are key points for survivorship of corals in shallow areas. However, there is still a gap in understanding trophic ecology of different functional groups of corals and of the relative susceptibility of these organisms when subjected to increasing anthropogenic impacts. Given the global current scenario of mortality and mass coral bleaching associated to climatic changes (increased temperature) and other local impacts (e.g. pollution, sedimentation, overfishing), understanding metabolic and physiological responses of corals to different environments is essential to support conservation actions in reef ecosystems. This thesis aimed to investigate physiological and metabolic plasticity, the relative importance of autotrophy and heterotrophy, and estimate the isotopic niche width of two species of corals (*Mussismilia braziliensis* and *Favia gravida*). With an interdisciplinary approach, data were collected on nearshore and offshore reefs exploring the effects of these environments on coral trophic dynamics. Physiological and metabolic parameters of corals were assessed employing flow cytometry to quantify *Symbiodinium* densities, mass spectrometry in stable isotopes analyzis (δ^{13}C and δ^{15}N) to quantify variabilities associated to nitrogen and carbon in symbionts and tissue, flow imaging technologies to assess *Symbiodinium* biovolume, and spectrophotometer, applied for pigment analysis. The results highlighted *M. braziliensis* and *F. gravida* showed contrasting trophic plasticity, isotopic niche width and nutrient demand. The endemic brain coral, *M. braziliensis*, showed narrower isotopic niche, lower nutritional plasticity, with higher contribution from autotrophy, and stronger coupling between metabolic and physiological parameters compared to the "weedy" coral *F. gravida*. Data suggest that *M. braziliensis* benefitted from autotrophy in protected offshore reefs, since significant reductions in physiological parameters of symbionts were observed near the coast. The study raises new hypothesis about trophic dynamics between corals of different functional groups and provide relevant information to support the selection of new protected areas for coral reef conservation in the Abrolhos Bank, Bahia, Brazil.

Key words: nutrition, food chain, nitrogen, isotopic niche, susceptibility, heterotrophy, autotrophy, carbon, symbionts, isotopes, marine protected area, functional groups, Abrolhos

CONTENTS

LIST OF TABLES

Supplementary material

LIST OF FIGURES

Chapter 1

Introduction

1 Coral reefs: value, services and threats

The complex biogenic structures of coral reefs are of utmost biological and economic importance as they sustain high productivity, marine biodiversity and critical ecosystem services (HUGHES, 1989; ODUM; ODUM, 1955), especially benefiting human health, wealth and security. Coral reefs ecosystem has been recognized to contribute $ 9.9 trillion/year to the global economy (COSTANZA et al., 2014) providing services such as the protection of the coastline from storms and erosion, support tourism industries, capture and storage of carbon, and nursery for the commercially important fish species (COSTANZA et al., 2014; HOEGH-GULDBERG, 1999).

Despite its recognized value, substantial negative impacts have been observed on corals reefs in the last decades (ALVAREZ-FILIP et al., 2009; GARDNER et al., 2003; PANDOLFI et al., 2003) as a result of local and global anthropogenic stressors (HUGHES et al., 2003; HUGHES; CONNELL, 1999). At the local scale, the impacts related to the decline of corals worldwide include: increased terrestrial sedimentation (BROWN, 1997; WILKINSON, 2008), nutrient enrichment (WOOLDRIDGE et al., 2016) over-exploitation of marine species (ESTES et al., 2011; HUGHES et al., 2007), mining and physical destruction by reef users. Among the local impacts mentioned, the influence of coastal waters on corals is central for conservation of reef systems (HUGHES et al., 2003). There is increasing pressure of population growth in coastal areas increasing continental materials as a result of land use change, erosion and dredging (BRUCE et al., 2012; COSTA; NIMMO; ATTRILL, 2008; SILVA et al., 2013). The

increase in sedimentation rate of terrestrial material is a stressor that will be amplified throughout the 21st Century, according to the IPCC climate change scenarios (2007). In some areas of the world where higher turbidity is a natural condition, the concern of continental contributions will be even more critical. In the South Atlantic, for example, higher turbidity seems to restrict richness and distribution of corals species and explains the high level of endemism (MOURA, 2000; MOURA et al., 2016). Nevertheless, the coastal negative impacts on coral reef remains incompletely understood and turbidity may show controversial effects (BROWNE, 2012; JOMPA; MCCOOK, 2002).

At a global scale, climate change is an emergent threat to corals, causing vast mortality and drastic decrease in coral resilience of reef system (SMITH; GILMOUR; HEYWARD, 2007; VAN WOESIK et al., 2011) through the disruption of the mutualistic relationship between host and symbionts (BAKER; GLYNN; RIEGL, 2008). Prolonged elevated sea temperatures trigger the egress of symbionts from the colony, a physiological response of host to thermal stress (HOEGH-GULDBERG; BRUNO, 2010), which turns the host organism white, explaining the term known as “coral reef bleaching” (BAKER; GLYNN; RIEGL, 2008). Trends in temperature in Tropical Oceans have become ~1-2 °C warmer in the last 100 years (HOEGH-GULDBERG, 1999), and bleaching associated to temperature anomalies have increased in frequency and are intensified (HUGHES et al., 2017, 2018a) in areas affected by El Niño Southern Oscillation (ENSO) (WALTHER et al., 2002). Temperature anomalies in shallow tropical oceans have become the most challenging impact on coral reefs (HOEGH-GULDBERG, 1999) until greenhouse gas emissions are reduced (HOEGH-GULDBERG; BRUNO, 2010). When symbionts are egressed, there is a temporary loss or reduction in autotrophic nutrition by the coral, and heterotrophic feeding may play a crucial role for their survivorship (FERRIER-PAGÈS et al., 2011; GROTTOLI; RODRIGUES; PALARDY, 2006; TREMBLAY et al., 2016). However, the magnitude of bleaching impacts on hard corals have been reported to vary according to the degree of species susceptibilities (HUGHES et al., 2018b; SMITH; GILMOUR; HEYWARD, 2007; WOOLDRIDGE, 2014). Species susceptibility is generally a function of a combination of factors, including *Symbiodinium* type, and, life history trait, reproduction mode and growth rate of host species (SMITH; GILMOUR; HEYWARD, 2007).

Since resources acquisition (e.g. light, nutrients) by corals is a strong fitness driver (WOOLDRIDGE, 2014), nutrition strategies can be strongly related to species susceptibilities and may drive acclimation and survivorship. In this sense, higher nutrition flexibility, here termed trophic plasticity, may be a key aspect to cope with disturbances and extreme events such as coral recurrent reef bleaching (HUGHES et al., 2017). Therefore, the assessment of trophic ecology and dynamics is

important to elucidate physiological strategies of symbionts and host (POGOREUTZ et al., 2017) and the relative susceptibility of corals in the scenario of climate change.

2 Nutrition of reef building corals

Scleractinian corals represent one of the main holobiont models (*sensu* Mindell 1992), involving associations between a macrobium (the cnidarian), microbes ("protists", bacteria, archeas and fungi), viruses (ROHWER et al., 2002) and autotrophs (e.g., algae and cyanobacteria) (HARTMANN et al., 2010; SCHLICHTER; KAMPMANN; CONRADY, 1997). This evolution of mutual associations allowed the photobiont to acquire energy through extremely diverse trophic pathways, living as a primary producer, consumer and detritivores, and occupying multiple trophic levels simultaneously (ANTHONY, 1999; GOREAU; GOREAU; YONGE, 1971; HOULBRÈQUE; FERRIER-PAGÈS, 2009).

Mixotrophic dinoflagellates of the genus *Symbiodinum* are key components of the nutrition of scleractinian corals (HOEGH-GULDBERG, 1999; MUSCATINE, 1990). Symbionts can supply up to 90% of the carbon daily metabolic needs (ILUZ; DUBINSKY, 2015) in some species of corals. Through photosynthesis, symbionts provide energy (carbohydrates and sugars) (TREMBLAY et al., 2012) for corals biomineralization (MUSCATINE, 1990; MUSCATINE; CERNICHIARI, 1969a; ROWAN; POWERS, 1991; TITLYANOV; TITLYANOVA, 2012) and for other costly processes.

The inorganic carbon and nitrogen assimilated by the symbionts are synthesized within a few hours and permanently transferred to the host in the form of organic compounds including glycerol, glucose, amino acids, glycoproteins, fatty acids, lipids among other compounds (TITLYANOV; TITLYANOVA, 2002). Phosphate and some forms of dissolved nitrogen (e.g. nitrate) are assimilated only by the symbiont, whereas both, host and symbiont can assimilate ammonium from the water. Most dissolved nutrients are absorbed through active and passive transport across the cell membranes of body wall (DAVY; ALLEMAND; WEIS, 2012).

2.1 Heterotrophy

In addition to autotrophic nutrition, essential nutrients are supplied to coral through heterotrophy, by the ingestion of microorganisms (FERRIER-PAGÈS et al., 1998), zooplankton (GROTTOLI; WELLINGTON, 1999; PALARDY; RODRIGUES; GROTTOLI, 2008), debris, suspended

particulate matter (SPM) (ANTHONY, 1999; MILLS; LIPSCHULTZ; SEBENS, 2004), dissolved organic matter (DOM) in the water (HOULBRÈQUE; FERRIER-PAGÈS, 2009) and associated bacterioplankton (LEWIS; PRICE, 1975; SOROKIN, 1973). Although corals obtain inorganic nitrogen directly from water (preferably in the form of nitrate and ammonium), symbionts also benefit from the nitrogen and other nutrients assimilated by the coral, via heterotrophic feeding, that become available to its endosymbionts (TREMBLAY et al., 2015). Under optimal environmental conditions both, symbionts and host, are benefited because there is transfer and partitioning (sharing) of nutrients between them in both directions (MUSCATINE; CERNICHIARI, 1969b; YONGE, 1931). Recent studies indicate nitrogen and carbon obtained through heterotrophic nutrition, are retained for a longer time compared to the autotrophic assimilated components, both in the host and in its symbiont (TANAKA; SUZUKI; SAKAI, 2018; TREMBLAY et al., 2015). There is growing evidence showing the importance of heterotrophic nutrition as a way to prevent or compensate bleaching in reef building corals (FERRIER-PAGÈS; SAUZÉAT; BALTER, 2018; HUGHES; GROTTOLI, 2013; TREMBLAY et al., 2016). Heterotrophic nutrition has recently been found to be an important source of copper, zinc, boron, calcium and magnesium that have anti-oxidant properties (FERRIER-PAGÈS; SAUZÉAT; BALTER, 2018) during heat stress.

In many cases, corals are opportunistic and capable of switching between autotrophy and heterotrophy according to the availability of resources (ANTHONY; FABRICIUS, 2000; FERRIER-PAGÈS et al., 2011; MUSCATINE; PORTER; KAPLAN, 1989) and their physiological state (GROTTOLI; RODRIGUES; PALARDY, 2006; HUGHES; GROTTOLI, 2013; PORTER et al., 1989). In turbid waters, for example, where light is reduced and there is high concentration of suspended particulate matter (MPS) and dissolved organic matter in the water, it was observed that the heterotrophy complement the nutrition of opportunistic species (ANTHONY, 2006; ANTHONY; FABRICIUS, 2000; HOOGENBOOM et al., 2012; SANDERS; BARON-SZABO, 2005; SCHLICHTER; BRENDELBERGER, 1998). However, corals found in turbid waters are not necessarily heterotrophic. For example, persistent massive species of small polyps, such as *Siderastraea,* the mechanisms of success may not be associated with heterotrophy compensation, but related to the ability to use light and also to remove particles deposited throughout the day (MILLS; LIPSCHULTZ; SEBENS, 2004).

2.2 Feeding strategies and behavior of South Western Atlantic species

There is a wide range of specialization in the nutrition of scleractinian corals. The quantity and quality of food items and the size of particles ingested by corals exhibit distinct possibilities as

determined by the size and form of the polyp (GOREAU; GOREAU; YONGE, 1971), maximum tentacle extension, presence or absence of nematocysts, the amount of mucus production, the location of colony on the reef and feeding behavior. Lewis and Price (1975) systematically divided Caribbean and Atlantic species into three groups, describing differences in feeding strategies. There are species that expand polyps during day and night, with short tentacles but able to capture and ingest zooplankton (brine shrimp), and feed primarily by tentacle capture with low mucus production, such as *Porites astreoides and Madracis decactis*. A second group is described to act primarily as suspension feeders, yield abundant mucus net dispersed by ciliary currents, aiding the entanglement of particles during day and night, with rudimentary tentacles and low prey capture, such as *Agaricia agaricites*. In the third group, corals use both mechanisms, tentacles and mucus nets to efficiently capture and ingest food. Many species could be included in the third group (*Favia fragum, Montastrea cavernosa, Siderastrea siderea, S. radians, Meandrina meandrites)* (LEWIS; PRICE, 1975), and most of them have long tentacles (except *Siderastrea* sp), using both strategies at night, but are also suspension feeders during the day. The endemic reef building corals of SWA representative of Mussidae (*Mussismilia braziliensis, M. hispida and M. harttii)*, present copious mucus net, large polyps and long tentacles actively at night, which could possibly be included in this third group too.

3 Resource partitioning, trophic plasticity and mixing models

In symbiotic and mixotrophic organisms, such as reef-building corals, the term “resource partitioning” has been used to investigate the degree of heterotrophic nutrition (acquisition of organic particles from the environment) in relation to autotrophic nutrition (acquisition of inorganic nutrients from sea water) (GOREAU; GOREAU; YONGE, 1971; MUSCATINE; KAPLAN, 1994; MUSCATINE; MCCLOSKEY; MARIAN, 1981; MUSCATINE; PORTER; KAPLAN, 1989; PORTER, 1976; YONGE, 1931). However, it does not exclude the classical meaning of how different species uses the resources available in the environment (SCHOENER, 1974). The latter is typically related to ecological niches[1] diversification at a community organization level and, responsible for maintaining high biodiversity status in several ecosystems (CONNELL, 2008). The term trophic plasticity is thus, used in this study to characterize nutrition possibilities, to understand specific sources requirement, such as the exclusive dependence on autotrophy versus the heterotrophic opportunistic feeding habits of some corals.

The natural abundance of stable isotopes of carbon ($\delta^{13}C$) and nitrogen ($\delta^{15}N$) is an important tool for the assessment of resource use in organisms (PETERSON; FRY, 1987; POST, 2002), which is

typically represented by δ-values as coordinates in a two-dimensional space (also known as the isotopic niche space[1] and trophic niche) (CHISHOLM; NELSON; SCHWARCZ, 1982; FRY; BRAND, 1992; FRY; DAVIS, 2015; NEWSOME et al., 2007; PETERSON; FRY, 1987). The technique has the advantage of obtaining information from what has been assimilated and absorbed in animal tissue in a recent period of time, since the chemical composition of an animal tissue reflects what was consumed (FRY; DAVIS, 2015; PETERSON; FRY, 1987). The variation among individuals in the isotopic space is the result of the variation in their nutrition sources. Therefore, if the source of nutrition comes from only one source, the range of $\delta^{13}C$ and $\delta^{15}N$ of the population will be narrow. Likewise, when a variety of food sources (of different $\delta^{13}C$ and $\delta^{15}N$ -values between them) is consumed, the range of δ-values will be larger.

In this context, trophic plasticity of a population can be investigated by analyzing individual-level dispersion from the isotopic space (LAYMAN et al., 2011). When a representative number of samples (n~30) (JACKSON et al., 2011) is integrated into a two-dimensional space ($\delta^{13}C$ and $\delta^{15}N$-values), the isotopic niche width of a given population is reliably estimated (JACKSON et al., 2011; LAYMAN et al., 2007; TURNER; COLLYER; J, 2010).

Bayesian mixing models are commonly used to estimate the isotopic niche and relative contribution of dietary sources in heterotrophic organisms (LAYMAN et al., 2011; PARNELL; JACKSON, 2015). In general, there is either an enrichment or a fractionation process associated with stable isotopes from source isotopic values to the final tissue value of a consumer, which vary according to food source and consumer. Nitrogen enrichment occurs when light isotopes ^{14}N are lost during protein conversion from source to tissue. For this reason, when using stable isotope mixing models (SIMMs), a trophic enrichment factor (TEF) is applied as a correction factor. Whenever is possible, TEF is obtained from laboratory studies and minimize a degree of uncertainty in data analysis (PARNELL et al., 2013).

In symbiotic and mixotrophic organisms, such as reef building corals, the application and interpretation of these models become more complex, as nutrition comes from heterotrophic and the autotrophic pathway for organic and inorganic nutrient assimilation. Therefore, to provide more accurate interpretation of coral trophic dynamics, natural abundance of stable isotopes in corals will be empowered with the use of complementary parameters of photobiology.

[1] Ecologic niche according to Hutchinson (1944) can be defined as the sum of factors influencing an organism; the niche is defined is a region of an n-dimensional hyper space, where conditions may be quantifiable.

Chapter 2 presents a review manuscript on the use of natural stable isotopes ($\delta^{13}C$ and $\delta^{15}N$) studies in reef-building corals. I consider it is a relevant contribution to the literature since no review with this theme is available up to date. It gathers the main studies in the subject in the last 50 years, explaining the use and interpretation of natural abundance of stable isotopes to investigate trophic dynamics within symbiotic shallow corals within tissue and symbiont compartments. It highlights the main species, and the challenges of using stable isotopes in mixotrophic/symbiotic organism.

Chapter 3 presents the dataset and manuscript of the thesis. It describes for the first time the trophic plasticity and the isotopic niche width of two species of corals (Mussimilia braziliensis and Favia gravida) in the Southwestern Atlantic, with an ecological functional approach. The manuscript was designed, executed and wrote by me with the help of many collaborations for laboratory and data analyses and discussion. It highlights the role of autotrophy and heterotrophy as components of nutrition in Atlantic species, comparing nearshore and offshore reef conditions.

Chapter 4 brings a short conclusion of the thesis with the main take home messages applied to coral reef conservation. It emphasizes species-specific responses to coastal impacts and the importance of Marine Protected area in offshore reefs conditions. The conclusions are supported by data presented in chapter 3 with relevant information for reef managers in Brazil, especially for the region of the Abrolhos Bank and for the Abrolhos Marine National Park.

The appendix is an article published in 2016, describing an extensive carbonate reef system at the Amazon River mouth, which I was co-author contributing with data collection in the first expedition. The finding of symbiotic corals under the Amazon River mouth raises important hypothesis related to the use of resources and heterotrophic potential of some species of corals. The Amazon River has been thought to work as a geographic barrier for many coral species, justifying the low diversity of corals comparing to the Caribbean reefs. This fact is strongly related to the theme of this thesis as *Favia gravida* was one of the species collected in this highly turbid zone.

Chapter 2

A review on the trophic ecology of mixotrophic/symbiotic corals using the natural abundance of stable isotopes ($\delta^{13}C$ and $\delta^{15}N$)

Abstract

Expanding knowledge on trophic ecology of reef building corals is a critical aspect to promote conservation of reef ecosystems. Studies on trophic ecology of symbiotic corals are key-points to address heterotrophic potential of corals, which have been recently associated to lower susceptibility to climate change as prevalence of bleaching events increase. Variation and proportion in autotrophy and heterotrophy of reef building corals is still poorly understood and the isotopic values ($\delta^{13}C$ and $\delta^{15}N$) allow exploring the origin and the exchange of nutrients between tissue and symbionts within corals. This review aimed to: 1) broaden the comprehension of the use of natural abundance of stable isotopes ($\delta^{13}C$ and $\delta^{15}N$) in mixotrophic corals to address questions on trophic ecologic; 2) investigate the main species and sites studied and the challenges of using stable isotopes in mixotrophic/symbiotic organism; 3) investigate patterns in spatial and temporal variation of stable isotopes ($\delta^{13}C$ and $\delta^{15}N$) in tissue and symbionts; 4) suggest future directions, in the use of stable isotopes in trophic studies of mixotrophic corals. For this purpose, a systematic search were conducted in the *Web of Science* platform between 1945 and 2015. The genus *Porites, Acropora, Montastraea, Pocillopora and Stylophora* represented the most studied species. The use of this tool to study trophic ecology of reef building corals have been efficiently addressed along with several physiological measurements to be able to comprehend the various responses and interactions between coral compartments. However fractionation of ^{15}N within coral compartments, including nitrogen cycling and retention remain unclear even in controlled

experiments. Spatial and temporal comparisons should be made with caution, as natural abundance of stable isotopes are highly context dependent.

Key words: heterotrophy, nutrients, sources, partitioning, bleaching, symbiosis

1 Introduction

Natural abundance of stable isotopes are useful tools to address trophic dynamics within the food web, where consumers are subjected to multiple nutritional sources of different origins (Peterson and Fry, 1987; Post, 2002). The isotopic ratio of carbon and nitrogen (^{13}C / ^{12}C; ^{15}N / ^{14}N) has been extensively used in heterotrophic organisms in terrestrial and marine environments to elucidate trophic pathways (Fry and Davis, 2015; Layman et al., 2011). However, fewer studies have assessed trophic relationships of mixotrophic corals in natural conditions to address metabolic exchanges and ecological interaction (Heikoop et al., 2000; Muscatine and Kaplan, 1994; Muscatine et al., 1989; Nahon et al., 2013; Risk et al., 1994; Susanto et al., 2013; Ziegler et al., 2014). Despite that, there is a growing interest in the research field of metabolic diversity of mixotrophic/symbiotic organisms, such corals and sponges (Freeman et al., 2014; Thacker and Freeman, 2012) by the scientific community as analytical techniques advances and reefs are under unprecedented decline (Bellwood et al., 2004; Carpenter et al., 2008; Hughes et al., 2017).

Stable isotopes is a comprehensive tool to elucidate the trophic changes and the mutualistic relationship between host and symbionts. These changes may include shifts from autotrophic to heterotrophic pathways (Freeman et al., 2015; Hoogenboom et al., 2015; Muscatine et al., 1989) which is associated to resilience and survivorship of corals (Ferrier-Pagès et al., 2018; Grottoli et al., 2006; Hughes and Grottoli, 2013) in recent times of climate change.

In general, the $\delta^{13}C$ of the organism will reflect the average of the assimilated $\delta^{13}C$ sources consumed (Phillips et al., 2014; Post, 2002; Post et al., 2007), because of the relatively small variation of $\delta^{13}C$ between consumer and sources (0 to 1.00‰) (Peterson and Fry, 1987). In heterotrophic organisms, nitrogen isotope ($\delta^{15}N$) provide an estimate of the trophic position of the organism in the community (Peterson and Fry, 1987). Therefore, consumer becomes 2.3 to 3.4 ‰

more enriched than their sources at each trophic level (McCutchan Jr et al., 2003; Minagawa and Wada, 1984). In corals, nitrogen is longer conserved and continuously recycled within host and symbionts (Tanaka et al., 2018; Tremblay et al., 2015) in relation to heterotrophic organisms. Therefore, the interpretation of δ^{15}N-values is not necessarily indicating the trophic position (Ferrier-Pagès et al., 2011; Hoogenboom et al., 2015; Reynaud et al., 2009). Mixotrophic corals function through a permanent exchange of carbon and nitrogen between host and symbionts. Values of δ^{15}N of host and symbionts will be the result of the proportional uptake of δ^{15}N-values of inorganic sources (e.g. nitrate, ammonium) and δ^{15}N-values of organic sources translocated by the host and recycled within symbiosis.

Isotopic differences may arise from fractionation or enrichment caused by discrimination between light and heavy isotopes in various reactions from assimilation to elimination of substances in the body (Peterson and Fry, 1987; Schoeller, 1999). Isotopic ratios of samples are compared with reference standards (Carbon isotopic ratio deviation per mil of Vienna Peedee Belemnite Limestone (V-PDB); and Nitrogen isotopic ratio deviation per mil of atmospheric Nitrogen). The international notation for carbon and nitrogen isotopes are expressed by equations 1 and 2, respectively:

$$\delta^{13}C=\{[(^{13}C/^{12}C)_{sample}/(^{13}C/^{12}C)_{standard}]-1\} \times 1000 \qquad \text{(eq. 1)}$$

$$\delta^{15}N=\{[(^{15}N/^{14}N)_{sample}/(^{15}N/^{14}N)_{standard}]-1\} \times 1000 \qquad \text{(eq. 2)}$$

When values increase, it denotes there is an increase of the heavy isotope in the sample, which denotes increase in elements with more neutrons. To detect isotopic ratios of elements, the quantitative yields of molecules are calculated after completely conversion of samples to simple gases, which is then detected by a isotope-ratio mass spectrometer IRMS (Peterson and Fry, 1987).

The carbon isotopic composition of symbiont is the result of isotopic discrimination of seawater bicarbonate (δ^{13}C value ~ 0.8 ‰). When fractionated and assimilated by symbionts, δ^{13}C-values result in molecules of organic carbon ranging from -18 ‰ to -9 ‰ (Land and Lang, 1975; Muscatine et al., 1989; Nahon et al., 2013). In addition to photosynthetic products, carbon sources of longer retention are consumed trough heterotrophy by host. The ingestion of particles, such as zooplankton (Grottoli and Wellington, 1999) is generally more depleted than photosynthetic carbon, with δ^{13}C-values varying from -21 ‰ to -15 (Swart et al., 2005a). Suspended particulate matter SPM is another relevant heterotrophic source more enriched than the SPM (Lamb and Swart, 2008; Rau et al., 1990; Susanto et al., 2013). SPM from tropical forests is depleted around -27.8 ‰, as the particulate organic carbon in the water is mostly from C_3 plants (Risk et al., 1994; Swart, 1983). The different carbon sources assimilated by multiple trophic pathways will constitute coral host tissue.

In order to give more power to new researchers in this field, here we intended to fill a scientific gap, writing a review of the studies using stable isotopes in trophic ecology of mixotrophic/symbiotic corals. The goal of this review article was: 1) to broaden the comprehension of the use of natural abundance of stable isotopes ($\delta^{13}C$ and $\delta^{15}N$) in mixotrophic corals to address questions on trophic ecology; 2) to investigate the main species and sites studied and the challenges of using stable isotopes in mixotrophic/symbiotic organism; 3) to investigate patterns in spatial and temporal variation of stable isotopes ($\delta^{13}C$ and $\delta^{15}N$) in tissue and symbionts; 4) to suggest future directions, in the use of stable isotopes in trophic studies of mixotrophic corals.

2 Materials and Methods

A search was conducted on the *Web of Science* platform in order to record articles published that associated stable isotopes and corals from 1945 to 2015. This criteria was delimited by searching the "Topic" field for the query "((isotope) or (isotopic) or (isotopes) and (corals) or (coral reefs) and (carbon) or (nitrogen) or (C) or (N))" and "Title" field for the query "((coral)) not (oxygen) and "Topic" field for the query "(not (fish or fishes))". Subsequently, a refinement of the search was conducted by reading the abstracts so that only articles related to the trophic ecology of corals were included. From the total articles recorded related to coral trophic ecology, 62 analyzed carbon and/or nitrogen isotopes in the tissue, symbionts or coral skeleton. From these 62 articles, the 45 studies related to tissue and/or symbionts in shallow environments (up to 30m) were used to compose a list of the most studies species and sites on the subject (Table 1). An extended and non-systematic search was used to write the results and discussion.

3 Results and Discussion

The genus *Porites, Acropora, Montastraea, Pocillopora and Stylophora*, represented the most studied species due to one or more favorable characteristics, such as wide spatial and depth distribution, for example. *Porites* represent persistent, robust and long-lived species, typically focused on paleoclimatic studies (Muscatine et al., 2005; Swart et al., 1996; Swart et al., 2005a). The species of the Pacific Ocean appear most frequently as the region with the highest number of publications, followed by the northern Atlantic Ocean and the Caribbean, and the Red Sea. Few studies were recorded for the Indian Ocean and no study was found for the South Atlantic region. Detailed information (site, species, depth) are shown in Table 1.

Table 1. Most assessed regions and species in studies related to trophic ecology of mixotrophic/symbiotic corals using stable isotopes of carbon and/or nitrogen recorded from 1945 to 2015 assessing Web of Science Platform

Year	Country	Site/Region	Species	Depth (m)	Reference
Atlantic Ocean and Caribbean					
1975	Jamaica	Discovery Bay	*Acropora cervicornis, Montastraea annularis, Agaricia undata*	1 - 64	(Land and Lang, 1975)
1989	United States	Virgin Islands	*Montastraea annularis, Agaricia lamarcki*	6 - 31	(Porter et al., 1989)
1996	United States	Florida	*Montastraea annularis*	5.5	(Swart et al., 1996)
2003	Curaçao	Buoy 1 reef	*Madracis mirabilis, Madracis formosa, Madradcis pharensis*	Not informed	(Maier et al., 2003)
2004	Bermuda	Castle harbour	*Diploria strigosa, Montastraea franksi, Siderastrea radians, Madracis mirabilis*	5	(Mills et al., 2004)
2004	United States and Bermuda	North Carolina and Bermuda	*Oculina arbuscula, Oculina diffusa*	8 - 10	(Piniak and Lipschultz, 2004)
2005	United States	Florida	*Montastraea faveolata*	3 - 8.5	(Swart et al., 2005b)
2005	United States	Florida	*Montastraea faveolata*	3 - 8	(Swart et al., 2005a)
2007	Bahamas and Mexico	Lee Stocking Island and Akumal	*Montastraea cavernosa*	15	(Lesser et al., 2007)
2010	Curaçao	Not informed	*Madracis auretenra, Madracis carmabi, Madracis formosa*	5 - 47	(Maier et al., 2010)

2013	Panamá	Almirante bay, Bocas del Toro	*Porites furcata, Agaricia tenuifolia*	1 - 4	(Seemann et al., 2013)
2014	United States	Georgia coast, Gray's Reef Nat. Mar. Sanctuary	*Oculina arbuscula*	20	(Leal et al., 2014)
Indian Ocean and Red Sea					
2002	Jordan	Gulf of Aqaba, Red Sea	*Stylophora pistillata*	Not informed	(Reynaud et al., 2002)
2006	Israel	Eilat, the Gulf of Aqaba, Red Sea	*Stylophora pistillata, Hydnophora exesa, Acropora eurystoma, Pocillopora dana, Galaxea fascicularis, Paltygyra lamellina Turbinaria mesenterina, Favia favus, Plerogyra sinuosa, Cladop-sammia gracilis, Favites halicora, Goniopora lobata, Lobophyllia corymbosa, Fungia scutaria*	4 - 10	(Levy et al., 2006)
2006	Monaco	Red Sea	*Stylophora pistillata*		(Grover et al., 2006)
2009	Israel	Eilat, the Gulf of Aqaba, Red Sea	*Stylophora pistillata*	5, 10, 30, 50, 65	(Einbinder et al., 2009)
2009	Israel	Red Sea	*Stylophora pistillata, Favia favus*	1 - 60	(Alamaru et al., 2009)
2009	Monaco	Red Sea	*Turbinaria reniformis*	Not informed	(Treignier et al., 2009)
2011	Monaco	Red Sea	*Turbinaria reniformis*	3	(Tolosa et al., 2011)
2012	Monaco	Red Sea	*Stylophora pistillata*	Not informed	(Tremblay et al., 2012)
2014	Monaco	Red Sea	*Stylophora pistillata*	Not informed	(Tremblay et al., 2014)

2014	Saudi Arabia	Red Sea	*Pocillopora verrucosa*	5, 10, 20	(Ziegler et al., 2014)
2015	Monaco	Red Sea	*Stylophora pistillata, Turbinaria reniformis*	Not informed	(Tremblay et al., 2015)
Pacific Ocean					
1994	Australia	Central Great Barrier Reef	*Porites lobata, Acropora formosa*	5 - 8	(Risk et al., 1994)
1995	Japan	Palau, Ishigaki, western Pacific Ocean	*Porites lutea, Porites rus, Pocillopora damicornis, Acropora cf. nasuta, Goniopora sp., Echinopora lamellosa, Goniastrea sp.*	0 - 2	(Yamamuro et al., 1995)
1996	Australia	Northern Great Barrier Reef	*Acropora formosa*	2, 12	(Juillet-Leclerc et al., 1997)
2002	Hawaii	Kaneohe Bay	*Porites compressa*	2	(Grottoli, 2002)
2002	Hawaii	Kaneohe Bay	*Porites compressa, Montipora verrucosa*	2	(Grottoli et al., 2004)
2004	Australia	One Tree Island's lagoon	*Pocillopora damicornis, Heliofungia actiniformis*	0.5 - 0.8	(Hoegh-guldberg et al., 2004)
2006	Japan	Shiraho Reef in Ishigaki Island	*Acropora pulchra*	Not informed	(Tanaka et al., 2006)
2008	Japan	Sesoko Island	*Porites lutea, Porites cylindrica*	1 - 2.5	(Sun et al., 2008)
2010	Hawaii	Moku O Lo'e Island	*Montipora capitata, Porites compressa*	2 - 4	(Hughes et al., 2010)
2012	French Polynesia	Moorea, Tahiti	*Porites rus*	2 - 3	(Padilla-Gamiño et al., 2012)

2013	French Polynesia	Moorea Lagoon	*Porites rus, Napopora irregulares, Acropora cytherea, Acropora hyacinthus, Acropora pulchra, Pocillopora damicornis, Pocillopora meandrina, Pavona cactus, Montipora tuberculosa*	1	(Nahon et al., 2013)
2013	Australia	Orpheus Island Great Barrier Reef	*Pocillopora damicornis*	Not informed	(Ceh et al., 2013)
2013	Indonesia	Berau, East Kalimantan, Coral Triangle	*Porites, Seriatopora and Stylophora*	3, 10	(Susanto et al., 2013)
2014	Hawaii	Kaneohe Bay	*Porites compressa, Montipora capitata*	2 - 4	(Baumann et al., 2014)
2015	Australia	Heron Island	*Porites lutea, Favia stelligera*	Not informed	(Erler et al., 2015)
2015	Japan	Sesoko Island, Okinawa	*Porites cylindrica, Montipora digitata*	1.5	(Tanaka et al., 2015)
Mediterranean sea					
2011	Italy	Ligurian Sea (northwest Mediterranean Sea)	*Cladocora caespitosa*	8 - 10	(Ferrier-Pagès et al., 2011)
2015	France	Aquarium Tropical, Palais de la Porte Dorée	*Pocillopora damicornis*	Not informed	(Kopp et al., 2015)
Multiple regions					

1989	Jamaica and Red Sea	Opposite Discovery Bay and/ Red Sea	*Madracis mirabilis, Agaricia agaricites, Acropora palmata, Porites astreoides, Montastraea annularis, Montastraea cavernosa, Acropora cervicornis, Eusmilia fastigiata, Dendrogyra cylindrus, Stylophora pistillata*	1 - 50	(Muscatine et al., 1989)
1998	Jamaica and Zanzibar	Discovery Bay/ Zanzibar	*Caribbean: Montastraea annularis, Porites astreoides, Agaricia agaricites; Indo Pacific: Porites lobata*	1, 5, 12, 22, 30	(Heikoop et al., 1998)
2000	Jamaica, Zanzibar, Australia, Costa Rica, Jepara, Maldives, Banda	Discovery Bay and others	*Caribbean: Montastraea annularis, Porites astreoides, Agaricia agaricites, Diploria sp., Porites furcata, Siderastraea radians; Indo Pacific: Porites lobata*	0 - 5	(Heikoop et al., 2000)

			Acropora sp., Fungia danai Merulina sp., Pavona decussata, Pocillopora damicornis, Stylophora pistillata, Fungia scutaria, Pocillopora damicornis, Oculina arbuscula (aposymbiotic), Stylophora sp., Acropora sp., Caryophyllia ambrosia, Dendrophyllia alcocki, Enallopsammia sp., Paracyathus sp., Solenosmilia variabilis,		
2005	Diverse collection	New Caledonia, Red Sea, Hawaii, North Carolina, Florida, Monaco, Celtic Sea, Great Barrier Reef, Indian Ocean, Mediterranean Sea, Turkey	*Stephanocyathus spiniger, Tubastrea coccinea, Tubastrea micrantha, Madrepora oculata, Madrepora oculata, Pachythecalis major*	1 - 425	(Muscatine et al., 2005)

3.1 $\delta^{13}C$: mechanisms of carbon acquisition and isotopic fractionation in mixotrophic corals

The natural isotopic fractionation in compartments (tissue, symbionts and skeleton) of coral is of fundamental importance for understanding the mechanism of carbon acquisition and fluxes (Muscatine et al., 1989; Omata et al., 2008; Swart, 1983). Isotopic fractionation during carbon assimilation occurs during photosynthesis, respiration, calcification (Swart, 1983) and feeding (Ferrier-Pagès et al., 2011). Tissue and symbionts are key compartments to investigate trophic relationships and nutrition in mixotrophic corals, since they are only affected by kinetic fractionation (metabolic processes), while the skeleton is controlled by kinetic and thermodynamic fractionation (respiration and photosynthesis) (Allison et al., 2014; Muscatine et al., 2005; Omata et al., 2008; Reynaud et al., 2002; Swart et al., 1996; Swart et al., 2005a). Therefore, coral tissue and symbionts will reflect more accurately the autotrophic and heterotrophic carbon sources acquired than the isotope of skeleton or organic matrix of skeleton (Hughes and Grottoli, 2013; Muscatine et al., 2005; Swart et al., 2005a).

The autotrophic carbon is transferred from symbionts to host tissue for rapid metabolic demands (Tremblay et al., 2012) and for skeletal calcification. The heterotrophic carbon is longer retained in the compartments as reserve sources (symbionts and tissue) (Tremblay et al., 2015) and mostly used in the constitution of host tissue (Hughes et al., 2010). For example, Reynaud et al. 2002 proposed a model with the *Stylophora pistillata* coral fed with Artemia sp. enriched in ^{13}C: in this model, the largest fractionation of carbon (-7 ‰) occurs when the bicarbonate of seawater ($\delta^{13}C$ ~ 0.8 ‰) is incorporated by the coral, which is CO_2 dehydration inside the tissue (Fig. 1). The dissolved inorganic carbon is accumulated in this pool (Furla et al., 2000) and then diffuses until it is assimilated by the symbionts ($\delta^{13}C$ ~ -10.5 ‰) when lighter isotopes are selected in the process of photosynthesis. Much of the photosynthetic fixed carbon compounds are translocated from symbionts to coral host, to be incorporated into the skeleton. Through this process, $\delta^{13}C$ carbon tissue (~ -12.5 ‰) derived from both autotrophic and heterotrophic sources will be more depleted than symbionts. (Reynaud et al., 2002).

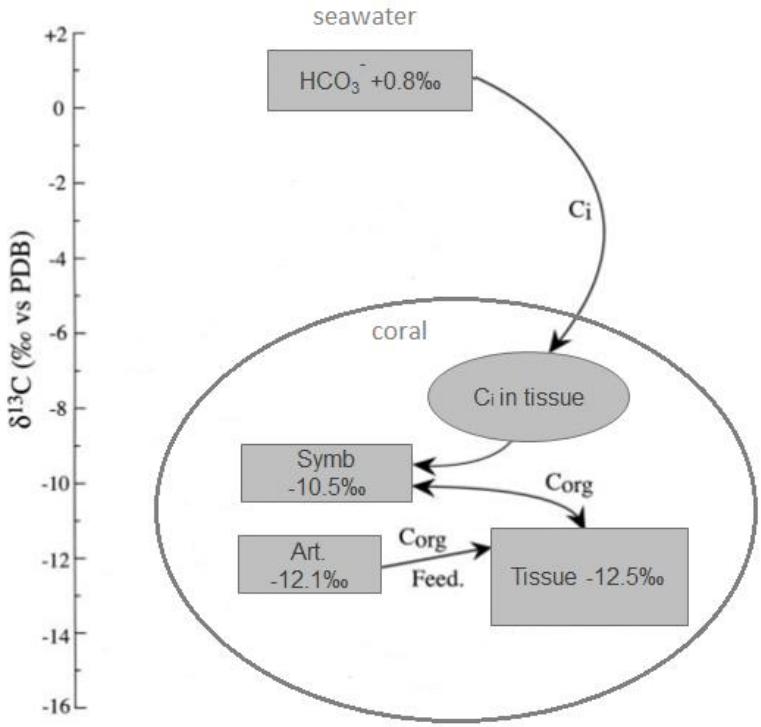

Fig. 1 Model of carbon flux and δ^{13}C-values within coral tissue and symbionts in *Stylophora pistillata* modified from Reynaud et al. (2002). In this model the coral was fed with labeled (enriched in ^{13}C) Arthemia sp. (Art). Bicarbonate of seawater (δ^{13}C ~ 0.8 ‰) is incorporated by the coral, when the largest fractionation of carbon (-7 ‰) occurs. Dissolved inorganic carbon (Ci) is accumulated then diffuses until it is assimilated by the symbionts (Symb). Symbionts transfer part of this as organic carbon (Corg). Through this process, δ^{13}C- values of carbon tissue (~ -12.5 ‰) derived from both autotrophic and heterotrophic sources will be more depleted than symbionts. Rectangles represent δ^{13}C-values pool measured by the authors, circle represent inferred values of carbon pool.

3.2 δ^{13}C as a measure of heterotrophy and autotrophy

Muscatine et al. (1989) was the first to study the natural isotopic ratio (δ^{13}C) of tissue and symbiont, separately, proposing the δ^{13}C differences as an indirect measure to quantify the degree of heterotrophy of the organism. More recently, other studies have used the same approach (Alamaru et al., 2009; Hoogenboom et al., 2015; Levy et al., 2006; Nahon et al., 2013; Swart et al., 2005b). Thus, the

closer the isotope ratio $\delta^{13}C$ between symbionts and tissue, the more autotrophic is the coral (Ferrier-Pagès et al., 2011).

Evidence of increasing heterotrophy was observed along a depth gradient. In deeper areas, with consequently reduction of light and photosynthetic rate, where $\delta^{13}C$-values of coral tissue and symbionts become more depleted and similar to plankton and SPM $\delta^{13}C$-values (Alamaru et al., 2009; Ferrier-Pagès et al., 2011; Land and Lang, 1975; Muscatine et al., 1989; Susanto et al., 2013). Similarly, $\delta^{13}C$-values within compartments generally become more depleted under increasing influence of terrigenous sources (Nahon et al., 2013; Risk et al., 1994). Both examples contribute to light attenuation and are expected to enhance heterotrophic feeding by corals.

The natural isotopes abundance has been applied with several metabolic and physiological parameters to assess the plasticity of a typically autotrophic branching coral *Pocillopora verrucosa* to acclimate after transplant depth (Ziegler et al., 2014). The $\delta^{13}C$ significantly decreased in host tissue and symbionts after 30 days in deeper condition. However, each isotope ($\delta^{13}C$, $\delta^{15}N$ of tissue and symbionts) explained 2 to 5% of the data dissimilarities between depths, while ~ 40% was explained by photophysiological and pigment parameters.

In order to understand the changes in carbon acquisition in bleached corals (i.e. with lower density of symbionts) affected by climate change, an increase in feeding rates (heterotrophy) may occur in some species to supply the energy required for daily metabolism (Grottoli et al., 2006; Hughes and Grottoli, 2013; Hughes et al., 2010). By establishing a more heterotrophic feeding mode and increasing nutritional status (Ferrier-Pagès et al., 2018; Grottoli et al., 2006; Hughes and Grottoli, 2013) with carbon and nitrogen of longer retention, susceptibility of corals to bleaching may be reduced. Thus, resilience after bleaching can be increased (Grottoli et al., 2006; Levas et al., 2015). In this sense, isotopic ratio and fatty acids trophic markers are used to identify zooplankton biochemical specificities in sources and associate to the nutritional status of corals (Naumann et al., 2015; Teece et al., 2011; Treignier et al., 2009).

Experimental investigations (Baumann et al., 2014; Grottoli et al., 2006; Hughes et al., 2010) sought to understand changes in carbon acquisition in bleached corals (i.e. corals that expelled symbionts) because in this condition the contribution of autotrophy is reduced (Swart et al., 2005a) and, it can occur the increase of heterotrophy to supply the necessary energy for daily metabolism (Grottoli et al., 2006; Hughes and Grottoli, 2013; Hughes et al., 2010). In a comparative study between bleached and non-bleached colonies of *Porites compressa* and *Montipora verrucosa* no increase in heterotrophy was

detected by differences between $\delta^{13}C$ of symbionts and $\delta^{13}C$ of tissue (Grottoli et al., 2004). However, a decrease in the total lipid concentration of bleached colonies of *P. compressa* showed significant physiological change. In another experiment with bleached corals under recovery, using inorganic and organic labeled ^{13}C, the expected increase of heterotrophy by *Montipora capitata* and *P. compressa* didn't happen until autotrophic carbon acquisition was normalized 4 months after bleaching (Hughes and Grottoli, 2013). Both experiments showed the complex and non-uniform trophic behavior of corals and challenging in using stable isotopes as a unique tool to detect metabolic responses.

Considering the fractionation variations in different compartments of corals, Alamaru et al. (2009) investigated increase in heterotrophy in two species (*Stylophora pistillata* and *Favia favus*) along a depth gradient, using two isotopes of different compartments: 1) isotope ($\delta^{13}C$) of the lipid fraction of tissue and lipid fraction of symbionts and 2) isotope ($\delta^{13}C$) of tissue and symbiont. Significant results was detected only by using the first method. The lipid isotope can provide specific responses to heterotrophic plasticity due to the typical differentiated synthesis of this reserve. The fractionation of the lipid fraction was 3.5‰ more depleted when compared to the tissue, and 2‰ compared to symbionts (Alamaru et al., 2009).

3.3 Variation in the degree of heterotrophy between different species

The advantage of analyzing the isotopic composition of tissue and symbiont separately, is to use the differences as a relative and comparable measure of heterotrophy. It is possible to compare data from different sampling times, places and species, increasing the possibilities from working with absolute values of $\delta^{13}C$ and $\delta^{15}N$. For most shallow corals of the tropics, the indicator of heterotrophy (differences between $\delta^{13}C$ of tissue and $\delta^{13}C$ of symbionts) usually ranges from 0 to ± 3‰ for $\delta^{15}N$ 0 to ± 9‰ for $\delta^{13}C$ (Hoogenboom et al., 2015; Muscatine and Kaplan, 1994; Muscatine et al., 1989). Differences are expected to be smaller for more autotrophic corals, and larger, in more heterotrophic corals. Variations in the degree of heterotrophy between species are explained by the different feeding mechanisms (Lewis and Price, 1975) due to morphological and physiological characteristics and the availability of resources (Anthony, 2000; Anthony and Fabricius, 2000; Anthony et al., 2005; Hoogenboom et al., 2015). Branched corals such as *Acropora*, *Pocillopora* and *Porites* are mostly autotrophic compared to corals with larger polyps with massive skeletons and adapted to capture plankton (Porter, 1976), such as *Favia favus, Favites halicora, Platygyra lamellina, Lobophyllia*

corymbosa, Plerogyra sinuosa, and *Fungia scutaria* (Levy et al., 2006). However, isotopic ratio comparisons between species of different morphology and feeding behaviours can be misleading. In a study with 11 species from the Red Sea, for example, corals with lower prey factor, small polyps, typically autotrophic, hosted symbionts with more depleted δ^{13}C-values than massive species of higher preying factor (Levy et al., 2006). The unexpected results of higher δ^{13}C in more species expected to be more heterotrophic was suggested to be caused by carbon-limitation in the cells related to lower tentacles activity during the day in the massive species.

3.4 δ^{15}N: mechanisms of nitrogen acquisition and isotopic fractionation

The use of δ^{15}N has an important role complementing the results of δ^{13}C since nitrogen enrichment is a possible way to estimate the trophic position of heterotrophic organisms (Layman et al., 2011; Minagawa and Wada, 1984). When combined with the carbon isotope enhance the understanding of trophic relationships within the ecosystem creating a bi-dimensional isotopic niche space (Fry and Davis, 2015; Layman et al., 2011). However, the pattern of δ^{15}N in symbiotic mixotrophic corals are still on its way towards a more comprehensible dynamic within the holobiont. Its trends have been inconclusive since many studies show conflicting results (Heikoop et al., 1998; Hoogenboom et al., 2015; Muscatine and Kaplan, 1994; Reynaud et al., 2009).

The most important inorganic nitrogen sources for symbionts are nitrate (Bythell, 1990; Grover et al., 2003) and ammonium obtained from seawater, and ammonium from host tissue waste products (Muscatine and Kaplan, 1994). In addition to ammonium, urea has shown to be an important source of nitrogen especially for tissue that presented values 5 times higher than symbionts in the presence of light (Grover et al., 2006). With regard to the flow of nitrogen between compartments, symbionts absorb dissolved inorganic nitrogen (DIN) from seawater (NO_3-, NO_2-, NH_4+) and from the internal DIN pool of coral tissue, producing organic nitrogen (Tanaka et al., 2015). Organic nitrogen is maintained in the symbionts or released into the tissue (Fig. 2). It is estimated that 80% and 50% of the nitrogen of the symbionts of *Porites cylindrica* and *Montipora digitata*, respectively, comes from the DIN pool of coral tissue compartment, which holds an important reserve to maintain vital metabolic functions of symbionts (Tanaka et al., 2015). On the other pathway, the symbiont can transfer more than 70% of the organic nitrogen synthesized from the nitrate (NO_3^-) to the coral (Tanaka et al., 2006). However, a recent research showed that symbionts are responsible for 99% of the total N measured in coral tissue

(Fig. 2), suggesting symbionts deliver nutrients through extracellular release and algal digestion (Tanaka et al., 2018).

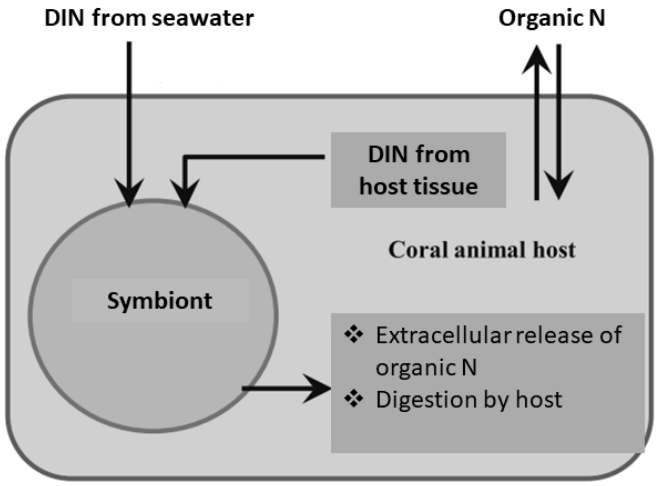

Fig. 2 Simplified model of nitrogen flux within a symbiotic coral from Tanaka et al. (2015). Dissolved inorganic nitrogen (DIN) is assimilated by symbionts from seawater and from the pool in host tissue, which holds an important reserve to maintain vital metabolic functions of symbionts (Tanaka et al., 2015). On the other pathway, the symbiont can transfer more than 70% of the organic nitrogen synthesized from the nitrate (NO_3^-) as extracellular release to the host.

The causes of the variations are directly affected by the isotopic composition of the nitrogen sources consumed (Heikoop et al., 2000; Minagawa and Wada, 1984; Muscatine and Kaplan, 1994). Therefore, $\delta^{15}N$ in tissue of mixotrophic/symbiotic corals will be lower than non-symbiotic (heterotrophic) corals as they will reflect a combination from $\delta^{15}N$ of the inorganic and organic sources assimilated (Muscatine et al., 2005). The $\delta^{15}N$ in coral tissue compartment presents values typically higher than symbionts (Alamaru et al., 2009; Muscatine and Kaplan, 1994; Muscatine et al., 2005; Nahon et al., 2013; Susanto et al., 2013) because of its heterotrophic derived nutrients and, for the same reason, the ratio of carbon to nitrogen (C:N) may double in *Symbiodinium* compared to host tissue (Ziegler et al., 2014). Symbionts values will also correspond to the $\delta^{15}N$ of organic matrix of coral skeleton (Erler et al., 2015; Muscatine et al., 2005). Yamazaki et al. (2011) found $\delta^{15}N$ in skeleton as a proxy for $\delta^{15}N$ of seawater nitrate with values around (4.09 ± 1.51‰) and, similarly, $\delta^{15}N$ symbionts of the coral *Porites* have been used as a pollution proxy for dissolved inorganic nitrogen in the seawater (Wong et al., 2017).

The drivers of fractionation of nitrogen within corals compartments have not been clear along environmental gradients. Fractionation of $\delta^{15}N$ within mixotrophic/symbiotic coral was first suggested to be influenced by light, based on investigations of different parts of colonies exposed to contrasting light levels (Heikoop et al., 1998). The results of this research were in agreement and explained the results of a previous study that described seven out of nine species in the Caribbean with a depleted trend of $\delta^{15}N$-values of tissue and symbionts with increasing depth in natural field conditions, but not exceeding 2 ‰ within the same species over 30 m (Muscatine and Kaplan, 1994). Therefore, It has been proposed that light drive the uptake and fractionation of DIN, because under low light level, there is a decreased in photosynthetic activity and reduction in the energy available to assimilate DIN, leading to increase fractionation factors, which reflect in depleted $\delta^{15}N$-values (Heikoop et al., 1998; Maier et al., 2010; Swart et al., 2005b). Contrasting the proposed hypothesis, in a more recent work about trophic plasticity, Alamaru et al. (2009) did not find any correlation between $\delta^{15}N$ of tissue or symbiont and depth (1-60m) sampling *Stylophora pistillata* and *Favia favus* in the Red Sea. Ziegler et al. (2014) observed the effect of depth on $\delta^{15}N$ investigate plasticity of *Pocillopora verrucosa* in the same region and found that only symbionts (not in the tissue) became enriched after 30 days transplanted from 5 to 20m depth (Ziegler et al., 2014). However, in theory, the values of $\delta^{15}N$ in the tissue may not follow symbionts in depth zones and can even show enriched values as observed for the host tissue of *Montastraea annularis* and *M. cavernosa* by Muscatine and Kaplan (1994) at 50 m (Muscatine and Kaplan, 1994).

3.5 $\delta^{15}N$ relationship with heterotrophy

In an experiment (Mills et al., 2004) to evaluate the SPM ingestion and nitrogen utilization by four species of corals (*Diploria strigosa, Montastrea franksi, Siderastrea radians, Madracis mirabilis*) from the North Atlantic, Mills et al. (2004) observed a preference for larger fractions and that the ability to use it varied according to colony species and morphology. *Siderastraea radians*, typically found in high sedimentation environments, did not use a greater amount of particulate matter as a source of nitrogen than other species found in places with lower turbidity (Mills et al., 2004). Nitrogen acquired via SPM remained only in coral tissue with no traces detected in symbionts, suggesting heterotrophic nitrogen is used for growth, cell maintenance, reproduction and others functions. In two studies related to trophic plasticity of transplanted corals, the physiological adjustment in symbionts concerning light levels (depth and turbidity changes) did not include changes in $\delta^{15}N$ of tissues (Padilla-Gamiño et al.,

2012; Ziegler et al., 2014). Branching and plating *Porites rus* (Padilla-Gamiño et al., 2012) in turbid and non-turbid environments in French Polynesia, did not differ in $\delta^{15}N$ between sites and morphologies, when transplanted between environments with different levels of turbidity, indicating low plasticity in the nitrogen source.

The available particulate material in the reefs can vary in quantity and quality, and the $\delta^{15}N$ of this sources (registered by some authors around 3 to 9 ‰) (Ferrier-Pagès et al., 2011; Lamb and Swart, 2008; Susanto et al., 2013) tend to be relatively more enriched in the size fractions smaller than 1 µm and larger than 75 µm at any depth (Rau et al., 1990), which may serve as an indicator of their origin (allochthonouse or autochthonous) (Peterson and Fry, 1987). With the increase in depth there seems to be cumulative losses of ^{14}N in the process of decomposition of the particulate material that become more enriched (between 5 and 1 ‰) in ^{15}N (Peterson and Fry, 1987) contrasting to the depleted directions driven by lack of light.

Recently, it has been suggested that differences in $\delta^{15}N$ between host and symbiont tissue from the same fragments could also be as an indicator for heterotrophy for experimentally fed corals (as it had been earlier proposed for $\delta^{13}C$) (Hoogenboom et al., 2015). Densities of symbionts was also correlated with differences in $\delta^{15}N$ between coral compartments (tissue and symbiont), with higher densities associated to higher $\delta^{15}N$ of tissue. These results agree with hypothesis by Heikoop et al. (1998) correlating light and photosynthetic activity with higher $\delta^{15}N$ in octocorals.

3.6 The effect of seasonality on $\delta^{13}C$ and $\delta^{15}N$

Seasonality should be considered in trophic studies of mixotrophic corals as variations of carbon and nitrogen isotopic ratio throughout the year can be higher than variations between reefs under different environmental conditions (Swart et al., 2005b). Seasonal variation can be expected to affect the photosynthetic active radiation and, the sources and concentration of particulate organic matter (POM) (Ferrier-Pagès et al., 2011; Susanto et al., 2013), influencing the $\delta^{13}C$ and $\delta^{15}N$ of the tissue if there is a marked change in the nutrition modes such as described for temperate regions. Therefore, it is expected to obtain higher $\delta^{15}N$ and more depleted and $\delta^{13}C$-values in tissue and symbiont in periods of higher heterotrophy when water turbidity increases and there is more nutrient in the form of available POM (Ferrier-Pagès et al., 2011). Swart et al. (2005a) collected monthly samples of *Montastraea faveolata* and did not detect seasonal differences in $\delta^{15}N$ in the tissue or symbionts, as found for the

δ^{13}C-values of the Florida reefs. The cause suggested for the intra-annual variation in the δ^{13}C of tissue and symbionts was the carbon limitation and increased fractionation of the inorganic carbon pool during the early summer and rainy season, when both compartments, as well as the difference between tissue and symbionts presented highest values (Swart et al., 2005b). When the ratio between photosynthesis and respiration is high, the CO_2 fractionation factor decreases, thus increasing δ^{13}C-values (Swart et al., 2005a).

Some studies found significant effect of seasonality on δ^{13}C in coral tissue and symbionts, as reported for the southern United States and Indonesia (Susanto et al., 2013; Swart et al., 2005b; Yamamuro et al., 1995). However, the temporal effect on the isotopic ratio may be minor in certain tropical regions and not biologically significant as recorded in French Polynesia (Nahon et al., 2013). Although showing differences in symbionts density (but not in chlorophyll *a* concentrations), Nahon et al. (2013) did not detect significant variation in δ^{15}N of the tissue between dry and rainy season. The authors assume that the absence of a marked seasonality would explain the small difference (less than 1‰) found in δ^{13}C for the same species that showed the highest seasonal variation in other geographic regions. Therefore, when comparing studies of different regions of the tropical zone, the specificities of each climate (Equatorial, Savana, and Tropical Monsoons) should be considered, as rainfall distribution, soil type and vegetation indexes, as these factors control the entry of light and nutrients in the reef ecosystem (Swart et al., 2005b). In a tropical region, Nahon et al. (2013) did not observe significant temporal variation (dry and rainy season), nor even in the difference between the tissue and symbionts. As occurs for δ^{13}C, seasonal variations may be non-existent or minor in some regions.

Nutritional mode was detected using stable isotopes of sources and consumers according to the season in a temperate region, at 10 m depth in three different sites levels of turbidity influenced by a river plume (Ferrier-Pagès et al., 2011). Autotrophic mode in summer shifted to heterotrophic mode in the winter in the coral *Cladocora caespitosa*. In the summer, δ^{13}C of symbionts and the tissue remained closer to each other and more distant from the δ^{13}C of plankton and SPM values. In the winter, δ^{13}C symbionts and tissue were 7 to 8 ‰ more depleted than in summer and closer to the values of potential heterotrophic carbon sources. In terms of nitrogen, δ^{15}N-values of tissue and symbionts were close to each other during the summer (δ^{15}N= 6 to 8‰). In winter, tissue and symbionts were 7‰ apart, indicating heterotrophy was higher (Ferrier-Pagès et al., 2011). In this study, the hypothesis of higher heterotrophy in winter was corroborated observing the δ^{13}C of sources and consumer, rather than the difference between coral compartments (tissue and symbionts). In addition to measurements of

carbon and nitrogen isotopic ratios, other physiological parameters that could explain the relationship between autotrophy and heterotrophy aided to explain the responses of corals, including chlorophyll *a* concentration, symbionts' density and protein concentration. However, results of physiological parameters were not conclusive, and the carbon and nitrogen isotopes measured in tissue, symbionts, plankton, particulate organic matter (POM) and suspended organic matter were fundamental in the interpretation of results, since concentration of proteins, chlorophyll *a* and density of symbionts did not vary significantly.

4 Conclusions

Studies using natural abundance of stable isotopes of nitrogen and carbon in mixotrophic and symbiotic corals are still scarse in the literature, especially considering seasonal or long-term sampling. However, the number of publications have been increasing since year 2000 and changing the poor-designed approach dating from 1989. Recent investigations tend to a multivariable approach, combining isotopes with several physiological and metabolic parameters within corals compartments, such as: protein content, lipid content, calcification rates, symbiont density, fatty acids, photosynthetic yield, electron transport rate, chlorophyll *a* content, among others. Along with stable isotopes, the approach combining multiple variables has been showing to be an efficient way to address the complex polytrophic mechanism of symbiotic corals and comprehend the responses in its multiple compartments (skeleton, tissue and symbionts). Stable isotopic ratios (δ^{13}C and δ^{15}N) of coral tissue and symbionts have been used to explore relative importance of autotrophy and heterotrophy, trophic plasticity, resources use, and niche width.

Stable isotopes are highly context dependent, which means that absolute comparisons in space and time may not be appropriate without an environmental background assessment of organic or/and inorganic nutrients as well as other physiological parameters to complement. The fractionation patterns of δ^{15}N between host and symbionts remain a scientific gap, as its results have been unpredictable and inconsistent even under controlled experiments. Despite being a science under construction, when planning a sampling design with nitrogen stable isotope (δ^{15}N), it is important to consider the factors reported to have caused fractionation on corals such as, depth gradients, light intensities and photosynthesis, and coral morphologies. Nevertheless, based on the articles reviewed here, δ^{13}C and δ^{15}N should be interpreted with caution, in the light of a broad environmental context.

5 References

Alamaru, A., Loya, Y., Brokovich, E., Yam, R. and Shemesh, A. (2009). Carbon and nitrogen utilization in two species of Red Sea corals along a depth gradient: Insights from stable isotope analysis of total organic material and lipids. *Geochim. Cosmochim. Acta* **73**, 5333–5342.

Allison, N., Cohen, I., Finch, A. a, Erez, J. and Tudhope, A. W. (2014). Corals concentrate dissolved inorganic carbon to facilitate calcification. *Nat. Commun.* **5**, 5741.

Anthony, K. R. N. (2000). Enhanced particle-feeding capacity of corals on turbid reefs (Great Barrier Reef, Australia). *Coral Reefs* **19**, 59–67.

Anthony, K. and Fabricius, K. (2000). Shifting roles of heterotrophy and autotrophy in coral energetics under varying turbidity. *J. Exp. Mar. Bio. Ecol.* **252**, 221–253.

Anthony, K. R. N., Hoogenboom, M. O. and Connolly, S. R. (2005). Adaptive variation in coral geometry and the optimization of internal colony light climates. *Funct. Ecol.* 17–26.

Baumann, J., Grottoli, A. G., Hughes, A. D. and Matsui, Y. (2014). Photoautotrophic and heterotrophic carbon in bleached and non-bleached coral lipid acquisition and storage. *J. Exp. Mar. Bio. Ecol.* **461**, 469–478.

Bellwood, D., Hughes, T. P., Folke, C. and Nystrom, M. (2004). Confronting the coral reef crisis ¨. *Nature* **429**, 827–833.

Bythell, J. C. (1990). Nutrient uptake in the reef-building coral Acropora palmata at natural environmental concentrations. *Mar. Ecol. Prog. Ser.* **68**, 65–69.

Carpenter, K. E., Abrar, M., Aeby, G., Aronson, R. B., Banks, S., Bruckner, A., Chiriboga, A., Cortés, J., Delbeek, J. C., Devantier, L., et al. (2008). One-third of reef-building corals face elevated extinction risk from climate change and local impacts. *Science (80-.).* **321**, 560–3.

Ceh, J., Kilburn, M. R., Cliff, J. B., Raina, J.-B., van Keulen, M. and Bourne, D. G. (2013). Nutrient cycling in early coral life stages: *Pocillopora damicornis* larvae provide their algal symbiont (*Symbiodinium*) with nitrogen acquired from bacterial associates. *Ecol. Evol.* **3**, 2393–2400.

Einbinder, S., Mass, T., Brokovich, E., Dubinsky, Z., Erez, J. and Tchernov, D. (2009). Changes in

morphology and diet of the coral *Stylophora pistillata* along a depth gradient. *Mar. Ecol. Prog. Ser.* **381**, 167–174.

Erler, D. V, Wang, X. C. T., Sigman, D. M., Scheffers, S. R. and Shepherd, B. O. (2015). Controls on the nitrogen isotopic composition of shallow water corals across a tropical reef flat transect. *Coral Reefs* **34**, 329–338.

Ferrier-Pagès, C., Peirano, A., Abbate, M., Cocito, S., Negri, A., Rottier, C., Riera, P., Rodolfo-Metalpa, R. and Reynaud, S. (2011). Summer autotrophy and winter heterotrophy in the temperate symbiotic coral Cladocora caespitosa. *Limnol. Oceanogr.* **56**, 1429–1438.

Ferrier-Pagès, C., Sauzéat, L. and Balter, V. (2018). Coral bleaching is linked to the capacity of the animal host to supply essential metals to the symbionts. *Glob. Chang. Biol.* 0–2.

Freeman, C. J., Easson, C. G. and Baker, D. M. (2014). Metabolic diversity and niche structure in sponges from the Miskito Cays, Honduras. *PeerJ* **2**, e695.

Freeman, C. J., Baker, D. M., Easson, C. G. and Thacker, R. W. (2015). Shifts in sponge-microbe mutualisms across an experimental irradiance gradient. *Mar. Ecol. Prog. Ser.* **526**, 41–53.

Fry, B. and Davis, J. (2015). Rescaling stable isotope data for standardized evaluations of food webs and species niches. *Mar. Ecol. Prog. Ser.* **528**, 7–17.

Furla, P., Galgani, I., Durand, I. and Allemand, D. (2000). Sources and mechanisms of inorganic carbon transport for coral calcification and photosynthesis. *J. Exp. Biol.* **203**, 3445–3457.

Grottoli, A. (2002). Effect of light and brine shrimp on skeletal δ 13 C in the Hawaiian coral Porites compressa: a tank experiment. *Geochim. Cosmochim. Acta* **66**, 1955–1967.

Grottoli, A. G. and Wellington, G. M. (1999). Effect of light and zooplankton on skeletal δ13C values in the eastern Pacific corals Pavona clavus and Pavona gigantea. *Coral Reefs* **18**, 29–41.

Grottoli, A. G., Rodrigues, L. J. and Juarez, C. (2004). Lipids and stable carbon isotopes in two species of Hawaiian corals, Porites compressa and Montipora verrucosa, following a bleaching event. *Mar. Biol.* **145**, 621–631.

Grottoli, G., Rodrigues, L. J. and Palardy, J. E. (2006). Heterotrophic plasticity and resilience in bleached corals. *Nature* **440**, 10–13.

Grover, R., Maguer, J.-F., Allemand, D. and Ferrier-Pagès, C. (2003). Nitrate uptake in the scleractinian coral Stylophora pistillata. *Limnol. Oceanogr.* **48**, 2266–2274.

Grover, R., Maguer, J. F., Allemand, D. and Ferrier-Pages, C. (2006). Urea uptake by the scleractinian coral Stylophora pistillata. *J. Exp. Mar. Bio. Ecol.* **332**, 216–225.

Heikoop, J. M., Dunn, J. J., Risk, M. J., Sandeman, I. M., Schwarcz, H. P. and Waltho, N. (1998). Relationship between light and delta 15N of coral tissue: Examples from Jamaica and Zanzibar. *Limnol. Oceanogr.* **43**, 909–920.

Heikoop, J. M., Dunn, J. J., Risk, M. J., Tomascik, T., Schwarcz, H. P., Sandeman, I. M. and Sammarco, P. W. (2000). δ15 N and δ13 C of coral tissue show significant inter-reef variation. *Coral Reefs* **19**, 189–193.

Hoegh-guldberg, O., Muscatine, L., Goiran, C., Siggaard, D. and Marion, G. (2004). Nutrient-induced perturbations to δ 13C and δ 15N in symbiotic dinoflagellates and their coral hosts. *Mar. Ecol. Prog. Ser.* **280**, 105–114.

Hoogenboom, M., Rottier, C., Sikorski, S. and Ferrier-page, C. (2015). Among-species variation in the energy budgets of reef-building corals : scaling from coral polyps to communities. *J. Exp. Biol.* **4**, 3866–3877.

Hughes, A. D. and Grottoli, A. G. (2013). Heterotrophic Compensation: A Possible Mechanism for Resilience of Coral Reefs to Global Warming or a Sign of Prolonged Stress? *PLoS One* **8**, e81172.

Hughes, A. D., Grottoli, A. G., Pease, T. K. and Matsui, Y. (2010). Acquisition and assimilation of carbon in non-bleached and bleached corals. *Mar. Ecol. Prog. Ser.* **420**, 91–101.

Hughes, T. P., Kerry, J. T., Álvarez-Noriega, M., Álvarez-Romero, J. G., Anderson, K. D., Baird, A. H., Babcock, R. C., Beger, M., Bellwood, D. R., Berkelmans, R., et al. (2017). Global warming and recurrent mass bleaching of corals. *Nature* **543**, 373–377.

Juillet-Leclerc, A., Gattuso, J., Montaggioni, L. F. and Pichon, M. (1997). Seasonal variation of primary productivity and skeletal δ13C and δ18O in the zooxanthellate scleractinian coral Acropora formosa. *Mar. Ecol. Prog. Ser.* **157**, 109–117.

Kopp, C., Domart-coulon, I., Escrig, S., Humbel, B. M., Hignette, M. and Meibom, A. (2015). Subcellular Investigation of Photosynthesis-Driven Carbon Assimilation in the Symbiotic Reef

Coral Pocillopora damicornis. *MBio* **6**, 1–9.

Lamb, K. and Swart, P. K. (2008). The carbon and nitrogen isotopic values of particulate organic material from the Florida Keys: A temporal and spatial study. *Coral Reefs* **27**, 351–362.

Land, L. S. and Lang, J. c. (1975). Preliminary observations on the carbon isotopic composition of some reef coral tissues and symbiotic zooxanthellae. *Limnol. Oceanogr.* **20**, 283–287.

Layman, C. A., Araujo, M. S., Boucek, R., Hammerschlag-peyer, C. M., Harrison, E., Jud, Z. R., Matich, P., Rosenblatt, A. E., Vaudo, J. J., Yeager, L. A., et al. (2011). Applying stable isotopes to examine food-web structure : an overview of analytical tools. *Biol. Rev. Camb. Philos. Soc.*

Leal, M. C., Ferrier-Pagès, C., Calado, R., Brandes, J. A., Frischer, M. E. and Nejstgaard, J. C. (2014). Trophic ecology of the facultative symbiotic coral Oculina arbuscula. *Mar. Ecol. Prog. Ser.* **504**, 171–179.

Lesser, M. P., Falcón, L. I., Rodríguez-Román, A., Enríquez, S., Hoegh-Guldberg, O. and Iglesias-Prieto, R. (2007). Nitrogen fixation by symbiotic cyanobacteria provides a source of nitrogen for the scleractinian coral Montastraea cavernosa. *Mar. Ecol. Prog. Ser.* **346**, 143–152.

Levas, S., Grottoli, A. G., Schoepf, V., Aschaffenburg, M., Baumann, J., Bauer, J. E. and Warner, M. E. (2015). Can heterotrophic uptake of dissolved organic carbon and zooplankton mitigate carbon budget deficits in annually bleached corals? *Coral Reefs*.

Levy, O., Dubinsky, Z., Achituv, Y. and Erez, J. (2006). Diurnal polyp expansion behavior in stony corals may enhance carbon availability for symbionts photosynthesis. *J. Exp. Mar. Bio. Ecol.* **333**, 1–11.

Lewis, J. B. and Price, W. S. (1975). Feeding mechanisms and feeding strategies of Atlantic reef corals. *J. Zool.* **176**, 527–544.

Maier, C., Pätzold, J. and Bak, R. P. M. (2003). The skeletal isotopic composition as an indicator of ecological and physiological plasticity in the coral genus Madracis. *Coral Reefs* **22**, 370–380.

Maier, C., Weinbauer, M. G. and Pätzold, J. (2010). Stable isotopes reveal limitations in C and N assimilation in the caribbean reef corals Madracis auretenra, M. carmabi and M. formosa. *Mar. Ecol. Prog. Ser.* **412**, 103–112.

McCutchan Jr, J. H., Lewis Jr, W. M., Kendall, C. and McGrath, C. C. (2003). Variation in trophic shift

for stable isotope ratios of carbon, nitrogen, and sulfur. *Oikos* **102**, 378–390.

Mills, M. M., Lipschultz, Æ. F. and Sebens, K. P. (2004). Particulate matter ingestion and associated nitrogen uptake by four species of scleractinian corals. *Coral Reefs* **23**, 311–323.

Minagawa, M. and Wada, E. (1984). Stepwise enrichment of 15N along food chains: Further evidence and the relation between δ15N and animal age. *Geochim. Cosmochim. Acta* **48**, 1135–1140.

Muscatine, L. and Kaplan, I. R. (1994). Resource Partitioning by Reef Corals as Determined from Stable Isotope Composition II. δ l5N of Zooxanthellae and Animal Tissue versus Depth. *Pacific Sci.* **48**, 304–312.

Muscatine, L., Porter, J. W. and Kaplan, I. R. (1989). Resource partitioning by reef corals as determined from stable isotope composition - I. 13C of zooxanthellae and animal tissue vs depth. *Mar. Biol.* **100**, 185–193.

Muscatine, L., Goiran, C., Land, L., Jaubert, J., Cuif, J. and Allemand, D. (2005). Stable isotopes (δ 13 C and δ15 N) of organic matrix from coral skeleton. *PNAS* **102**, 1525–1530.

Nahon, S., Richoux, N. B., Kolasinski, J., Desmalades, M., Ferrier Pages, C., Lecellier, G., Planes, S. and Berteaux Lecellier, V. (2013). Spatial and temporal variations in stable carbon (δ13C) and nitrogen (δ15N) isotopic composition of symbiotic scleractinian corals. *PLoS One*.

Naumann, M. S., Tolosa, I., Taviani, M., Grover, R. and Ferrier-Pag??s, C. (2015). Trophic ecology of two cold-water coral species from the Mediterranean Sea revealed by lipid biomarkers and compound-specific isotope analyses. *Coral Reefs* **34**, 1165–1175.

Omata, T., Suzuki, A., Sato, T., Minoshima, K., Nomaru, E., Murakami, A., Murayama, S., Kawahata, H. and Maruyama, T. (2008). Effect of photosynthetic light dosage on carbon isotope composition in the coral skeleton: Long-term culture of Porites spp. *J. Geophys. Res.* **113**, G02014.

Padilla-Gamiño, J. L., Hanson, K. M., Stat, M. and Gates, R. D. (2012). Phenotypic plasticity of the coral Porites rus: Acclimatization responses to a turbid environment. *J. Exp. Mar. Bio. Ecol.* **434–435**, 71–80.

Peterson, B. J. and Fry, B. (1987). Stable isotopes in ecosystem studies. *Annu. Rev. Ecol. Syst.* **18**, 293–320.

Phillips, D. L., Inger, R., Bearhop, S., Jackson, A. L., Moore, J. W., Parnell, A. C., Semmens, B. X. and Ward, E. J. (2014). Best practices for use of stable isotope mixing models in. *Can. J. Zool.* **835**, 823–835.

Piniak, G. A. and Lipschultz, Æ. F. (2004). Effects of nutritional history on nitrogen assimilation in congeneric temperate and tropical scleractinian corals. *Mar. Biol.* **145**, 1085–1096.

Porter, J. W. (1976). Autotrophy, heterotrophy and resource partitioning in Caribbean reef-building corals. *Am. Nat.* **110**, 731–742.

Porter, J. W., Fitt, W. K., Spero, H. J., Rogers, C. S. and White, M. W. (1989). Bleaching in reef corals: Physiological and stable isotopic responses. *Proc. Natl. Acad. Sci. U. S. A.* **86**, 9342–6.

Post, D. M. (2002). Using stable isotopes to estimate trophic position: models, methods, and assumptions. *Ecology* **83**, 703–718.

Post, D. M., Layman, C. A., Arrington, D. A., Takimoto, G., Quattrochi, J. and Montaña, C. G. (2007). Getting to the fat of the matter: Models, methods and assumptions for dealing with lipids in stable isotope analyses. *Oecologia* **152**, 179–189.

Rau, G., Teyssie, J.-L., Rassoulzadegan, F. and Fowler, S. (1990). 13C/12C and 15N/14N variations among size-fractionated marine particles: implications for their origin and trophic relationships . *Mar. Ecol. Prog. Ser.* **59**, 33–38.

Reynaud, S., Ferrier-Pagès, C., Sambrotto, R., Juillet-Leclerc, A., Jaubert, J. and Gattuso, J. P. (2002). Effect of feeding on the carbon and oxygen isotopic composition in the tissues and skeleton of the zooxanthellate coral Stylophora pistillata. *Mar. Ecol. Prog. Ser.* **238**, 81–89.

Reynaud, S., Martinez, P., Houlbrèque, F., Billy, I., Allemand, D. and Ferrier-Pagès, C. (2009). Effect of light and feeding on the nitrogen isotopic composition of a zooxanthellate coral: Role of nitrogen recycling. *Mar. Ecol. Prog. Ser.* **392**, 103–110.

Risk, M. J., Sammarco, W. P. and Schwarcz, H. P. (1994). Cross-continental shelf trends in 13c in coral on the Great Barrier Reef. *Mar. Ecol. Prog. Ser.* **106**, 121–130.

Schoeller, D. a. (1999). Isotope Fractionation: Why Aren't We What We Eat? *J. Archaeol. Sci.* **26**, 667–673.

Seemann, J., Berry, K. L., Carballo-Bolaños, R., Struck, U. and Leinfelder, R. R. (2013). The use of 13C

and 15N isotope labeling techniques to assess heterotrophy of corals. *J. Exp. Mar. Bio. Ecol.* **442**, 88–95.

Sun, D., Su, R., McConnaughey, T. a. and Bloemendal, J. (2008). Variability of skeletal growth and d13C in massive corals from the South China Sea: Effects of photosynthesis, respiration and human activities. *Chem. Geol.* **255**, 414–425.

Susanto, H. A., Komoda, M., Yoneda, M., Kano, A., Tokeshi, M. and Koike, H. (2013). A Stable isotope study of the relationship between coral tissues and zooxanthellae in a seasonal tropical environment of East Kalimantan, Indonesia. *Int. J. Mar. Sci.* **3**, 285–294.

Swart, P. K. (1983). Carbon and Oxygen Isotope Fractionation in Scleractinian Corals: a Review. *Earth-Science Rev.* **19**, 51–80.

Swart, P. K., Leder, J. J., Szmant, A. M. and Dodge, R. E. (1996). The origin of variations in the isotopic record of scleractinian corals: II. Carbon. *Geochim. Cosmochim. Acta* **60**, 2871–2885.

Swart, P. K., Szmant, A., Porter, J. W., Dodge, R. E., Tougas, J. I. and Southam, J. R. (2005a). The isotopic composition of respired carbon dioxide in scleractinian corals: Implications for cycling of organic carbon in corals. *Geochim. Cosmochim. Acta* **69**, 1495–1509.

Swart, P. K., Saied, A. and Lamb, K. (2005b). Temporal and spatial variation in the d15N and d13C of coral tissue and zooxanthellae in Montastraea faveolata collected from the Florida reef tract. *Limnol. Oceanogr.* **50**, 1049–1058.

Tanaka, Y., Miyajima, T., Koike, I., Hayashibara, T. and Ogawa, H. (2006). Translocation and conservation of organic nitrogen within the coral-zooxanthella symbiotic system of Acropora pulchra, as demonstrated by dual isotope-labeling techniques. *J. Exp. Mar. Bio. Ecol.* **336**, 110–119.

Tanaka, Y., Grottoli, A. G., Matsui, Y., Suzuki, A. and Sakai, K. (2015). Partitioning of nitrogen sources to algal endosymbionts of corals with long-term 15N-labelling and a mixing model. *Ecol. Modell.* **309**–**310**, 163–169.

Tanaka, Y., Suzuki, A. and Sakai, K. (2018). The stoichiometry of coral-dinoflagellate symbiosis: carbon and nitrogen cycles are balanced in the recycling and double translocation system. *ISME J.* 1–9.

Teece, M. A., Estes, B., Gelsleichter, E. and Lirman, D. (2011). Heterotrophic and autotrophic assimilation of fatty acids by two scleractinian corals , Montastraea faveolata and Porites astreoides. *Limnol. Oceanogr.* **56**, 1285–1296.

Thacker, R. W. and Freeman, C. J. (2012). *Sponge-Microbe Symbioses: Recent Advances and New Directions*. 1st ed. Elsevier Ltd.

Tolosa, I., Treignier, C., Grover, R. and Ferrier-Pagès, C. (2011). Impact of feeding and short-term temperature stress on the content and isotopic signature of fatty acids, sterols, and alcohols in the scleractinian coral Turbinaria reniformis. *Coral Reefs* **30**, 763–774.

Treignier, C., Tolosa, I., Grover, R., Reynaud, S. and Ferrier-Pagés, C. (2009). Carbon isotope composition of fatty acids and sterols in the scleractinian coral Turbinaria reniformis: Effect of light and feeding. *Limnol. Oceanogr.* **54**, 1933–1940.

Tremblay, P., Grover, R., Maguer, J. F., Legendre, L. and Ferrier-Pagès, C. (2012). Autotrophic carbon budget in coral tissue: a new 13C-based model of photosynthate translocation. *J. Exp. Biol.* **215**, 1384–93.

Tremblay, P., Grover, R., Maguer, J. F., Hoogenboom, M. and Ferrier-Pagès, C. (2014). Carbon translocation from symbiont to host depends on irradiance and food availability in the tropical coral Stylophora pistillata. *Coral Reefs* **33**, 1–13.

Tremblay, P., Maguer, J. F., Grover, R. and Ferrier-Pages, C. (2015). Trophic dynamics of scleractinian corals: A stable isotope evidence. *J. Exp. Biol.* 1223–1234.

Wong, M. C. W., Duprey, N. N. and Baker, D. M. (2017). New insights on the nitrogen footprint of a coastal megalopolis from coral-hosted. *Environ. Sci. Technol.*

Yamamuro, M., Kayanne, H. and Minagawa, M. (1995). Carbon and nitrogen stable isotopes of primary producers in coral reef ecosystems. *Limnol. Oceanogr.* **40**, 617–621.

Ziegler, M., Roder, C. M., Büchel, C. and Voolstra, C. R. (2014). Limits to physiological plasticity of the coral Pocillopora verrucosa from the central Red Sea. *Coral Reefs* **33**, 1115–1129.

Chapter 3

Trophic plasticity of the shallow corals Mussimilia braziliensis and Favia gravida in a turbid-zone reef system

Abstract

Coral reefs are facing the major decline ever registered, especially because of massive bleaching events when corals lose their symbiotic partner (the dinoflagellate *Symbiodinium*). This organism perform a major role in the nutrition and growth of symbiotic corals, but mixotrophic species have developed a wide repertoire of trophic pathways to acquire nutrients and adapt to diverse environments. Thus, although trophic relationships in coral reefs is a key point for survivorship, there is still a gap in understanding natural nutritional requirements of different functional groups of corals in contrasting environments. Here, we investigated trophic plasticity and the isotopic niche size of a large and long lived coral *Mussimilia braziliensis*, and of a small weedy coral, *Favia gravida,* both harboring, mainly, clade C *Symbiodinium.* We combined physiological parameters of host and symbionts (density/cm², biovolume/cm², biovolume/cell, *Chla*/cm², *Chla*/cell, FL3/cell, symbionts productivity given by Margalef index) with metabolic parameters (δ^{15}N and δ^{13}C) in nearshore and offshore reefs in Abrolhos, Brazil. The site effect was significant on δ^{15}N-values of host of both corals with enriched tissue in offshore reefs. However, only symbionts of *M. braziliensis* were significantly affected by site. This species showed 2.1X higher symbionts' density ($0.93x10^6$/cm²), 2.7X higher biovolume of cells/cm² (392µm³x10^6/cm²) and 3X higher *Chla*/cm² in offshore protected reefs, while no changes were observed for *F. gravida*. In *M. braziliensis*, symbiont densities, biovolume/cm², *Chla*/cm² and Margalef Index were significantly correlated to δ^{15}N- values of host tissue. An increase in nitrogen status of host did not affect physiological response of symbionts in *F. gravida,* suggesting different demand and

strategies to acquire and use nutrients. Therefore, symbionts of *F. gravida* showed a weak correlation with host metabolic parameters, contrasting with *M. braziliensis*. The coral *M. braziliensis* showed higher nitrogen requirements with stronger correlations between host and symbionts, and strong coupling of metabolic and physiological parameters, suggesting larger nutrient flux between the partners in relation to *F. gravida*. Our findings show the two species have different demand and strategies to acquire and use nutrients, *M. braziliensis* showed narrower isotopic niche, lower nutritional plasticity and lower proportion of heterotrophic sources. These results highlights the higher susceptibility to climate impacts related to the coral *M. braziliensis*, that can be benefited from protected offshore reefs, thus raising concern about increased coral susceptibilities on coastal areas.

Key words: coral sources, food web, resources use, isotopic niche, susceptibility, stable isotope, marine protected area, Abrolhos (Brazil)

1 Introduction

Coral reefs are major builders in the ocean and function as key components of a highly diverse ecosystem (Bellwood et al., 2004; Jones et al., 2004). Most representative reef building organisms in shallow waters (~798 species) has established a symbiotic association with favored *Symbiodinium* spp (Baker et al., 2004; Ziegler et al., 2015). This symbiosis may comprise one or more clades of *Symbiodinium* which perform a major role in the nutrition and growth of the coral holobiont via photosynthesis (Baker, 2003; Muscatine and Porter, 1977; Wooldridge, 2014). The great density of *Symbiodinium spp.* hosted by healthy corals (>10^6 cells cm^{-2}) (Iluz and Dubinsky, 2015; Muscatine et al., 1989a; Wooldridge, 2016) highlights their importance to coral nutrition, from larvae through adulthood. *Symbiodinium* spp. may represent 27% of the biomass of a planula and 14% of a coral polyp (Odum and Odum, 1955). Within the polyp, symbionts translocate around 90% of the organic fixed carbon to their host (Falkowski et al., 1984; Tremblay et al., 2014) delivering sugars rapidly consumed mainly by host respiration (Tremblay et al., 2015). Given the genetic diversity of host and of symbionts (~ 160 distinct *Symbiodinium* strains) and all possible combinations in space and time between these partners, a range of metabolic relationships is bound to emerge (Gordon and Leggat, 2010).

The diverse use of resources by different organisms integrates the concept of resource partitioning (Muscatine and Kaplan, 1994; Porter, 1976; Schoener, 1974). Different strategies in assimilating nutrients or in selecting food sources typically results from changes throughout evolutionary times in the morphological structures of organisms in responses to selective pressures from competitive interactions (Porter, 1976). Together, symbionts and hosts have developed impressive adaptive strategies to acquire carbon and nitrogen with a broad repertoire of mechanisms to retain, cycle and transfer nutrients between the symbiotic partners (Hoogenboom et al., 2015; Leal et al., 2015; Tremblay et al., 2015; Tremblay et al., 2016). On the host-symbiont direction, heterotrophic-derived nitrogen and phosphorus from host excretion become available to their symbionts through an efficient nutrient cycling system (Houlbrèque and Ferrier-Pagès, 2009; Titlyanov and Titlyanova, 2002). Importantly, endosymbionts are very efficient to acquire small amounts of essential inorganic nutrients (nitrate, ammonium and phosphate) from sea water (Bythell, 1990; den Haan et al., 2016; Radecker et al., 2015). They may fix 14 to 23 times more ammonium than the host for example (Kopp et al., 2013; Pernice et al., 2012). To avoid over-exploitation by symbionts, the host may regulate the metabolism (Cunning et al., 2015; Davy et al., 2012) of symbionts by controlling nutrient fluxes, releasing biochemical substances such as amino-acids (Gates et al., 1995; Leletkin, 2000), or by removing symbionts through digestion or expulsion (Titlyanov and Titlyanova, 2002). Dissolved organic matter, phytoplankton, zooplankton (Ferrier-Pagès et al., 2011; Houlbrèque and Ferrier-Pagès, 2009) and bacterioplankton (which includes bacteria and bacteria associated with various particulate organic matter, mucus or dead material) (Sorokin, 1973) are examples of heterotrophic sources of food that supplement the autotrophic nutrition in mixotrophic corals (Houlbrèque and Ferrier-Pagès, 2009).

Despite this large trophic potential, food requirements can be very specific for some corals, while other may have opportunistic behavior obtaining their optimum nutritional status from what is available in their surroundings (Anthony, 1999; Anthony, 2000) and by alternating the proportion of autotrophic and heterotrophic nutrition (Anthony and Fabricius, 2000; Leal et al., 2015). For example, previous studies have investigated trophic patterns in corals using natural abundance of stable isotopes reported a shift in metabolic status from autotrophy to heterotrophy along a depth gradient (Alamaru et al., 2009; Muscatine and Kaplan, 1994; Muscatine et al., 1989b) and seasonal range (Ferrier-Pagès et al., 2011; Nahon et al., 2013; Susanto et al., 2013).

Carbon and Nitrogen stable isotopes ($\delta^{13}C$ $\delta^{15}N$) are useful tracers of the nutritional sources (autotrophic and heterotrophic) incorporated (Lorrain et al., 2017; Muscatine et al., 1989b) and can be

informative for the isotopic niche width (Jackson et al., 2011) and trophic potential of organisms. The isotopic composition, $\delta^{15}N$ and $\delta^{13}C$, measured in host and symbionts will be the result of an isotopic mixture from the contribution of multiple sources (autotrophic and heterotrophic) assimilated, retained and exchanged between the symbiotic partners (Tremblay et al., 2015). Carbon isotope indicate the assimilated sources and $\delta^{15}N$ values is a proxy for trophic position obtained through all trophic pathways. Complementary to the typical bi-plot data of carbon and nitrogen, heterotrophy in corals is usually assessed by subtracting the isotopic composition between host and symbionts (Hoogenboom et al., 2015). Recent advances have been made towards the understanding of nutrients exchange and carbon and nitrogen turnover rates within the symbiotic partners (Reynaud et al., 2009; Tanaka et al., 2015; Tanaka et al., 2018; Tremblay et al., 2012; Tremblay et al., 2015). Moreover, possible shifts from a mutualist relationship to competition or parasitism may occur between the partners when temperature condition become stressful (Baker et al., 2013; Baker et al., 2018).

The importance of trophic plasticity lies in understanding the cost and potential for acclimatization to increasing impacts and environmental changes, such as what has been gradually observed in coastal tropical areas (Costa et al., 2008; Duprey et al., 2016; Silva et al., 2013). As coral reefs are generally closely connected to the coast line, coral cover has been dramatically declining worldwide due to the effect of multiple anthropogenic factors (overfishing, land use change, and pollution) but, especially, coral bleaching driven by climate change (Bellwood et al., 2004; Bruno and Selig, 2007; Hoegh-Guldberg, 1998; Hoegh-Guldberg, 1999; Hughes and Connell, 1999). However, some evidence points out species have different thermal susceptibility (Wooldridge, 2014) and are differently affected by bleaching (Carpenter et al., 2008; Hughes et al., 2018; Loya et al., 2001; van Woesik et al., 2011). A possible explanation is because species have different metabolic requirements (Hoogenboom et al., 2015), for example, it has been recently suggested inorganic nitrogen fixation compensates for low heterotrophic acquired nitrogen in more autotrophic corals (Pogoreutz et al., 2017). The outcome of nutrient acquisition from autotrophic and heterotrophic sources will eventually influence physiological responses of symbionts (Fagoonee et al., 1999; Muscatine et al., 1989a; Stambler et al., 1991; Wooldridge, 2016) consequently, affecting the host capacity to resist to or recover from bleaching experiences (Baumann et al., 2014; Béraud et al., 2013; Hughes et al., 2010). Wider isotopic niche space would indicate higher trophic plasticity (i.e., consumers feed on diverse resources) (Jackson et al., 2011; Layman et al., 2007; Newsome et al., 2007), while narrower niche boundaries combined with greater physiological variation would indicate restricted trophic plasticity and greater susceptibility to disturbances. In this context, when physiological responses of endosymbionts are significantly affected

by environmental conditions, corals may be more susceptible to extinction. If trophic possibilities are ample and physiological parameters are maintained in contrasting environments (nearshore and offshore reefs, for example), then there is greater trophic plasticity to acquire nutrients to their demand (Grottoli et al., 2006; Riera, 2009) and more chances for survivorship in future scenarios.

Yet, there is still a gap in understanding natural variation of trophic and physiological responses of corals (Pogoreutz et al., 2017) from different coral functional groups (i.e. different tolerances to stress, growth strategies, reproduction modes, and energy allocation) and the scarcity of data is even greater in the Atlantic Ocean. To fill this extensive knowledge gap, the goal of this study was to investigate natural trophic and physiological response of two symbiotic corals comparing nearshore and offshore reefs. They are two closely-related species of massive scleractinian corals (Fukami et al., 2004; Nunes et al., 2008) representative of mussids and favids, both inhabitants of shallow reefs and mainly associated with clade C *Symbiodinium* (C1 and C3 in *F. gravida*, C3 and A4 in *M. braziliensis*) (Silva-Lima et al., 2015), but with different life history strategies (Darling et al., 2012; Knowlton, 2001). Our hypothesis was that the small and short-lived weedy coral *Favia gravida* (Verril, 1868), widely distributed in the South Atlantic, would exhibit higher trophic plasticity than the larger, long-lived and narrowly distributed coral *Mussismilia braziliensis* (Verril 1968). Both differ in their geographic distribution (Castro and Pires, 2001) (Fig. 1; Fig. 1S), reproductive traits and dispersal potential (Nunes et al., 2011). The spawner and long lived coral *Mussismilia braziliensis* (Verril 1968) grows slower than *F. gravida*, reaches more than 1 m in diameter and is restricted to a narrow range of 1500 km along the SWA coast (Moura, 2000). The brooder *Favia gravida* (Verril, 1868) does not reach more than 10 cm in diameter and is found along 3000 km of the SWA coast (Castro and Pires, 2001) as well as along the Atlantic coast of Africa (Hoeksema, 2012). It dominates tidepools, with highly variable sedimentation and salinity conditions and may occur under extremely turbid waters such as the Amazon River plume (Moura et al., 2016). The coral *F. gravida* has been known to be one of the oldest living genera of corals (210-140 million years ago) (Veron 1995), to be highly tolerant to temperature anomalies (Kelmo et al., 2003; Kelmo et al., 2014) and to show a high morphological plasticity (Amaral and Ramos, 2007; Hoeksema, 2012).

2 Materials and Methods

2.1 Study Area

The study was conducted in the Abrolhos Bank Reefs, the most extensive and biodiverse coral reef system in the Southern Western Atlantic (SWA) (Moura, 2000). Two contrasting reefs in terms of water quality (Bruce et al., 2012), management regimes and environmental conditions were sampled: Pedra de Leste (-17.78 S; -39.05 W), a nearshore reef (14 km offshore) and Parcel dos Abrolhos (-17.99 S; -38.67 W) an offshore reef (61 km offshore), located within the Abrolhos Marine National Park (Fig. 1). Sampling occurred in the end of the summer in February and March 2016, when eastern winds prevails and the water is clearer. Turbidity and sedimentation rates are historically higher nearshore and remain under higher variability (Segal et al., 2008; Zoffoli et al., 2013). Sedimentation rate reaches 5mg cm^{-2} day^{-1} (Segal et al., 2008), being predominantly carbonate-derived (~90%) in offshore reefs (Parcel dos Abrolhos) and contrasting to terrigenous-derived constituents (40%-60% of silt and clay) in coastal reefs sites (Pedra de Leste) (Leão and Kikuchi 2005; Segal et al. 2008), which have been increasing since 2002 due to land use changes (Leão and Kikuchi, 2005; Silva et al., 2013).

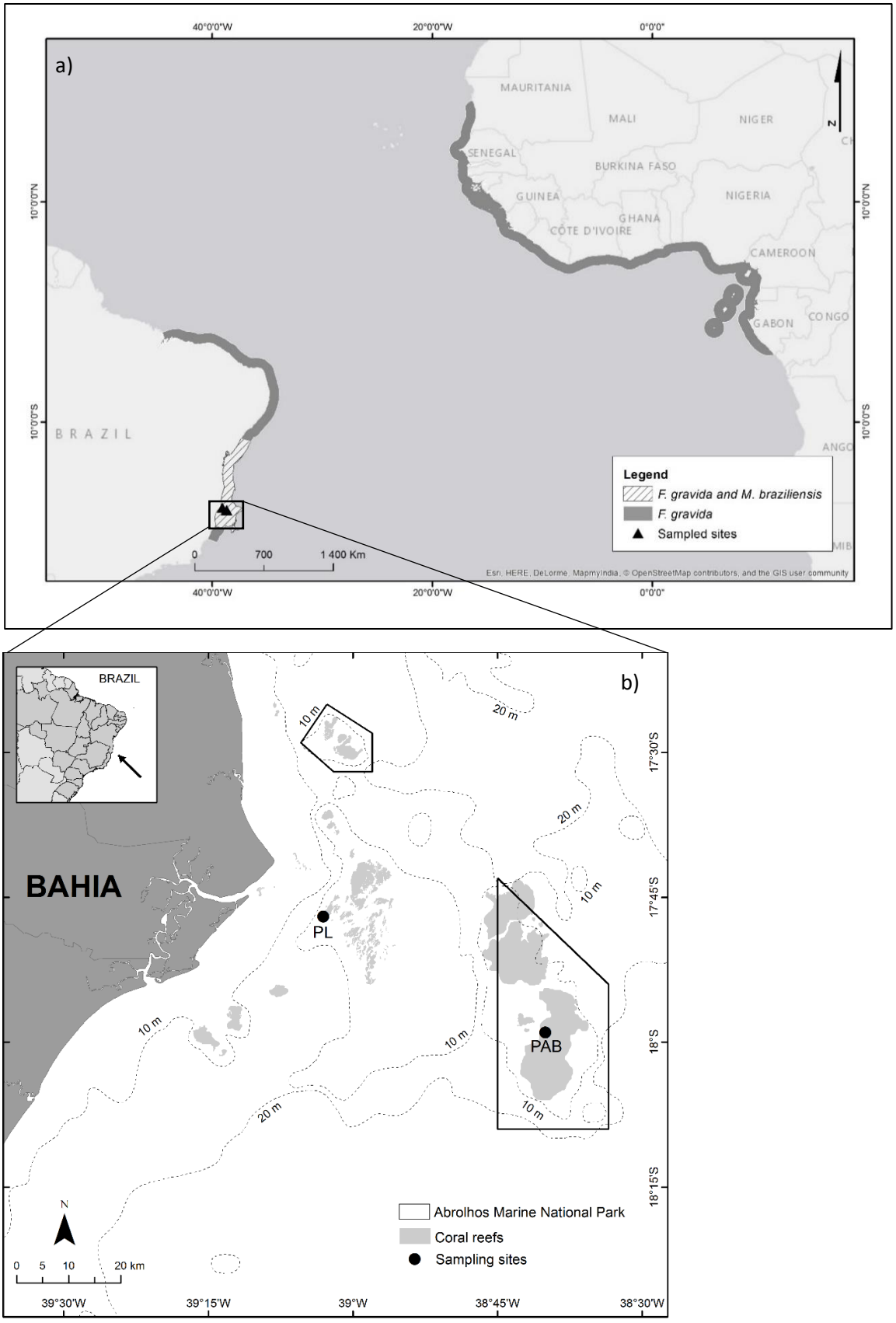
a)
40°0'0"W
20°0'0"W
0°0'0"
10°0'0"N
10°0'0"S
MAURITANIA
MALI
NIGER
SENEGAL
BURKINA FASO
GUINEA
NIGERIA
GHANA
CÔTE D'IVOIRE
CAMEROON
GABON
CONGO
BRAZIL
Legend
F. gravida and M. braziliensis
F. gravida
Sampled sites
0
700
1 400 Km
Esri, HERE, DeLorme, MapmyIndia, © OpenStreetMap contributors, and the GIS user community
b)
BRAZIL
BAHIA
PL
PAB
10 m
20 m
17°30'S
17°45'S
18°S
18°15'S
N
0 5 10 20 km
Abrolhos Marine National Park
Coral reefs
Sampling sites
39°30'W
39°15'W
39°W
38°45'W
38°30'W

Fig. 1 a) Distribution range of *Favia gravida* and *Mussismilia braziliensis* (after Laborel 1969, 1974) along the Atlantic Ocean modified from Aronson et al. 2008 for *Favia fragum*, and; b) Study area and sampling sites nearshore and offshore reefs of Abrolhos, Bahia, Brazil.

2.2 Sample collection and preparation for analysis

In February and March of 2016, at each site, colonies were collected from three (at Pedra de Leste) and two (at Parcel dos Abrolhos) patch reefs approximately 20m apart, at 5 m depth. Maximum colony diameter ranged from 53-124 mm (*M. braziliensis*) and from 21-49mm (*F. gravida*). Corals were collected by SCUBA diving, with a hammer and chisel and put into numbered bags. On the boat, colonies were transferred to 20 L buckets filled with seawater and immediately processed. Corals were rinsed with Milli-Q water and coral tissue from the whole colony area was airbrushed into a 10 L beaker using a dive cylinder. The total slurry volume obtained from each colony of *M. braziliensis* was registered, vigorously homogenized and divided into three subsamples. Two subsamples were frozen in liquid nitrogen, one for stable isotope analysis and the other for chlorophyll-*a* (*Chla)* content quantification while the third subsample was suspended in 10mL of filtered (0.22 µm) seawater, preserved in 10% paraformaldehyde, and kept in the dark at 4°C for symbiont densities and biovolume measurements. Because of the small size of *F. gravida* and limited slurry content obtained, the isotopic composition was analyzed from different colonies from which *Chla* content, symbiont densities and biovolume were measured. All skeletons were labeled and kept for skeletal surface area (SSA) measurements (cm^2). SSA were estimated through the aluminum foil method (Marsh, 1970; Veal et al., 2010). *Chla* content and symbiont density parameters were standardized to SSA. Samples were collected under permit number 50339-1, emitted by the Brazilian Environmental Authority (SISBIO License).

2.3 Symbiont density and optical properties

In the laboratory, the diluted homogenate was vortexed (1 min) and sonicated for 10 s (30 pulses of 1 s with 3 s intervals, 20% power, ultrasonic processor, Cole-Palmer). Symbiont counts were determined using a flow cytometer (FCM, BD Accuri™ C6 flow cytometer). Aliquots of 1 mL (triplicates) from the preserved subsample was filtered in 45 µm mesh to remove any carbonates. The filtered fraction was read for 2 min in the FCM allowing quantification of cells and characterization of optical properties of

Symbiodinium spp. To determine photosynthetic potential all samples were characterized according to mean and coefficient variation (CV) of Fluorescence (FL3) of *Symbiodinium* spp.

2.4 Symbiont biovolume

Biovolume was measured with an automated inflow imaging system (FlowCAM®, Fluid Imaging Technologies) set with a 90-µm flow cell, using a x10 magnification objective in auto-image mode. Images were taken at 100 µl/min sample flow, for 5 min. Biovolume was estimated assuming cells showed an ellipsoid form and was determined by $V = \frac{4\pi.\left(\frac{l}{2}\right).\left(\frac{w}{2}\right).\left(\frac{w}{2}\right)}{3}$ (where l= cell length and w=cell width). A minimum of 177 (*F. gravida*) and 272 (*M. braziliensis*) of focused and well delimited cells (checked by the particle edge trace and edge gradient parameters) were measured in each sample and the mean biovolume per colony was used in analysis.

2.5 Pigment analysis

Photosynthetic pigments content of corals were extracted from an aliquot of slurry in 90% acetone (1:5; v:v) (overnight, at 4°C in the dark). The extracts were centrifuged at 2000 rpm for 15 min and optical densities (OD) were read at 750, 664, 647, 630, and 430 nm in a spectrophotometer (SHIMADZU®, UV-160A) using a 10 mm glass cuvette to assess the turbidity of the sample and the concentration of chlorophyll-*a* (*Chla),* chlorophyll-b *(Chlb)*, chlorophyll-c *(Chlc)*, and carotenoids, respectively. Concentration of *Chla* was calculated according to the trichromatic method of Jeffrey and Humphrey (1975). The Margalef index (OD430/ OD664, i.e., carotenoid to *Chla* ratio) was calculated to determine the maturity state of the *Symbiodinium* population by taking into account the diversity of pigments found within a colony, a method described by Margalef (1983) established for phytoplankton pigments applied here in *Symbiodinium*. For phytoplankton reference, values around 2 represent a young algal association with high productivity while higher values (between 5 and 7) correspond to a lower rate of cell renovation and lower productivity (Margalef, 1983).

2.6 Environmental parameters of water

Sea water samples were collected few centimeters above corals at 12:00 h and ~17:30h (high and low photosynthetic activity) to quantify concentrations of suspended particulate matter (SPM), dissolved and particulate organic carbon (DOC and POC, respectively), total dissolved nitrogen (TDN), and stable isotopes of carbon and nitrogen ($\delta^{13}C$ and $\delta^{15}N$). Turbidity (expressed in NTU) and pH were measured *in situ* using a turbidimeter (LaMotte 2020we) and a portable potentiometer (Digimed DM-PV) with Ag/AgCl electrode. Temperature was registered with a HOBO every 6 hours, during three months before the experiment on both sites. SPM was obtained in duplicate by filtering seawater (gravimetric method) using precombusted (350°C/4h) and pre-weighed GF/F filters (Whatman, nominal pore size 0.7 µm). To remove salt, after filtration, filters were rinsed in the field with ultra-pure water, dried at 60° C (~ 72h) in the laboratory and SPM (mg/L) concentrations were determined by subtracting the initial from the final weight of filters. SPM was acidified (48h) acidic atmosphere (HCl) and dried (4h, 110°C). A subsample of dried filters containing SPM were weighed into tin disc plates for POC isotopic analyses. Filtered sea water samples were preserved in amber glass vials (previously soaked overnight in HCl 10%, rinsed with ultra-pure water, dried at 60° C and precombusted at 350° C, 4h) and stored at 4° C until DOC and TDN concentrations analysis. Samples of DOC were acidified with HCl (37%, analytical grade) to pH 2 and purged with ultra-pure synthetic air for 5 minutes to remove the inorganic carbon content. Concentrations (mg/L) of DOC and TDN were determined in duplicate through the high-temperature catalytic oxidation (680° C) method using an infrared TOC-VCPH (Shimadzu) (Non dispersive infra Red – detector). A fraction of dissolved organic matter (DOM) was isolated and concentrated in the field via solid-phase extraction (SPE-DOM) (Dittmar et al., 2008) with pre-packaged PPL (styrene divinyl benzene polymer, Varian Bond Elut) cartridges. In the cartridges, DOM were desalted with 0.01mol L^{-1} HCl and dried with a stream of N_2. SPE-DOM was eluted with 8 mL of methanol (HPLC grade) and the extracted DOM was stored in the freezer at -18°C pending isotopic analysis. An aliquot (800–1600 µL, ~20 µg) of SPE-DOM was re-dissolved in 50 µL of methanol, transferred into tin Smooth wall capsules and dried at 60◦C for 24 h until DOC isotopic analysis.

Microplankton and mesoplankton were collected horizontally on the reefs using plankton nets, of 60 and 200 µm mesh sizes, respectively, (30 cm mouth diameter, 1 m length), at night (7 and 11 pm) and day time (9 am and 4 pm) to estimate biomass density and isotopic composition in the study area. Samplings were carried out for 10 min (2x5 minutes) on a small boat, with average speed of 2.5 knots. A subsample of 15% from the whole homogenized sample was preserved in formaldehyde (5%) for taxonomic identification. The remaining fraction (85%) of each sample was preserved in 4°C and in the dark for biomass and isotopic analyses. In the laboratory, samples were desalted by several

centrifugations (2500 rpm, 10 min), changing Milli-Q water until reaching 300 µS. Samples were freeze-dried and dried biomass was quantified. The density of dried microplankton and mesoplankton was expressed in g/m^3. Plankton density was calculated using the formula $V = (\pi r^2 h)(0.85d)$, where *r* corresponded to the mouth net diameter divided by 2, *h* to the length of plankton net and d the distance traveled. Taxonomic identification of microplankton were conducted using a magnifying glass (Leica S8APO). Samples collected with 200 µm mesh sizes were counted either taking the whole subsample or using the quartering method when abundance was high (Erdoğan et al., 2014). In the latter method, counts should reach at least 300 individuals allowing extrapolation for the aliquot. Microplankton community collected with 64 µm was divided into two fraction: <100 µm, composed mainly by debris, analyzed with an automated inflow imaging system (FlowCAM) and, > 100 µm, composed mainly by copepods' feces and smaller copepods, analyzed using a microscope. Only dried biomass' density of these samples are shown here.

2.7 Elemental composition and stable isotopes (δ^{15}N and δ^{13}C) of tissue and symbiont

In the laboratory, tissue and symbiont were separated adding Milli-Q water to the samples in 15mL tubes, followed by sonication and vortexing for 1 min. Tubes were centrifuged (1600 rpm x5 min) and the supernatant (tissue fraction) was separated from the pellet (symbiont fraction). Additional Milli-Q water was added to the pellet to rinse and remove any remaining tissue. Samples were centrifuged 2x to remove most symbiont from tissue fraction and vice-versa. After processing, the separated fractions were verified in the microscope where minimum cross contamination remained. Symbiont and tissue were frozen in liquid nitrogen and freeze-dried until further analysis. In addition to field measurements, we investigated the isotopic composition (δ^{15}N and δ^{13}C) and C:N ratio of cultured *Symbiodinium* (clade D), lineage A4 (ITS2), isolated from *Mussismilia braziliensis* aiming to have a reference for free living *Symbiodinium* in different growth stages of population (Suplementary Material).

Elemental composition of N (%) and δ^{15}N of coral tissue and symbiont were determined from 1.5 mg. For elemental composition of C (%) and δ^{13}C analysis, approximately 2 mg were weighed in silver capsules, followed by acidification through the addition of HCl (2M) to remove carbonates (Brodie et al., 2011). Analysis were performed with an Elemental Analyzer (Flash 2000) coupled to an isotope ratio mass spectrometer Delta V Advantage (Thermo Scientific, Germany). Carbon and nitrogen content was

expressed as percent (%) element and the detection limits were 0.05% and 0.02% for C and N, respectively. Carbon and nitrogen isotope ratios were expressed as ‰ relative to Pee Dee Belemnite (PDB) and atmospheric nitrogen, respectively, with analytical precision of 0.1‰.

2.8 Statistical analysis

To test for significant differences in water parameters between sites, a Welch's t-test was performed after conducting a Shapiro-Wilk test for normality. Concentrations of SPM, TDN and δ^{15}N of DOC were log transformed. The similarity in zooplankton community composition among reefs was evaluated with a Multi-Dimensional Scaling (MDS) analysis, based on Bray Curtis dissimilarity matrix with fourth root-transformed data (Clarke, 1993). Analyses were conducted using the software package PRIMER (PRIMER-E Ltd.). Significant differences in physiological parameters were evaluated with Factorial ANOVA with site and species as fixed factors, followed by the Tukey HSD for multiple comparisons to identify homogeneous group. Pearson correlations with a 95% Confidence interval were used to investigate the relationship between δ^{15}N of host and symbiont in each species separately and to investigate the association between the trophic status of the colony (symbiont and host) on symbiont traits. The following transformations were used to meet homoscedasticity and normality assumptions of residuals in ANOVA: Relative percentage of coral cover and coefficient of variation of FSC H were logit transformed (Warton and Hui, 2011); To avoid negative values from the subtraction between δ^{15}N host and δ^{15}N symbiont, 2.5 were added to the result of each sample. This addition applied was necessary fit a square root transformation to the data while keeping the correct proportions and; *Chla* per cell were square root transformed; *Symbiodinium* density, *Symbiodinium* biovolume/cm², δ^{13}C of host and δ^{13}C of symbiont were log transformed. The analyses were conducted using the linear model and *lm* function in R.

*Stable Isotopic Analysis (*SIAR) was used to estimate the relative contribution of the potential nutrition sources (Layman et al., 2011) associated to coral host tissue of corals in Abrolhos. The model assumes target values comes from a Gaussian distribution with an unknown mean and standard deviation and the mean is a weighted combination of the nutrition sources' isotopic values (Parnell and Jackson, 2015). *Stable Isotope Bayesian Ellipses* (SIBER) (Jackson et al., 2011) (p-interval of 0.05) and convex-hull-based quantitative analysis (Turner et al., 2010) were applied to estimate relative niche width of host and symbiont within the two species studied. The Bayesian framework was used as a

complementary metric for trophic plasticity. The Standard Ellipses Area corrected (SEAc) allows robust comparison of among data sets with unequal sample sizes (Jackson et al., 2011).

3 Results

3.1 Environmental parameters

The three months temperature measurements revealed daily temperature fluctuations was more variable nearshore than offshore reefs with differences up to 3.7°C (Fig. 2).

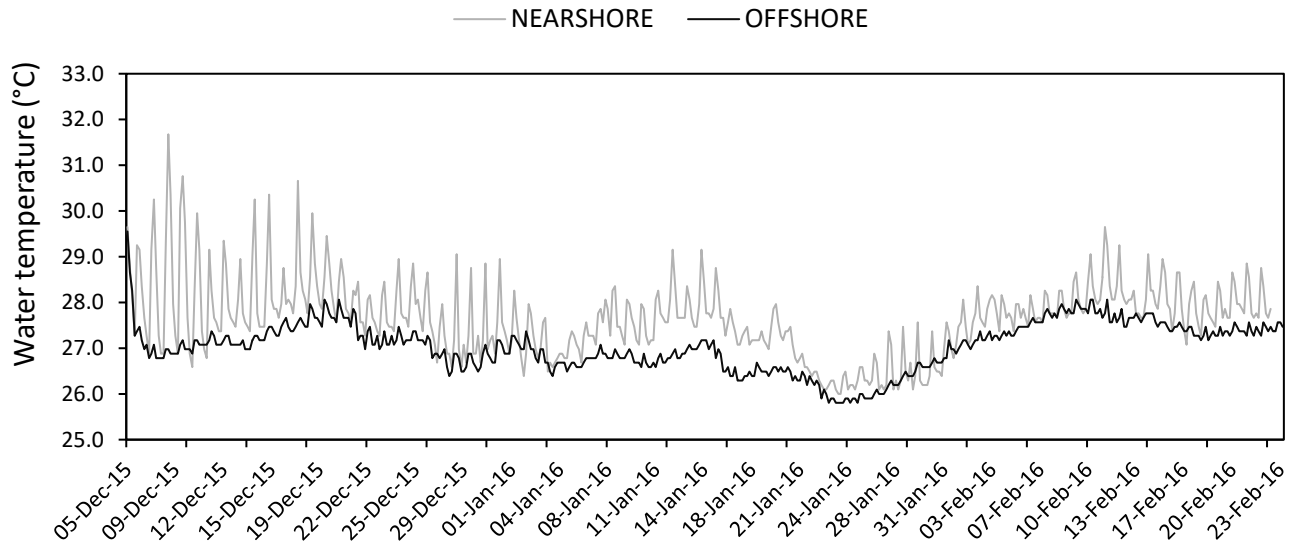

Fig. 2 Seawater temperature measured every 6 hours in the sampling areas, during three months before the experiment

Water turbidity and pH showed significant differences regarding nearshore and offshore reefs (Table 1S; Fig. 3). Turbidity was 1.6 times higher nearshore, reflecting the contribution of dissolved organic matter from river discharges as water pH was significant lower nearshore, and where DOC reached higher values, but not statistically different from offshore reefs (Table 1S; Fig. 3). Likewise, TDN and SPM concentrations did not differ between sites. However, SPM concentrations was higher and more variable offshore. The bi-plot of carbon ($\delta^{13}C$) and nitrogen ($\delta^{15}N$) isotopic composition of potential

nutritional sources collected from the water column were distinct between them, but remained similar between nearshore and offshore sites (Fig. 4; Table 1).

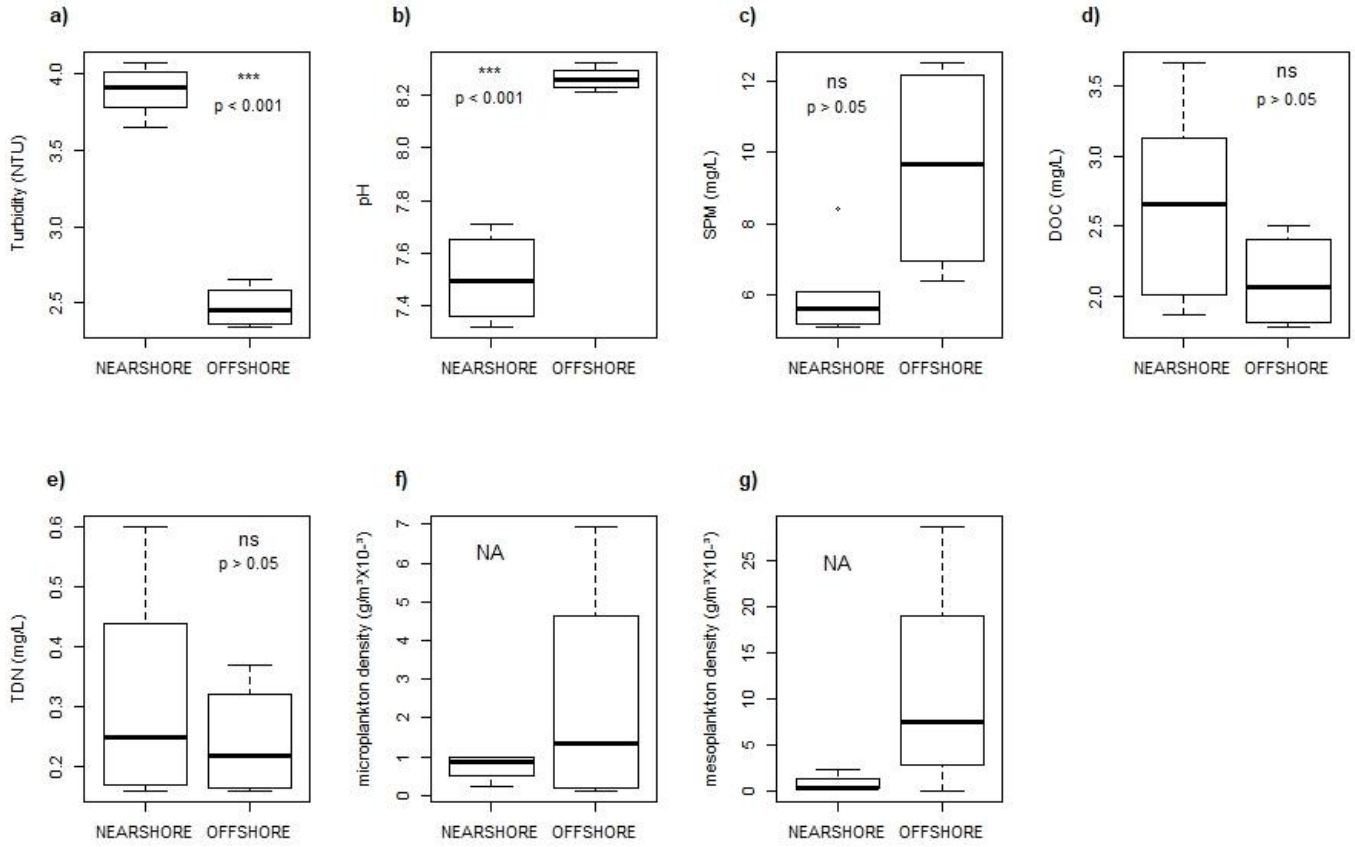

Fig. 3 Boxplots with the range of data for a) water turbidity (n=6; n=4); b) pH (n=6; n=4) c) suspended particulate matter (SPM) (n=6; n=4); d) dissolved organic carbon (DOC) (n=6; n=4); e) total dissolved nitrogen (TDN) (n=6; n=4); f) microplankton density (n=6; n=4), and; g) mesoplankton density on nearshore and offshore reefs (n=4;n=4), with respective results of Welch's t-test analysis comparing parameters between sites. Ns=not statically significant; NA= not applicable, when assumptions of Welch's t-test were not met. The midline across each box represents the median, and the upper and lower limits of the box are the third and first quartiles (50% of data). Diamonds express outliers (when data extends 1.5 times the interquartile range of the box).

3.2 Mesoplankton community

Higher variability (all samples) and greater contribution (night samples) of micro and mesoplankton was observed in offshore when compared to nearshore reefs (Fig. 3). Marked differences in mesoplankton density between sites was registered at 11pm, reaching 29 x10^{-3} g/m³ offshore against 0.40 x10^{-3} g/m^3 on nearshore reefs. Mesoplankton community nearshore and offshore showed a similarity index of 40% (Bray Curtis similarity) (Fig. 2S). Among the main taxonomic groups identified, Copepoda was the most abundant at both sites. Foraminifera, Gastropoda, Polychaeta and Stomatopoda (Crustacea) were exclusively sampled offshore, while Isopoda, Chaetognatha, Bryozoa, one group of Decapoda (Lucyfer) and two orders of Copepoda (Harpacticoida, Monstrilloida) were only registered nearshore. Other Copepoda (Calanoida, Cyclopoida), Decapoda, Crustacea (Mysida, Amphipoda, Cumacea, Tanaidacea), and ichthyoplankton were common on both sites.

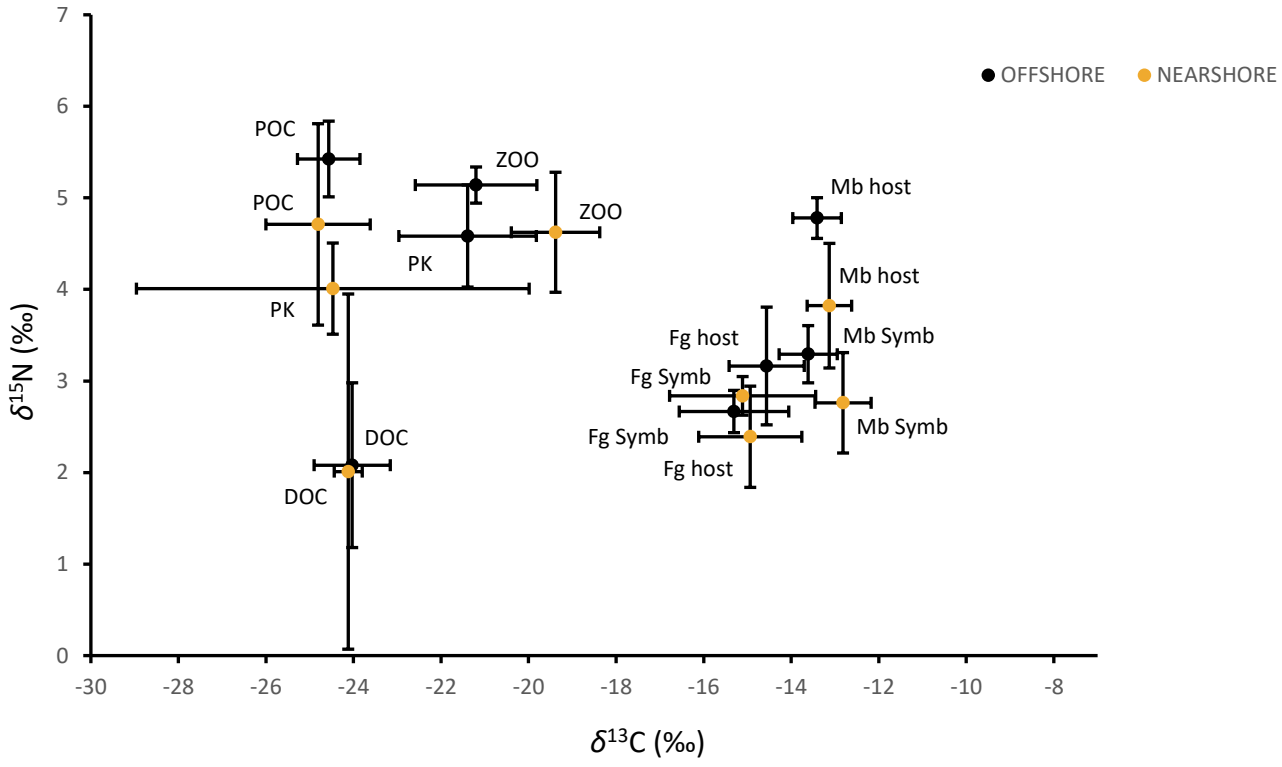

Fig. 4 δ^{13}C and δ^{15}N (mean±SD) of potential nutrition sources (DOC: dissolved organic carbon; POC: particulate organic carbon; PK:microplankton (60µm mesh size); ZOO: mesoplankton (200µm mesh size); Symb=symbiont) for the corals *Favia gravida* (Fg) and *Mussismilia braziliensis* (Mb) for nearshore and offshore reefs.

Table 1 Results from Welch's t-test comparing differences biogeochemical parameters from water and plankton samples on nearshore and offshore reefs with the number of samples (n) by site. Significant differences ($p < 0.05$) are shown in bold.

	Parameter	Mean Nearshore	Mean Offshore	t-value	df	p	n Nearshore	n Offshore
water	**DOC**							
	$\delta^{13}C$	**-24.1**	**-24.7**	**3.51**	**3.3**	**0.034**	4	3
	$\delta^{15}N$	2.0	1.4	0.33	3.8	0.760	4	3
	$C:N_a$	15.20	18.33	-2.60	4.72	0.051	4	3
	POC							
	$\delta^{13}C$	-24.8	-24.6	-0.41	8.0	0.693	6	4
	$\delta^{15}N$	4.7	5.4	-1.43	6.8	0.197	6	4
	$C:N_a$	11.68	11.60	0.05	4.11	0.956	6	4
plankton	**60 mesh**							
	$\delta^{13}C$	-24.5	-21.4	-1.30	3.7	0.243	4	4
	$\delta^{15}N$	4.0	4.6	-1.54	5.9	0.176	4	4
	$C:N_a$	7.39	6.08	0.79	3.39	0.483	4	4
	200 mesh							
	$\delta^{13}C$	-19.4	-21.2	2.12	5.5	0.079	4	4
	$\delta^{15}N$	4.6	5.2	-1.65	3.7	0.179	4	3
	$C:N_a$	**5.76**	**4.07**	**3.67**	**3.27**	**0.030**	**4**	**3**

3.3 Symbiont and host tissue isotopic composition

Host tissue (ANOVA; $\delta^{15}N$: $F(1,52)= 115.87$, $P<0.001$; $\delta^{13}C$: $F(1,53)= 52.45$, $P<0.001$) and symbiont (ANOVA; $\delta^{15}N$: $F(1,52)= 6.54$, $P=0.014$; $\delta^{13}C$: $F(1,46)= 30.84$, $P<0.001$) of *M. braziliensis* were significant enriched in ^{15}N and ^{13}C compared with *F. gravida* (Table 3. Fig. 5a). Differences between the two species accounted for 1.6‰ for $\delta^{15}N$ and 1.5‰ for $\delta^{13}C$ in host tissue fractions, and 0.3‰ for $\delta^{15}N$, and 2‰ for $\delta^{13}C$ for the symbiont fractions.

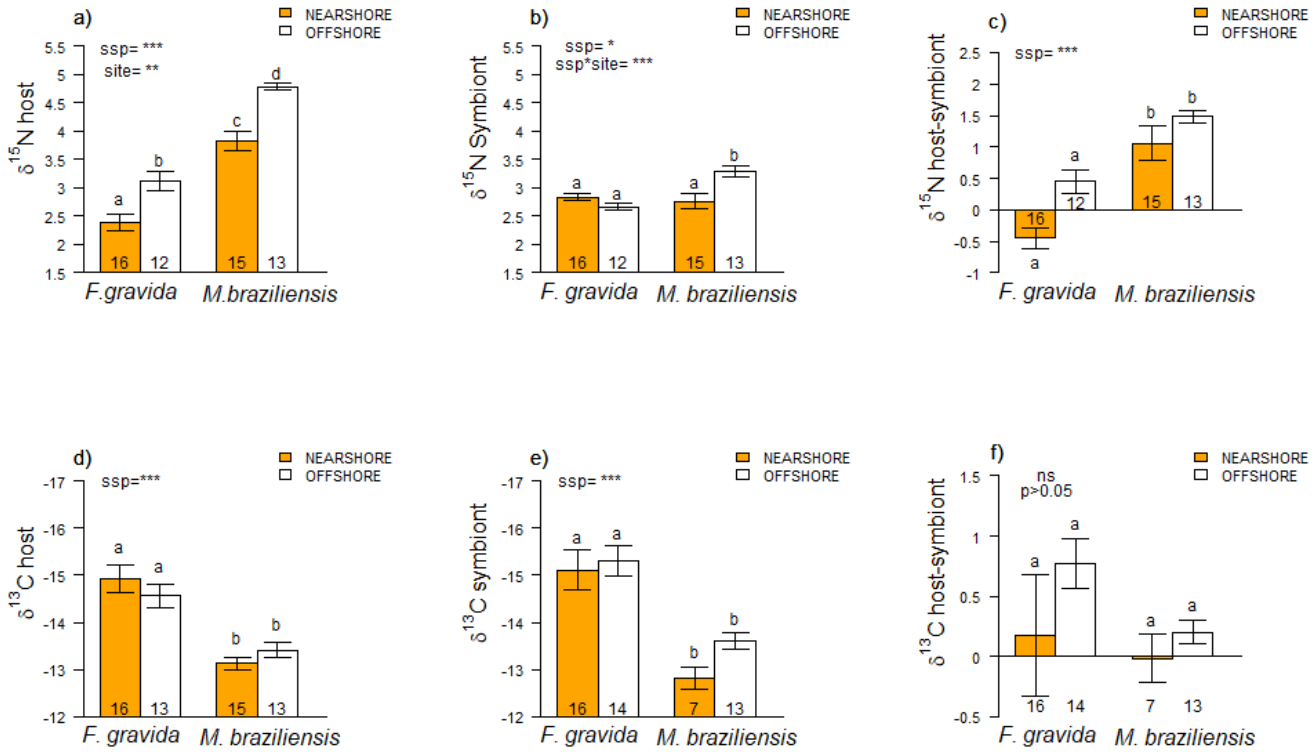

Fig 5 Means ±SE in $\delta^{15}N$ and $\delta^{13}C$ (‰) of host and symbiont showing differences between nearshore and offshore reefs in *Favia gravida* and *Mussismilia braziliensis*; a) $\delta^{15}N$ of host, b) $\delta^{15}N$ of symbiont; c) $\delta^{15}N$ host-symbiont; d) $\delta^{13}C$ of host; e) $\delta^{13}C$ of symbiont; f) $\delta^{13}C$ of host-symbiont. Significant results of Two-factorial ANOVA are summarized on the top of barplots: * = p<0.05; ** = p<0.01; ***= p<0.001; Letters indicate homogeneous group from Tukeys HSD comparisons. Number of samples are shown inside the plots.

There was a significant effect of site on $\delta^{15}N$ of hosts' tissues (ANOVA, F(1,52)= 32.78, P=0.002) (Fig. 5a), which was on average 0.7‰ (*F. gravida*) and 1‰ (*M. braziliensis*) enriched in ^{15}N offshore. There was an interaction effect between species and site on $\delta^{15}N$ symbionts (Fig. 5b): *M. braziliensis* (ANOVA, F(1,52)= 13.16, P<0.001) offshore was more enriched in ^{15}N than nearshore, following the same pattern of its host fraction, whereas $\delta^{15}N$ symbiont of *F. gravida* was similar nearshore and offshore with a different pattern of its host (Fig. 5a and 5b). No differences between sites and no interaction effects were detected in $\delta^{13}C$ of host tissue and of symbionts fractions (Fig. 5d and 5e).

Differences in $\delta^{15}N$ between host and symbiont ($\delta^{15}N_{host\text{-}symbiont}$) was significantly larger in *M. braziliensis* (1.3‰), compared to *F. gravida* (0.0‰) (ANOVA, F(1,52)= 44.32, P<0.001) (Fig. 5c). The $\delta^{15}N_{host\text{-}symbiont}$

of *F. gravida* averaged ±0.4‰, being negative nearshore and positive offshore, against +1‰ nearshore and +1.5‰ offshore for *M. braziliensis*. Overall differences in the $\delta^{13}C_{host\text{-}symbiont}$ were small, averaging 0.3‰ with no significant effect of site or species (Fig. 5f). Given the small differences between host and symbiont (<0.8‰) in both species, the results indicate carbon was mostly derived from photosynthesis.

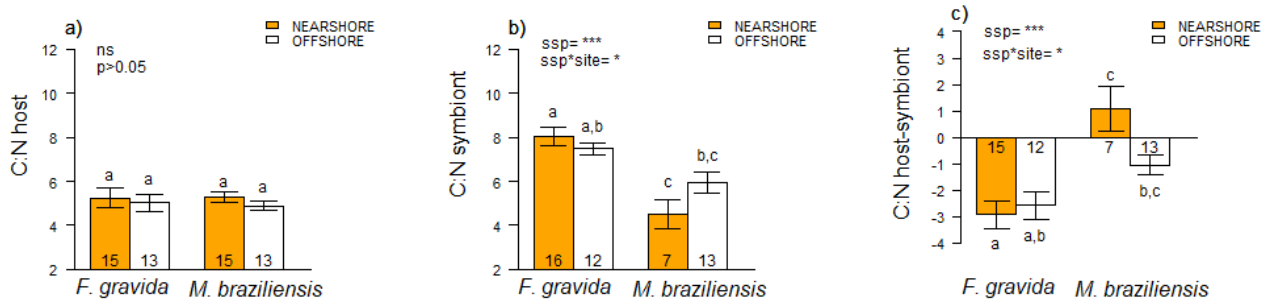

Fig. 6 Means ±SE in C:N_a ratio of host (a) and symbiont(b) showing differences between sites and species. Significant results of Two-Factorial ANOVA are summarized on the top of barplots: * = p<0.05; ** = p<0.01; ***= p<0.001; Letters indicate rom Tukeys HSD comparisons. Number of samples are shown inside or below the plots.

Carbon to nitrogen ratio (C:N_a) of host tissue fractions were equivalent between species and sites (Fig. 6a), but differed between species in the symbiont fraction. Symbionts of *F. gravida* showed higher C:N_a ratio (ANOVA, F(1, 44)= 28.64, P<0.001) (Fig. 6b). There was an interaction effect between site and species (ANOVA, F(1, 44)= 4.73, P<0.05) as C:N_a ratio of symbionts of *M. braziliensis* were lower nearshore compared to offshore reefs, while they were less contrasting for *F. gravida*. C:N_a ratio of *F. gravida* symbiont (8:1) was 1.6 times higher than C:N_a ratio of its host (5:1) on both sites, resulting significantly larger differences between symbiont and host compared with *M. braziliensis* (Fig. 6c) (ANOVA, F(1, 44)= 21.63, P<0.01). Despite the small differences in C:N_a ratio between compartments in *M. braziliensis,* they were contrasting between sites (ANOVA, F(1, 44)= 5.31, P<0.05). In offshore reefs C:N_a ratio was higher in symbionts than its host whereas nearshore the opposite was observed.

3.4 Isotopic niche space and relative contribution of potential nutritional sources

Convex hull and Standard Ellipse Area of hosts tend to be broader nearshore reefs, as *δ*-values of individuals were more dispersed, due to higher variability in resources use than offshore reefs (Fig. 7a; Fig. 7b). These changes were carbon-driven in the coral *F. gravida*, but nitrogen-driven in *M. braziliensis.* In the coral *M. braziliensis* offshore*,* host and symbiont were further apart when compared to nearshore reefs, indicating heterotrophy was enhanced offshore. The comparison of isotopic niche area between species in Abrolhos included all data set (Fig. 7c; Fig. 7d). Standard Ellipse Area corrected (SEAc) in *F. gravida* host was 1.9 times wider the area of *M. braziliensis*, while Total Area of Convex Hull was almost 3 times larger (Table 2; Fig. 7c). Isotopic niche area symbionts were not different between species (Table 2; Fig. 7c).

a)

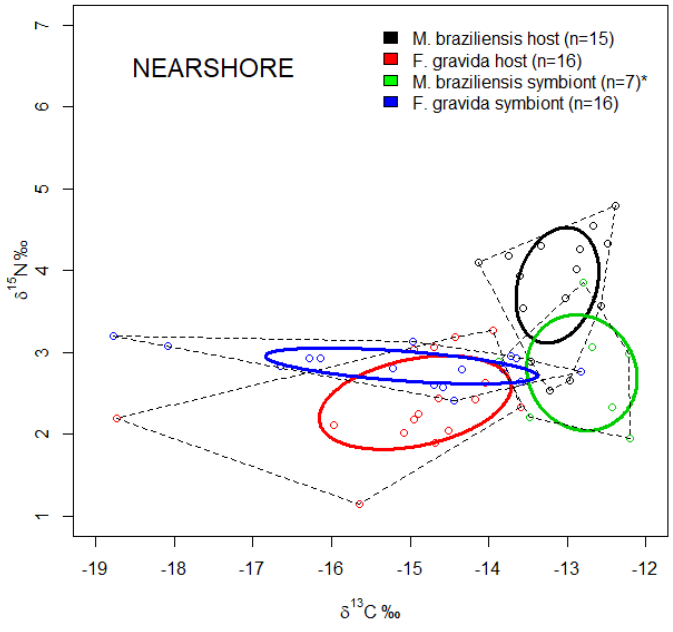

b)

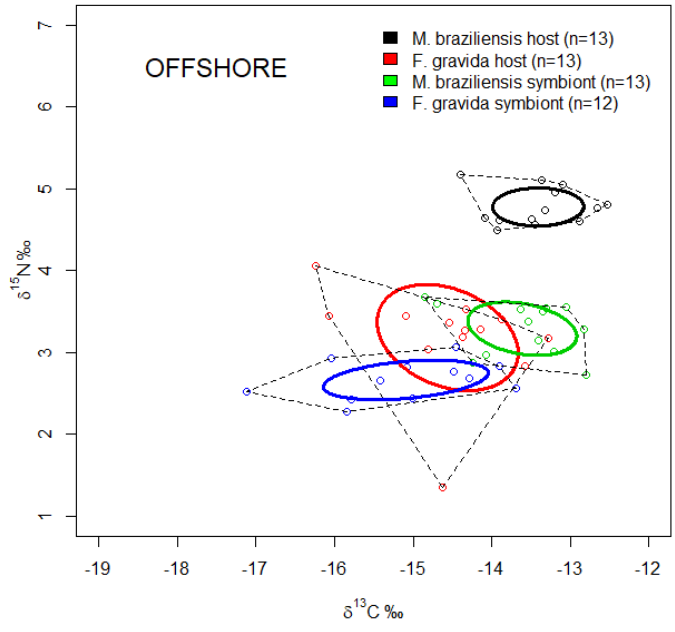

c)

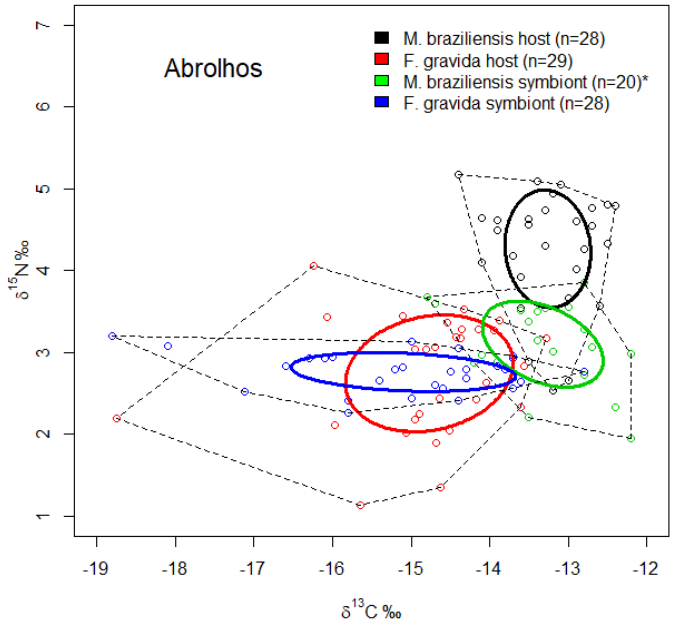

d)

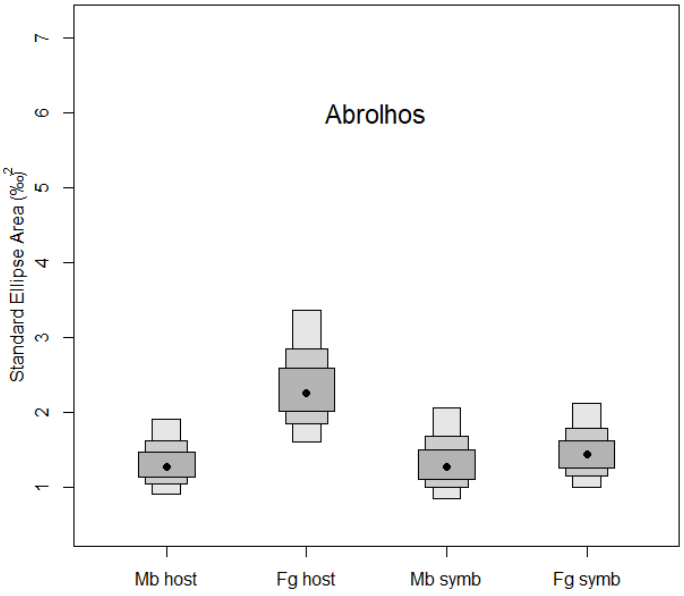

Fig.7 $\delta^{13}C$ and $\delta^{15}N$ bi-plot of host and symbiont (symb) of *Mussismilia braziliensis* (Mb) and *Favia gravida (Fg)* in: a) nearshore reefs; b) offshore reefs, and c) Abrolhos (nearshore + offshore reefs). Number of samples are indicated in parenthesis; *= samples lost. Standard Ellipse Area (SEAc) (solid thick lines) (d.f. = 2) represent the isotopic niche space and was used for comparison between species. Convex hull (dotted lines) represents the total niche width; d) Bayesian estimates of the Standard Ellipse Area between species (as plotted in figure c).

Table 2 Bayesian estimates of multivariate ellipse-based metrics of *Mussismilia braziliensis* (Mb) and *Favia gravida (Fg)* in: a) nearshore reefs; b) offshore reefs, and c) Abrolhos.

	***M. braziliensis* (Mb) host**	***F. gravida* (Fg) host**	***M. braziliensis* (Mb) symbiont**	***F. gravida* (Fg) symbiont**
Total Area (TA) of convex hull	3.2	9.4	3.14	3.18
Standard Ellipse Area (SEA)	1.18	2.27	1.15	1
Standard Ellipse Area corrected (SEAc)	1.23	2.36	1.17	1.03
Bayesian estimates (mean ±SD) for SEA (SEAb)	***1.39 (0.27)***	***2.44 (0.46)***	***1.42 (0.32)***	***1.54 (0.30)***
Comparisons[1] estimates between groups	Mb host < Fg host (p=0.99)		Mb symbionts = Fg symbionts (p=0.62)	

[1] To test whether group 1 (G1) SEA is smaller than group 2 (G2), the proportion of G1 ellipses that are smaller than G2 are calculated and significant results are given when p> 0.95.

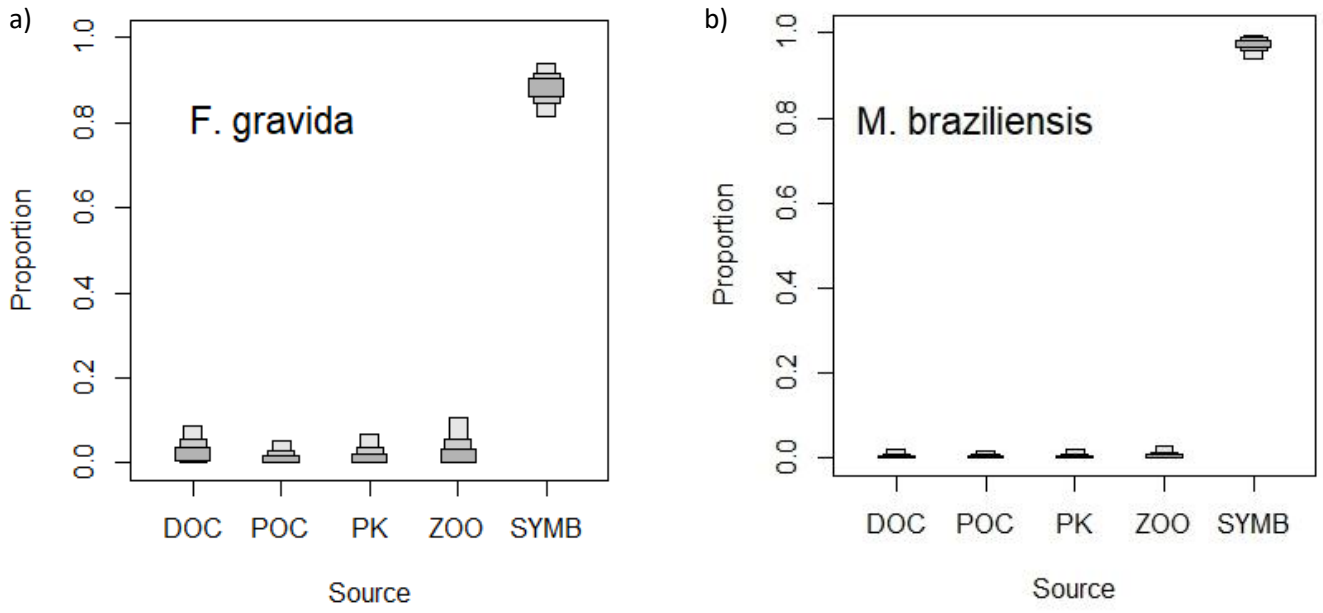

Fig. 8 Boxplot showing the estimates proportion (%) of potential nutrition sources assimilated by the host: a) *Favia gravida* (n=29), and; b) *Mussismilia Braziliensis* (n=28). DOC: dissolved organic carbon; POC: particulate organic carbon; PK: microplankton (60µm mesh size); ZOO: mesoplankton (200µm mesh size); SYMB=symbiont). Results were calculated using SIAR (Stable Isotope Analysis in R) with the trophic enrichment factor of*:* 1.6 ± 0.6‰ for $\delta^{13}C$ and 3.5 ± 0.7‰ for $\delta^{15}N$ (Minagawa and Wada, 1984). Boxplots are shown as the probability range with 25, 75 and 95% of credibility intervals.

Symbiont was the main nutritional source for both corals with an overall contribution (with 95% C.I) of 81 to 83% in *F. gravida* and 97% in *M. braziliensis* (Fig. 8). The model indicated symbionts contribution was higher offshore than nearshore. Heterotrophic sources showed relatively higher proportion nearshore, with dissolved organic matter and mesoplankton playing a more important role in nutrition, followed by microplankton and particulate organic matter (Table3).

Table 3 Probability range contribution (%) of potential sources assimilated by the host within 95% credibility interval (C.I.) for *Favia gravida* and *Mussismilia Braziliensis.* Results generated using *Stable Isotopic Analysis (*SIAR) with the trophic enrichment factor (TEF) of*:* 1.6 ± 0.6‰ for δ^{13}C and 3.5 ± 0.7 ‰ for δ^{15}N.

	DOC	POC	Microplankton	Mesoplankton	Symbiont
Abrolhos					
***F. gravida* (n=29)**	4.7-7.8%	0.4-1.3%	0.4-1.6%	0.5-2.4%	81-83%
***M braziliensis* (n=28)**	0.1-0.4%	0.1-0.3%	0.1-0.4%	0.1-0.06%	97%
F. gravida					
Nearshore (n=16)	0.9-3.8%	0.5-1.8%	0.5-2.1%	1-4.6%	75-79%
Offshore (n=13)	0.5-2.3%	0.4-1.4%	0.5-2.3%	0.5-2.2%	82-84%
M braziliensis					
Nearshore (n=15)	5.1%-9%	0.4-1.5%	0.5-1.7%	0.7-3.4%	79-81%
Offshore (n=13)	1.3-4.6%	0.4-1.4%	0.5-2.2%	0.5-1.9%	82-84%

3.4 Relationship between δ^{15}N and δ^{13}C of host and Symbiodinium

Host of *F. gravida* showed predominantly (96% of samples) δ^{15}N values lower than 3.5‰ while δ^{15}N of *M. braziliensis* host samples were predominantly (88% of samples) higher than 3.5‰. This was an arbitrary value (3.5‰) observed, which also corresponded to the TEF applied in the models. We analyzed the correlation between δ^{15}N of host and δ^{15}N *of Symbiodinium* for each species separately to further explore the coupling effect with physiological parameters. For *M. braziliensis,* we ran two correlation analyses as there was a clear pattern of positive correlation (Pearson, r=0.65, p<0.001) between host and symbionts when δ^{15}N of host > 3.5‰ (i.e, excluding three outliers). The second and non-significant correlation included all samples (Table 4). A weaker and negative correlation between the δ^{15}N of host and symbionts was observed for *F. gravida* (r=-0.40, p<0.05) (Fig. 9a). Likewise, the relationship in δ^{13}C of symbiotic partners in *M. braziliensis* were stronger correlated, while this relationship was not significant for *F. gravida* (Fig. 9b).

Table 4 Results from Pearson correlations between δ^{15}N and δ^{13}C between host and symbiont of *F. gravida* and *M. braziliensis.*

Metabolic relationships	Pearson correlation coefficient	p	t	df
M. braziliensis				
δ^{15}N symbiont X δ^{15}N host	0.09	0.640	0.47	26
δ^{15}N symbiont X δ^{15}N *host* (δ^{15}N > 3.5‰)	**0.65**	**0.000**	**4.12**	**23**
δ^{13}C symbiont X δ^{13}C host	**0.82**	**0.000**	**6.09**	**18**
F. gravida				
δ^{15}N symbiont X δ^{15}N *host*	**-0.40**	**0.034**	**-2.23**	**26**
δ^{13}C symbiont X δ^{13}C *host*	0.27	0.156	1.46	27

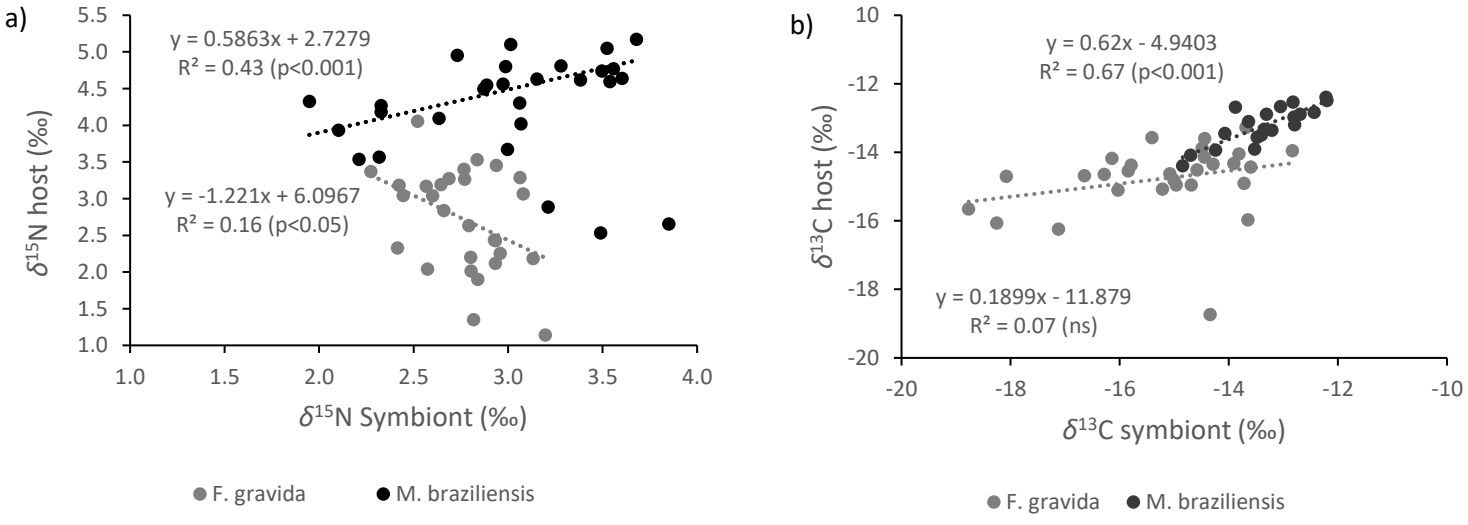

Fig. 9 Relationship between δ^{15}N (a) and δ^{13}C (b) of host and symbiont in *Mussismilia braziliensis* and *Favia gravida.*

3.5 Differences in physiological parameters

Physiological parameters were consistently different between species (Fig. 10; Table 3S), whereas differences between sites were only observed within *M. braziliensis* (Fig. 10a, b, d). The number of symbionts/cm² was 2.9 times higher in *M. braziliensis* ($0.74x10^6$) than in *F. gravida* ($0.25x10^6$). Hosting lower *Symbiodinium* densities, symbionts of *F. gravida* concentrated higher (~15%) *Chla* content per cell (15.86 pg/cm²) compared with *M. braziliensis* (6.55 pg/cm²) (Fig. 10). Conversely, fluorescence (measured as FL3) was not significantly different between species or sites (ANOVA, $F3(3,57)=0.53$, $P=0.66$) (Fig. 10; Table 3S), but *F. gravida* showed slightly lower variation in the overall fluorescence (CVFL3) than *M. braziliensis*. The interaction effect between sites and species in some parameters, indicated symbionts of *M. braziliensis* benefited from offshore reef conditions, while symbionts of *F. gravida* were not affected by site (Fig. 10). The coral *M. braziliensis* in offshore reefs responded with 2.1 times higher symbionts' density ($0.93x10^6$/cm²) than nearshore reefs ($0.43x10^6$/cm²), 2.7 times higher biovolume of cells/cm² ($392x10^6$/cm²) and 3 times higher *Chla*/cm² (Fig. 10a, b, d). There was significant differences between sites in productivity of symbiont population, given by the Margalef index (ANOVA, $F(3,31)=5.6$, $P=0.004$) (Fig. 10; Table 3S), as lower index indicated productivity was higher offshore for both species. Considering all samples, the Margalef index of cell renovation ranged between 1.25 (high renovation) and 5.75 (low renovation)

.

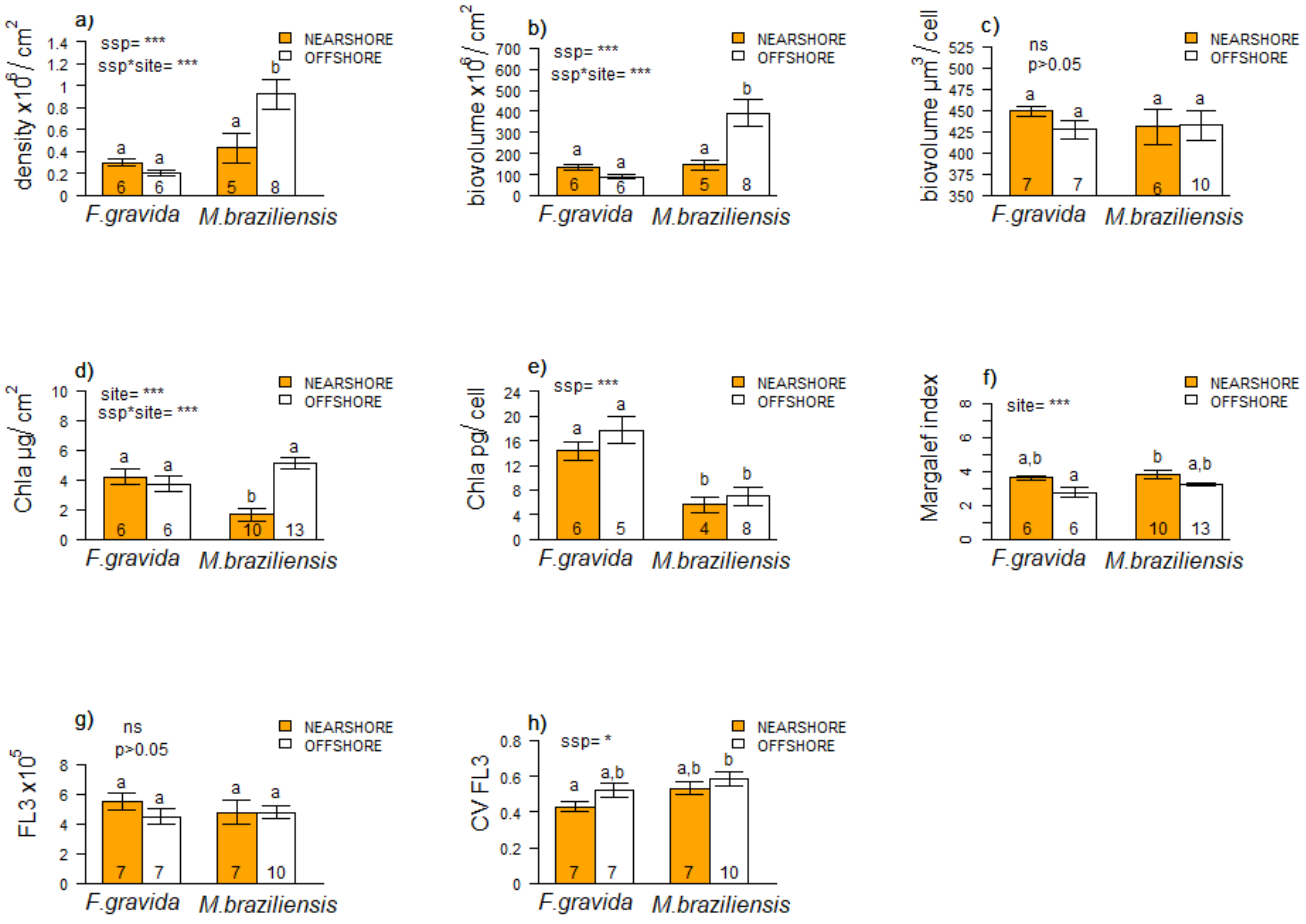

Fig. 10 Means ±SE of physiological parameters of symbiont from host tissue showing differences between sites and species: a) Density per skeletal surface area b) Biovolume per skeletal surface, area, c) Biovolume per cell, d) Chlorophyll-*a* content per skeletal surface area, e) Chlorophyll-a content per cell, f) Margalef index, g) Fluorescence in FL3 and, h) coefficient of variation of FL3. Significant results of Two- Factorial ANOVA are summarized on the top of barplots: * = p<0.05; ** = p<0.01; ***= p<0.001; Letters indicate homogeneous groups from Tukeys HSD comparisons. Number of samples are shown inside the bars.

3.6 Relationship between $\delta^{15}N$ and $\delta^{13}C$ and physiological traits in M. braziliensis

As $\delta^{15}N$ and $\delta^{13}C$ of symbionts and host were closely correlated in *M. braziliensis* (Fig. 9a and 9b), each physiological parameter of its symbionts were further correlated with $\delta^{15}N$, $\delta^{13}C$ and C:N_a ratio of

symbionts and host to investigate patterns and metabolic relationships. Surprisingly, most physiological and population parameters showed higher correlations with the host rather than symbionts, and mostly, strongly correlated to the nitrogen status rather than $\delta^{13}C$ (Table 5). Physiological parameters of symbionts (density/cm², biovolume/cm², chl*a*/cm² and productivity index) increased linearly until $\delta^{15}N$ reached ~4.5‰. After this value, $\delta^{15}N$ stabilized in relation to the increase in physiological parameters, reaching its maximum value of 5.2‰. While highest trophic status ($\delta^{15}N$) in *M. braziliensis* host stabilized ~ 5‰, symbionts density/cm² (Fig. 11a), biovolume of cells/cm² (Fig. 11b), *chla*/cm² (Fig. 11c) and productivity index (Fig. 11d) continued to increase. These results also suggest a high capacity for autotrophy reaches a limit to $\delta^{15}N$ values, which may serve as evidence that fractionation is reduced to zero in highly autotrophic scenarios.

Table 5 Results of Pearson correlation coefficients between physiological and metabolic parameters in *M. braziliensis.* Significant correlations ($p<0.05$) are in bold. In parentheses t value, and degrees of freedom to be included.

Physiological /metabolic parameters	**Density /cm²**	**Biovolume /cm²**	**Biovolume /cell**	**Chl *a* /cm²**	**Chl *a* /cell**	**Margalef index**	**Fluorescence (FL3)**
Host							
$\delta^{13}C$	-0.14	-0.30	-0.48	-0.17	0.47	0.16	**-0.55**
$\delta^{15}N$	**0.58**	**0.59**	0.05	**0.69**	0.09	**-0.64**	-0.22
C:N$_a$	0.04	-0.18	**-0.63**	-0.34	-0.12	**0.44**	**-0.70**
Symbiont							
$\delta^{13}C$	-0.42	-0.65	**-0.69**	-0.29	0.29	0.42	-0.59
$\delta^{15}N$	0.35	0.44	0.25	0.12	0.25	0.09	-0.13
C:N$_a$	-0.19	-0.36	-0.41	0.15	0.21	-0.30	-0.51

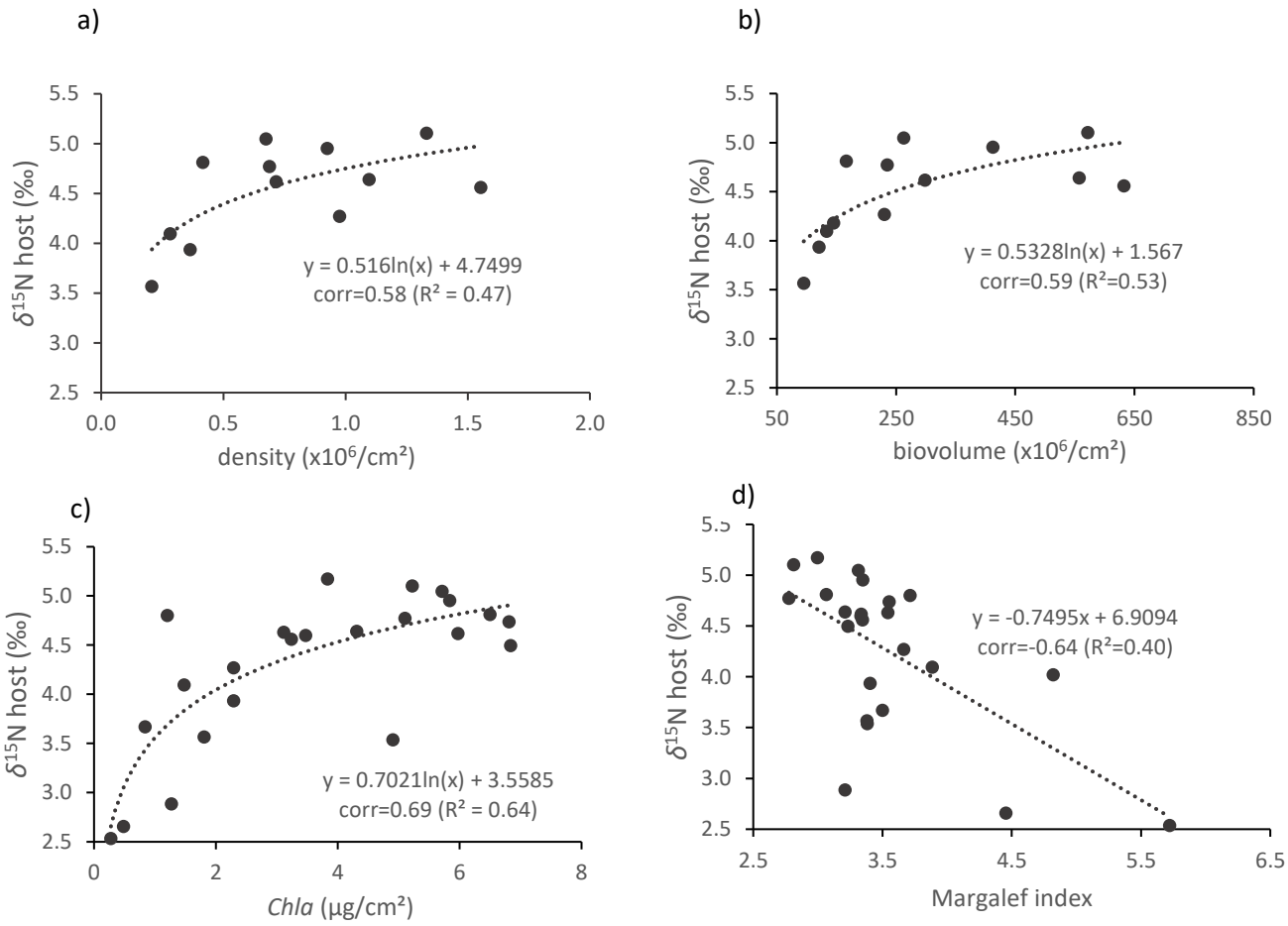

Fig. 11 Significant relationship between δ^{15}N of host and physiological parameters of symbionts: a) density, b) biovolume, c) chlorophyll-*a* and Margalef index in the coral *Mussismilia Braziliensis.*

4. Discussion

Trophic relationships and physiological responses were investigated using a natural field experiment to reveal the interaction of coastal effect on two corals, mainly associated with the clade C *Symbiodinium* (Teshima et al. 2016) (Silva-Lima et al., 2015) but belonging to distinct functional groups. The present study expands the knowledge on holobiont functioning, and potential susceptibilities in the current scenario of coral reefs decline, coastal degradation and climate change. The species *Favia gravida* and *Mussismilia braziliensis* were investigated under two conditions: 1) Unprotected nearshore reefs subjected to higher anthropogenic impacts, higher temperature fluctuations, higher water turbidity and lower seawater pH compared to offshore reefs (Fig. 2; Fig. 3) within the Abrolhos Marine National Park that has contrasting characteristics with the nearshore site.

4.1 Differences in nitrogen between sites

The lack of significant difference regarding total N concentration in both sites corroborated a previous study (Bruce et al. 2012) showing that nitrate concentration in Abrolhos were similarly low between nearshore (0.41±0.0 to 1.22±0.11 µM) and offshore (0.20 ± 0.09 to 0.97±0.04 µM) reefs and *Chla* does not exceed 0.50 $\mu g.L^{-1}$ (Bruce et al., 2012). The authors observed 2 to 3 times more ammonium offshore, but not exceeding 0.28 µM. The low inorganic nitrogen concentrations possibly reflect the highly dynamic pool of bioavailable nitrogen in a limited nitrogen environment (Crandall and Teece, 2012). Most sources (POM, mesozooplankton, microplankton and symbionts) were slightly enriched offshore reefs, suggesting that $\delta^{15}N$ of dissolved inorganic nitrogen was also enriched. The derived detritus from the nearby mangroves may drive the trend of lower $\delta^{15}N$ detected in coastal reefs of Abrolhos (Spano et al., 2014). In addition to that, offshore reefs that have been fully protected for more than 30 years harboring three times higher fish biomass (Bruce et al., 2012) and possibly generated a cascade effect in ^{15}N enrichment along the food web, including phytoplankton, zooplankton and corals. Abundance of mesoplankton (200 µm mesh) was often higher (9am, 7pm and 11pm) offshore. At 11pm, for example, density of mesoplankton yielded 75 times higher biomass than nearshore caused by a copepod aggregation. We also observed higher SPM concentration offshore, despite turbidity levels being approximately two times lower (Fig. 2), indicating SPM offshore was dominated by phytoplankton. Therefore, the snapshot assessment of reefs provided evidence of higher abundance and more enriched ^{15}N food sources availability offshore. An increase in food abundance may increase feeding rates by host (Anthony, 2000), leading to ^{15}N enrichment of tissues (Ferrier-Pagès et al., 2011; Hoogenboom et al., 2015; Nahon et al., 2013). What support this hypothesis is the slow turnover rate of N coupled with higher retention of heterotrophic derived nitrogen, due to high efficiency in nutrient recycling (Tanaka et al., 2018; Tremblay et al., 2015), contrasting to the fast turnover rate of carbon in host and symbionts cells (Fig. 8).

4.2 Differences between species

Larger differences in isotopic composition between symbionts and host can be interpreted as a result of heterotrophic feeding (Hoogenboom et al., 2015; Muscatine and Kaplan, 1994). While differences in $\delta^{13}C_{\text{host-symbiont}}$ showed similar values in both species, the overall differences in $\delta^{15}N_{\text{host-symbiont}}$ were more pronounced in *M. braziliensis* suggesting higher retention of heterotrophic nitrogen sources or either preying items of higher trophic level compared to *F. gravida* (Tremblay et al., 2015). Using these relative

proxy for heterotrophy as proposed by Hoogenboom et al. (2015), heterotrophic nitrogen in *M. braziliensis* was greater than to what has been reported for *Galaxea fascicularis*, *Turbinaria reniformis* and *Stylophora pistillata* in fed experimental conditions (Hoogenboom et al., 2015).

The ^{15}N enrichment (averaging 0.7‰ in *F. gravida* and 1‰ in *M. braziliensis*) in offshore reefs (Fig. 5a) was accompanied by significant physiological changes in symbionts of *M. braziliensis*, but not in *F. gravida* (Fig. 10). Although the two hosts showed relative higher trophic status offshore, it was inferred their symbionts were differently affected by the host nitrogen status. By the differences observed in $\delta^{15}N$ in host and symbionts, it is possible to compare these two corals with plants of different successional stages. With different demand and strategies to use available resources, fast-growing species from early successional stages, such as weedy species (*F. gravida*), are reported to be more efficient in nitrogen acquisition, which allow them to colonize more easily poor nitrogen environments than long-lived and slow-growing ones, typically of late successional stages (Tilman, 1986). As observed in other studies (Alamaru et al., 2009; Hoogenboom et al., 2015; Nahon et al., 2013; Seemann et al., 2013; Susanto et al., 2013), trophic response is expected to be specie-specific since corals can be highly selective heterotrophic feeders (Sorokin 1995). Both species show similar feeding behavior and strategies, as they use tentacles and mucus nets to capture and ingest food, especially at night (Lewis and Price, 1975). Faviids and mussidae have good ability and levels of prey captured compared to diurnal species, such as *Porites astreoides* (Levy et al., 2001; Levy et al., 2006). Despite their similarities, the larger polyps of mussidae may allow them to ingest larger items of higher trophic level, such as small fishes. With lower nitrogen status (Fig. 5a) and reduced number of symbionts (Fig. 10a), *F. gravida* may keep its fast growth rate (0.7 cm^2/year) by active feeding on lower trophic level and small particle sizes, such as dissolved organic matter and mesoplankton (Fig. 8) and from inorganic nitrogen uptake from seawater. Therefore, *F. gravida* may accept broader options of food sources (Fig. 8) as it is widely distributed along the Atlantic Ocean, while *M. braziliensis* is geographically more restricted, which may be associated to its smaller isotopic niche space.

4.3 Differences between host and symbionts

Carbon and nitrogen flux between host and symbionts will likely have different efficiency in exchange and delivery under contrasting environmental conditions, such as temperature (Baker et al., 2018; Hoogenboom et al., 2015; Tanaka et al., 2018). Therefore, the temperature fluctuations may also have an effect on nutrition of *M. braziliensis* (as observed nearshore), which must be further investigated. In the perspective of increasing thermal anomalies, recent attention has been given to the relationship

between trophic status of corals and nutrient acquisition capability (Béraud et al., 2013; Sawall et al., 2011; Tremblay et al., 2015). It has been demonstrated that by elevating the holobiont trophic status through heterotrophy (Borell et al., 2008; Houlbrèque et al., 2003; Hughes and Grottoli, 2013) or by direct uptake of inorganic nitrogen from the seawater (Béraud et al., 2013), corals may increase resilience and better respond to thermal stress since metabolism is maintained. In the specific context of this study, symbionts of *M. braziliensis* were benefitted from offshore reefs by reaching higher nitrogen status, maximum densities, biovolume and *chla* per skeletal surface area and higher productivity (Fig. 11). It is relevant to highlight that maximum symbionts densities in *M. braziliensis* was 1.6 $x10^6/cm^2$, and was interpreted as being positive for the host. The two species were differently affected by the coastal effect, indicating relative susceptibilities according to metabolic strategies. While *M. braziliensis* benefited from protected offshore reefs, symbionts of *F. gravida* was not significantly affected, corroborating the initial hypothesis of higher plasticity, wider isotopic niche, suggesting lower susceptibility to disturbance.

Despite the similarities of increased $\delta^{15}N$ in the two host species offshore, they had clearly different nitrogen status (Fig. 5) as $\delta^{15}N$ of *F. gravida* host was generally lower than 3.5‰ while *M. braziliensis* was typically higher than 3.5‰. The weak and negative relationship between $\delta^{15}N$ host and $\delta^{15}N$ symbionts of *F. gravida* versus contrasted the stronger and positive correlation found within *M. braziliensis* (Table 4; Fig. 8) ($\delta^{15}N$ host > 3.5‰) may suggest nitrogen retention and partitioning work differently in these corals. Because symbionts and host nitrogen status were highly correlated in *M. braziliensis* (Fig. 11), a lower trophic status is expected to have corresponding lower *Chla* content, symbiont size, and symbionts densitities, thus, compromising autotrophic nutrition, which was found to be its main nutritional source of these species. The increasing availability of ^{15}N in host correlated to higher densities of symbionts, biovolume and Chlorophyll *a* (Fig. 11a; Fig. 11b; Fig. 11c) which also suggest decreasing fractionation of $\delta^{15}N$ with increasing symbiont load. In previous studies exploring heterotrophy in a turbid environmental gradient with shallow corals from South Pacific Ocean, Nahon et al. (2013) found high correlation (r= 0.73) between $\delta^{15}N$ of host and $\delta^{15}N$ of symbionts, suggesting high nutrient partitioning within the species studied such as seen for *M. braziliensis*. The weak and negative correlation between $\delta^{15}N$ of symbionts and host in *F. gravida* (Fig 9) possibly suggest symbionts would have an autonomous mode of nitrogen acquisition and storage as the $\delta^{15}N$ of host is low and $C:N_a$ ratio is high. Tanaka et al. (2015) proposed that host with lower nitrogen biomass in their tissues, instead of assessing internal host N pool would switch to assimilate DIN from seawater (Tanaka et al., 2015). Our data suggest there may be a shift in nutrient dynamics (sharing) between symbionts

and host according to the nitrogen status. A possible hypothesis is when $\delta^{15}N$ of host> 3.5‰ (Table 4, Fig. 9), symbionts in *F. gravida* and *M. braziliensis* share the same source of nitrogen with their host, but it may shift it to an alternative source (possibly inorganic sources) below this value.

4.4 Conclusions

Previous studies using natural abundance of isotopes in corals that investigate trophic relationships focused on species from Caribbean, Mediterranean and the Pacific Ocean and this is the first study to report trophic plasticity of Southern Atlantic shallow corals. The few studies reporting natural isotopic abundance of shallow corals (Ferrier-Pagès et al., 2011; Hoogenboom et al., 2015; Nahon et al., 2013; Swart et al., 2005; Ziegler et al., 2014) used fewer number of samples per species and rarely used an ecological functional approach (except Alamaru et al. 2009). Other recent studies concerning trophic relationships are set in laboratory conditions and cannot simulate the natural environment dynamic complexity. Although we measured important parameters to describe and to contrast nearshore and offshore reefs, we could not distinguish what caused the changes in physiological parameters in *M. braziliensis.* Nevertheless, it deserves relevant attention the fact that offshore protected reefs (No take area) may serve as a refugee for *M. braziliensis* providing a healthy and unique environment for this species and, possibly, to other related corals of similar size and ecological requirements, such as the two other mussidae (*M. harttii* and *M. hispida*). The South Western Atlantic region harbors relatively low diversity of scleractinian corals (~18 species) and the three mussidae corals, together with *Montastraea cavernosa,* are the main reef builders in the region (Francini-Filho et al., 2013). Offshore reefs of Abrolhos Marine National Park is officially listed as a priority area for conservation in Brazil and the country is currently expanding its MPA network from 1.5 to 10% of the total Brazilian marine territory by 2020 (MMA, 2018), aiming to accomplish the target established by the Convention on Biological Diversity (CBD, 2010). Abrolhos, as well as most MPAs of the world have limited information of the benefits and impacts of no take areas on coral reefs functioning and physiology (Graham et al., 2011). Impacts of MPAs are generally evaluated by simply measuring the relative change in cover of corals and algae (Francini-Filho et al., 2013; Graham et al., 2011) caused by grazing intensities of herbivores. Therefore, the information provided here may contribute to fill this ecological gap on corals and ecosystem functioning and help decision makers when selecting new areas for protection.

However, the following considerations are important for a wider extrapolation of our results, we propose the need of future experiments that: 1) measure calcification rates to investigate whether reef growth is positively or negatively affected when *Symbiodinium* was benefitted in the magnitude here observed in *M. braziliensis*; 2) test if nitrogen status of host will govern the trophic relationship and the amount of nutrients translocation between the partners using labeled ^{15}N (*in situ)* in both species ; 3) Further investigation of *Symbiodinium* clades within *F. gravida* and *M. brazilienis* colonies.

Acknowledgments:

Carlos E Rezende is a member of Future Earth Coasts. Thanks to Rede Abrolhos for finantial and technical support in the field and the *Laboratório de Ciências Ambientais* of the *Centro de Biociências e Biotecnologia* at the *Universidade Estadual do Norte Fluminense* for the use its infrastructure and financial support from CNPq (305217/2017-8) and FAPERJ (E-26/202.916/2017).

Competing interests

The authors declare no competing or financial interests.

Author contributions

NLO, CER, MALF, MSS, and RLM designed the experiment. NLO, TPR and MA collected data. NLO, CER, MALF, MSS, MGA, BCVO, DQRA, GFS, MA, PSS analyzed samples. NLO, MALF, PSS, IECJ, DMB analyzed data. NLO wrote the paper and all authors contributed to reviewing the paper.

5 References

Alamaru, A., Loya, Y., Brokovich, E., Yam, R. and Shemesh, A. (2009). Carbon and nitrogen utilization in two species of Red Sea corals along a depth gradient: Insights from stable isotope analysis of total organic material and lipids. *Geochim. Cosmochim. Acta* **73**, 5333–5342.

Amaral, F. and Ramos, C. (2007). Skeletal variability of the coral Favia gravida (Verrill , 1868) from Brazil. *Biota Neotrop.* **7**, 245–251.

Anthony, K. R. . (1999). Coral suspension feeding on fine particulate matter. *J. Exp. Mar. Bio. Ecol.* **232**, 85–106.

Anthony, K. R. N. (2000). Enhanced particle-feeding capacity of corals on turbid reefs (Great Barrier Reef, Australia). *Coral Reefs* **19**, 59–67.

Anthony, K. and Fabricius, K. (2000). Shifting roles of heterotrophy and autotrophy in coral energetics under varying turbidity. *J. Exp. Mar. Bio. Ecol.* **252**, 221–253.

Baker, A. C. (2003). Flexibility and specificity in coral-algal symbiosis: diversity, ecology, and biogeography of Symbiodinium. *Annu. Rev. Ecol. Evol. Syst.* **34**, 661–89.

Baker, A. C., Starger, C. J., Mcclanahan, T. R. and Glynn, P. W. (2004). Corals ' adaptive response to climate change. *Nature* **430**, 2004–2004.

Baker, D. M., Andras, J. P., Jordán-Garza, A. G. and Fogel, M. L. (2013). Nitrate competition in a coral symbiosis varies with temperature among Symbiodinium clades. *ISME J.* **7**, 1248–1251.

Baker, D. M., Freeman, C. J., Wong, J. C. Y., Fogel, M. L. and Knowlton, N. (2018). Climate change promotes parasitism in a coral symbiosis. *ISME J.*

Baumann, J., Grottoli, A. G., Hughes, A. D. and Matsui, Y. (2014). Photoautotrophic and heterotrophic carbon in bleached and non-bleached coral lipid acquisition and storage. *J. Exp. Mar. Bio. Ecol.* **461**, 469–478.

Bellwood, D. R., Hughes, T. P., Folke, C. and Nystro, M. (2004). Confronting the coral reef crisis ¨. *Nature* **429**,.

Béraud, E., Gevaert, F., Rottier, C. and Ferrier-Pagès, C. (2013). The response of the scleractinian coral Turbinaria reniformis to thermal stress depends on the nitrogen status of the coral holobiont. *J. Exp. Biol.* **216**, 2665–2674.

Borell, E. M., Yuliantri, A. R., Bischof, K. and Richter, C. (2008). The effect of heterotrophy on photosynthesis and tissue composition of two scleractinian corals under elevated temperature. *J. Exp. Mar. Bio. Ecol.* **364**, 116–123.

Brodie, C. R., Leng, M. J., Casford, J. S. L., Kendrick, C. P., Lloyd, J. M., Yongqiang, Z. and Bird, M. I. (2011). Evidence for bias in C and N concentrations and δ13C composition of terrestrial and aquatic organic materials due to pre-analysis acid preparation methods. *Chem. Geol.* **282**, 67–83.

Bruce, T., Meirelles, P. M., Garcia, G., Paranhos, R., Rezende, C. E., de Moura, R. L., Filho, R.-F., Coni, E. O. C., Vasconcelos, A. T., Amado Filho, G., et al. (2012). Abrolhos bank reef health evaluated by means of water quality, microbial diversity, benthic cover, and fish biomass data. *PLoS One* **7**, e36687.

Bruno, J. F. and Selig, E. R. (2007). Regional Decline of Coral Cover in the Indo-Pacific : Timing , Extent , and Subregional Comparisons. *Methods*.

Bythell, J. C. (1990). Nutrient uptake in the reef-building coral Acropora palmata at natural environmental concentrations. *Mar. Ecol. Prog. Ser.* **68**, 65–69.

Carpenter, K. E., Abrar, M., Aeby, G., Aronson, R. B., Banks, S., Bruckner, A., Chiriboga, A., Cortés, J., Delbeek, J. C., Devantier, L., et al. (2008). One-third of reef-building corals face elevated extinction risk from climate change and local impacts. *Science (80-.).* **321**, 560–3.

Castro, C. B. and Pires, D. O. (2001). Brazilian coral reefs: What we already know and what is still missing. *Bull. Mar. Sci.* **69**, 357–371.

Costa, O. S., Nimmo, M. and Attrill, M. J. (2008). Coastal nutrification in Brazil: A review of the role of nutrient excess on coral reef demise. *J. South Am. Earth Sci.* **25**, 257–270.

Crandall, J. B. and Teece, M. A. (2012). Urea is a dynamic pool of bioavailable nitrogen in coral reefs. *Coral Reefs* **31**, 207–214.

Cunning, R., Vaughan, N., Gillette, P., Capo, T. R., Mate, J. L., Baker, A. C. and Morgan, S. G. (2015). Dynamic regulation of partner abundance mediates response of reef coral symbioses to environmental change. *Ecology* **96**, 1411–1420.

Darling, E. S., Alvarez-Filip, L., Oliver, T. A., McClanahan, T. R. and Côté, I. M. (2012). Evaluating life-history strategies of reef corals from species traits. *Ecol. Lett.* **15**, 1378–86.

Davy, S. K., Allemand, D. and Weis, V. M. (2012). Cell Biology of Cnidarian-Dinoflagellate Symbiosis. *Microbiol. Mol. Biol. Rev.* **76**, 229–261.

den Haan, J., Huisman, J., Brocke, H. J., Goehlich, H., Latijnhouwers, K. R. W., van Heeringen, S., Honcoop, S. A. S., Bleyenberg, T. E., Schouten, S., Cerli, C., et al. (2016). Nitrogen and phosphorus uptake rates of different species from a coral reef community after a nutrient pulse. *Sci. Rep.* **6**, 28821.

Dittmar, T., Koch, B. P., Hertkorn, N. and Kattner, G. (2008). A simple and efficient method for the solid-phase extraction of dissolved organic matter (SPE-DOM) from seawater. *Limnol. Oceanogr.* **6**, 230–235.

Duprey, N. N., Yasuhara, M. and Baker, D. M. (2016). Reefs of tomorrow: eutrophication reduces coral biodiversity in an urbanized seascape. *Glob. Chang. Biol.* **22**, 3550–3565.

Erdoğan, Ş., Yerli, M. B. and Middle (2014). *Phytoplankton counting and identification methods*.

Fagoonee, I., Wilson, H. B., Hassell, M. P. and Turner, J. R. (1999). The dynamics of zooxanthellae populations: a long-term study in the field. *Science (80-.).* **633**, 843–845.

Falkowski, P. G., Dubinsky, Z., Muscatine, L. and Porter, J. W. (1984). Light and the Bioenergetics of a Symbiotic Coral. *BioScienceScience* **34**, 705–709.

Ferrier-Pagès, C., Peirano, A., Abbate, M., Cocito, S., Negri, A., Rottier, C., Riera, P., Rodolfo-Metalpa, R. and Reynaud, S. (2011). Summer autotrophy and winter heterotrophy in the temperate symbiotic coral Cladocora caespitosa. *Limnol. Oceanogr.* **56**, 1429–1438.

Francini-Filho, R. B., Coni, E. O. C., Meirelles, P. M., Amado-Filho, G. M., Thompson, F. L., Pereira-Filho, G. H., Bastos, A. C., Abrantes, D. P., Ferreira, C. M., Gibran, F. Z., et al. (2013). Dynamics of coral reef benthic assemblages of the Abrolhos Bank, Eastern Brazil: inferences on natural and anthropogenic drivers. *PLoS One* **8**, e54260.

Fukami, H., Budd, A. F., Paulay, G., Sole, A., Chen, C. A., Iwao, K. and Knowlton, N. (2004). Conventional taxonomy obscures deep divergence between Pacific and Atlantic corals. *Nature* **427**, 0–3.

Gates, R. D., Hoegh-Guldbergt, O., McFall-Ngai, M. J., Bil, K. Y. and Muscatine, L. (1995). Free amino acids exhibit anthozoan “host factor” activity: They induce the release of photosynthate from symbiotic dinoflagellates in vitro. *Procedings Natl. Acad. Sci.* **92**, 7430–7434.

Gordon, B. R. and Leggat, W. (2010). Symbiodinium - Invertebrate symbioses and the role of metabolomics. *Mar. Drugs* **8**, 2546–2568.

Graham, N. A. J., Ainsworth, T. D., Baird, A. H., Ban, N. C., Bay, L. K., Cinner, J. E., Freitas, D. M. de, Diaz-Pulido, G., Dornelas, M., Dunn, S. R., et al. (2011). From microbes to people: tractable benefits of no-take areas for coral reefs. *Oceanogr. Mar. Biol. An Annu. Rev.* **49**, 105–136.

Grottoli, G., Rodrigues, L. J. and Palardy, J. E. (2006). Heterotrophic plasticity and resilience in bleached corals. *Nature* **440**, 10–13.

Hoegh-Guldberg, O. (1998). Climate Change, coral bleaching and the future of the world' s coral reefs II. *Symbiosis*.

Hoegh-Guldberg, O. (1999). Climate change, coral bleaching and the future of the world's coral reefs. *Mar. Freshw. Res.* **50**, 839–66.

Hoeksema, B. W. (2012). Extreme morphological plasticity enables a free mode of life in Favia gravida at Ascension Island (South Atlantic). *Mar. Biodivers.* **42**, 289–295.

Hoogenboom, M., Rottier, C., Sikorski, S. and Ferrier-page, C. (2015). Among-species variation in the energy budgets of reef-building corals : scaling from coral polyps to communities. *J. Exp. Biol.* **4**, 3866–3877.

Houlbrèque, F. and Ferrier-Pagès, C. (2009). Heterotrophy in tropical scleractinian corals. *Biol. Rev. Camb. Philos. Soc.* **84**, 1–17.

Houlbrèque, F., Tambutté, E. and Ferrier-Pagès, C. (2003). Effect of zooplankton availability on the rates of photosynthesis, and tissue and skeletal growth in the scleractinian coral Stylophora pistillata. *J. Exp. Mar. Bio. Ecol.* **296**, 145–166.

Hughes, T. P. and Connell, J. H. (1999). Multiple stressors on coral reefs: A long-term perspective. *Limnol. Oceanogr.* **44**, 932–940.

Hughes, A. D. and Grottoli, A. G. (2013). Heterotrophic Compensation: A Possible Mechanism for Resilience of Coral Reefs to Global Warming or a Sign of Prolonged Stress? *PLoS One* **8**, e81172.

Hughes, A. D., Grottoli, A. G., Pease, T. K. and Matsui, Y. (2010). Acquisition and assimilation of carbon in non-bleached and bleached corals. *Mar. Ecol. Prog. Ser.* **420**, 91–101.

Hughes, T. P., Kerry, J. T., Baird, A. H., Connolly, S. R., Dietzel, A., Eakin, C. M., Heron, S. F., Hoey, A. S., Hoogenboom, M. O., Liu, G., et al. (2018). Global warming transforms coral reef assemblages. *Nature* 1–5.

Iluz, D. and Dubinsky, Z. (2015). Coral photobiology: new light on old views. *Zoology* **118**, 71–78.

Jackson, A. L., Inger, R., Parnell, A. C. and Bearhop, S. (2011). Comparing isotopic niche widths among

and within communities: SIBER - Stable Isotope Bayesian Ellipses in R. *J. Anim. Ecol.* **80**, 595–602.

Jones, G. P., McCormick, M. I., Srinivasan, M. and Eagle, J. V (2004). Coral decline threatens fish biodiversity in marine reserves. *Proc. Natl. Acad. Sci. U. S. A.* **101**, 8251–3.

Kelmo, F., Attrill, M. J. and Jones, M. B. (2003). Effects of the 1997-1998 El Niño on the cnidarian community of a high turbidity coral reef system (northern Bahia, Brazil). *Coral Reefs* **22**, 541–550.

Kelmo, F., Bell, J. J., Moraes, S. S., Gomes, R. D. C. T., Mariano-Neto, E. and Attrill, M. J. (2014). Differential responses of emergent intertidal coral reef fauna to a large-scale el-niño southern oscillation event: Sponge and coral resilience. *PLoS One* **9**,.

Knowlton, N. (2001). The future of coral reefs. *PNAS* **98**, 5419–5425.

Kopp, C., Pernice, M., Domart-Coulon, I., Djediat, C., Spangenberg, J. E., Alexander, D. T. L., Hignette, M., Meziane, T. and Meibom, A. (2013). Highly dynamic cellular-level response of symbiotic coral to a sudden increase in environmental nitrogen. *MBio* **4**, 1–9.

Layman, C. A., Arrington, D. A., Montan, C. G. and Post, D. M. (2007). Can stable isotope ratios provide for community-wide measures of trphic structure? *Ecology* **88**, 42–48.

Layman, C. A., Araujo, M. S., Boucek, R., Hammerschlag-peyer, C. M., Harrison, E., Jud, Z. R., Matich, P., Rosenblatt, A. E., Vaudo, J. J., Yeager, L. A., et al. (2011). Applying stable isotopes to examine food-web structure : an overview of analytical tools. *Biol. Rev. Camb. Philos. Soc.*

Leal, M. C., Hoadley, K., Pettay, D. T., Grajales, A., Calado, R. and Warner, M. E. (2015). Symbiont type influences trophic plasticity of a model cnidarian-dinoflagellate symbiosis. *J. Exp. Biol.* **218**, 858–863.

Leão, Z. and Kikuchi, R. (2005). A relic coral fauna threatened by global changes and human activities, Eastern Brazil. *Mar. Pollut. Bull.* **51**, 599–611.

Leletkin, V. a. (2000). Trophic status and population density of zooxanthellae in hermatypic corals. *Russ. J. Mar. Biol.* **26**, 231–240.

Levy, O., Mizrahi, L. and Achituv, Y. (2001). Factors controlling the expansion behavior of Favia favus (Cnidaria : Scleractinia): effects of light, flow, and planktonic prey. *Biol. Bull.* **200**, 118–126.

Levy, O., Dubinsky, Z., Achituv, Y. and Erez, J. (2006). Diurnal polyp expansion behavior in stony corals

may enhance carbon availability for symbionts photosynthesis. *J. Exp. Mar. Bio. Ecol.* **333**, 1–11.

Lewis, J. B. and Price, W. S. (1975). Feeding mechanisms and feeding strategies of Atlantic reef corals. *J. Zool.* **176**, 527–544.

Lorrain, A., Houlbrèque, F., Benzoni, F., Barjon, L., Tremblay-Boyer, L., Menkes, C., Gillikin, D. P., Payri, C., Jourdan, H., Boussarie, G., et al. (2017). Seabirds supply nitrogen to reef-building corals on remote Pacific islets. *Sci. Rep.* **7**, 1–11.

Loya, Y., Sakai, K., Yamazato, K., Nakano, Y., Sambali, H. and Van Woesik, R. (2001). Coral bleaching: The winners and the losers. *Ecol. Lett.* **4**, 122–131.

Marsh, J. A. (1970). Primary Productivity of Reef-Building Calcareous Red Algae. *Ecology* **51**, 255–263.

Minagawa, M. and Wada, E. (1984). Stepwise enrichment of 15N along food chains: Further evidence and the relation between δ15N and animal age. *Geochim. Cosmochim. Acta* **48**, 1135–1140.

Moura, R. L. (2000). Brazilian reefs as priority areas for biodiversity conservation in the Atlantic Ocean. *Proc. 9th Int. Coral Reef Symp. Bali, Indones.* **2**,.

Moura, R. L., Amado-Filho, G. M., Moraes, F. C., Brasileiro, P. S., Salomon, P. S., Mahiques, M. M., Bastos, A. C., Almeida, M. G., Silva, J. M., Araujo, B. F., et al. (2016). An extensive reef system at the Amazon River mouth. *Sci. Adv.* **2**, e1501252–e1501252.

Muscatine, L. and Kaplan, I. R. (1994). Resource Partitioning by Reef Corals as Determined from Stable Isotope Composition II. δ l5N of Zooxanthellae and Animal Tissue versus Depth. *Pacific Sci.* **48**, 304–312.

Muscatine, L. and Porter, J. W. (1977). Reef Corals : Mutualistic Symbioses Adapted to Nutrient-Poor Environments. *Bioscience* **27**, 454–460.

Muscatine, L., Falkowski, P. G., Dubinsky, Z., Cook, P. A. and McCloskey, L. R. (1989a). The effect of external nutrient resources on the population dynamics of zooxanthellae in a Reef Coral. *Proc. R. Soc. B Biol. Sci.* **236**, 311–324.

Muscatine, L., Porter, J. W. and Kaplan, I. R. (1989b). Resource partitioning by reef corals as determined from stable isotope composition - I. 13C of zooxanthellae and animal tissue vs depth. *Mar. Biol.* **100**, 185–193.

Nahon, S., Richoux, N. B., Kolasinski, J., Desmalades, M., Ferrier Pages, C., Lecellier, G., Planes, S. and Berteaux Lecellier, V. (2013). Spatial and temporal variations in stable carbon (δ13C) and nitrogen (δ15N) isotopic composition of symbiotic scleractinian corals. *PLoS One*.

Newsome, S. D., Rio, C. M. del, Bearhop, S. and Phillips, D. L. (2007). A niche for isotopic ecology. *Front. Ecol. Environ.* **5**, 429–436.

Nunes, F., Fukami, H., Vollmer, S. V., Norris, R. D. and Knowlton, N. (2008). Re-evaluation of the systematics of the endemic corals of Brazil by molecular data. *Coral Reefs* **27**, 423–432.

Nunes, F. L. D., Norris, R. D. and Knowlton, N. (2011). Long Distance Dispersal and Connectivity in Amphi- Atlantic Corals at Regional and Basin Scales. *PLoS One* **6**, e22298.

Odum, H. T. and Odum, E. P. (1955). Trophic structure and productivity of a windward coral reef community on Eniwetok Atoll. *Ecol. Monogr.* **25**, 291–320.

Parnell, A. and Jackson, A. (2015). Package 'siar': Stable Isotope Analysis in R. *R Found. Stat. Comput. Vienna* 34.

Pernice, M., Meibom, A., Heuvel, A. Van Den, Kopp, C., Domart-coulon, I., Hoegh-guldberg, O. and Dove, S. (2012). A single-cell view of ammonium assimilation in coral – dinoflagellate symbiosis. *Int. Soc. Microb. Ecol.* **6**, 1314–1324.

Pogoreutz, C., Rädecker, N., Cárdenas, A., Gärdes, A., Wild, C. and Voolstra, C. R. (2017). Nitrogen fixation aligns with nifH abundance and expression in two coral trophic functional groups. *Front. Microbiol.* **8**, 1–7.

Porter, J. W. (1976). Autotrophy, heterotrophy and resource partitioning in Caribbean reef-building corals. *Am. Nat.* **110**, 731–742.

Radecker, N., Pogoreutz, C., Voolstra, C. R., Wiedenmann, J. and Wild, C. (2015). Nitrogen cycling in corals : the key to understanding holobiont functioning ? *Trends Microbiol.* **23**, 490–497.

Reynaud, S., Martinez, P., Houlbrèque, F., Billy, I., Allemand, D. and Ferrier-Pagès, C. (2009). Effect of light and feeding on the nitrogen isotopic composition of a zooxanthellate coral: Role of nitrogen recycling. *Mar. Ecol. Prog. Ser.* **392**, 103–110.

Riera, P. (2009). Trophic plasticity in similar habitats: an example which severely limits generalization among ecosystems. *Mar. Biodivers. Rec.* **2**, 1–3.

Sawall, Y., Teichberg, M. C., Seemann, J., Litaay, M., Jompa, J. and Richter, C. (2011). Nutritional status and metabolism of the coral Stylophora subseriata along a eutrophication gradient in Spermonde Archipelago (Indonesia). *Coral Reefs* **30**, 841–853.

Schoener, T. W. (1974). Resource partitioning in ecological communities. *Science (80-.).* **185**, 27–39.

Seemann, J., Berry, K. L., Carballo-Bolaños, R., Struck, U. and Leinfelder, R. R. (2013). The use of 13C and 15N isotope labeling techniques to assess heterotrophy of corals. *J. Exp. Mar. Bio. Ecol.* **442**, 88–95.

Segal, B., Evangelista, H., Kampel, M., Gonçalves, A. C., Polito, P. S. and dos Santos, E. A. (2008). Potential impacts of polar fronts on sedimentation processes at Abrolhos coral reef (South-West Atlantic Ocean/Brazil). *Cont. Shelf Res.* **28**, 533–544.

Silva-Lima, A. W., Walter, J. M., Garcia, G. D., Ramires, N., Ank, G., Meirelles, P. M., Nobrega, A. F., Siva-Neto, I. D., Moura, R. L., Salomon, P. S., et al. (2015). Multiple Symbiodinium strains are hosted by the Brazilian endemic corals Mussismilia spp. *Microb. Ecol.* **70**, 301–310.

Silva, a. S., Leão, Z. M. a. N., Kikuchi, R. K. P., Costa, a. B. and Souza, J. R. B. (2013). Sedimentation in the coastal reefs of Abrolhos over the last decades. *Cont. Shelf Res.* **70**, 159–167.

Sorokin, Y. I. (1973). On the feeding of some scleractinian coral with bacteria and dissolved organic matter. *Limnol. Oceanogr.* **18**, 380–385.

Spano, S., Belem, A. L., Doria, R. N., Zucchi, M. do R., Souza, J. R. B. de, Costa, A. B., Lentini, C. A. D. and Azevedo, A. E. G. de (2014). Application of organic carbon and nitrogen stable isotope and C/N ratios as source indicators of organic matter of Nova Viçosa-Caravelas estuarine complex, southern Bahia, Brazil. *Brazilian J. Geol.* **44**, 13–21.

Stambler, N., Popper, N., Dubinsky, Z. and Stimson, J. S. (1991). Effects of nutrient enrichment and water motion on the coral Pocillopora damicornis. *Pacific Sci.* **45**, 299–307.

Susanto, H. A., Komoda, M., Yoneda, M., Kano, A., Tokeshi, M. and Koike, H. (2013). A Stable isotope study of the relationship between coral tissues and zooxanthellae in a seasonal tropical environment of East Kalimantan, Indonesia. *Int. J. Mar. Sci.* **3**, 285–294.

Swart, P. K., Saied, A. and Lamb, K. (2005). Temporal and spatial variation in the d15N and d13C of coral tissue and zooxanthellae in Montastraea faveolata collected from the Florida reef tract.

Limnol. Oceanogr. **50**, 1049–1058.

Tanaka, Y., Grottoli, A. G., Matsui, Y., Suzuki, A. and Sakai, K. (2015). Partitioning of nitrogen sources to algal endosymbionts of corals with long-term 15N-labelling and a mixing model. *Ecol. Modell.* **309**–**310**, 163–169.

Tanaka, Y., Suzuki, A. and Sakai, K. (2018). The stoichiometry of coral-dinoflagellate symbiosis: carbon and nitrogen cycles are balanced in the recycling and double translocation system. *ISME J.* 1–9.

Tilman, D. (1986). Nitrogen-limited growth in plants from different succesional stages. *Ecology* **67**, 555–563.

Titlyanov, E. A. and Titlyanova, T. V. (2002). Reef-building corals - Symbiotic autotrophic organisms: 1. General structure, feeding pattern, and light-dependent distribution in the shelf. *Russ. J. Mar. Biol.* **28**,.

Tremblay, P., Grover, R., Maguer, J. F., Legendre, L. and Ferrier-Pagès, C. (2012). Autotrophic carbon budget in coral tissue: a new 13C-based model of photosynthate translocation. *J. Exp. Biol.* **215**, 1384–93.

Tremblay, P., Grover, R., Maguer, J. F., Hoogenboom, M. and Ferrier-Pagès, C. (2014). Carbon translocation from symbiont to host depends on irradiance and food availability in the tropical coral Stylophora pistillata. *Coral Reefs* **33**, 1–13.

Tremblay, P., Maguer, J. F., Grover, R. and Ferrier-Pages, C. (2015). Trophic dynamics of scleractinian corals: A stable isotope evidence. *J. Exp. Biol.* 1223–1234.

Tremblay, P., Gori, A., Maguer, J. F., Hoogenboom, M. and Ferrier-Pagès, C. (2016). Heterotrophy promotes the re-establishment of photosynthate translocation in a symbiotic coral after heat stress. *Sci. Rep.* **6**, 1–14.

Turner, T. F., Collyer, M. L. and J, K. T. (2010). A general hypothesis-testing framework for stable isotope ratios in ecological studies. *Ecology* **91**, 2227–2233.

van Woesik, R., Sakai, K., Ganase, A. and Loya, Y. (2011). Revisiting the winners and the losers a decade after coral bleaching. *Mar. Ecol. Prog. Ser.* **434**, 67–76.

Veal, C. J., Holmes, G., Nunez, M., Hoegh-Guldberg, O. and Osborn, J. (2010). A comparative study of methods for surface area and three-dimensional shape measurement of coral skeletons. *Limnol.*

Oceanogr. Methods **8**, 241–253.

Warton, D. I. and Hui, F. K. C. (2011). The arcsine is asinine: the analysis of proportions in ecology. *Ecology* **92**, 3–10.

Wooldridge, S. A. (2014). Differential thermal bleaching susceptibilities amongst coral taxa : re-posing the role of the host. *Coral Reefs* **33**, 15–27.

Wooldridge, S. A. (2016). Excess seawater nutrients, enlarged algal symbiont densities and bleaching sensitive reef locations: 1. Identifying thresholds of concern for the Great Barrier Reef, Australia. *Mar. Pollut. Bull.* 1–8.

Ziegler, M., Roder, C. M., Büchel, C. and Voolstra, C. R. (2014). Limits to physiological plasticity of the coral Pocillopora verrucosa from the central Red Sea. *Coral Reefs* **33**, 1115–1129.

Ziegler, M., Roder, C., Bchel, C. and Voolstra, C. R. (2015). Niche acclimatization in Red Sea corals is dependent on flexibility of host-symbiont association. *Mar. Ecol. Prog. Ser.* **533**, 149–161.

Zoffoli, M. L., Kampel, M. and Frouin, R. (2013). Temporal characterization of the diffuse attenuation coefficient in Abrolhos Coral Reef Bank, Brazil. *An. XVI Simpósio Bras. Sensoriamento Remoto - SBSR, Foz do Iguaçu, PR, Bras.*

6 Supplementary material

6.1 Figures

a) Favia gravida

b) Mussismilia braziliensis

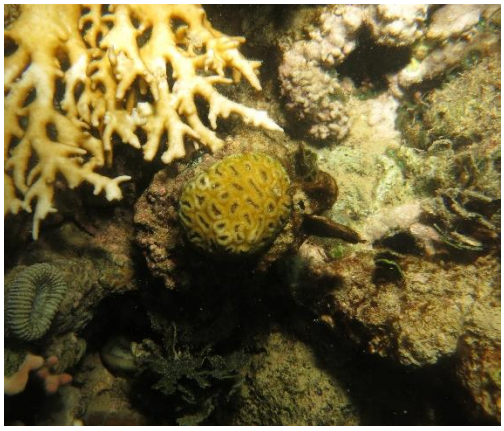

c) Favia gravida

d) Mussismilia braziliensis

e) Tissue removal

f) Mussismilia braziliensis and Favia gravida

g) Tissue removal

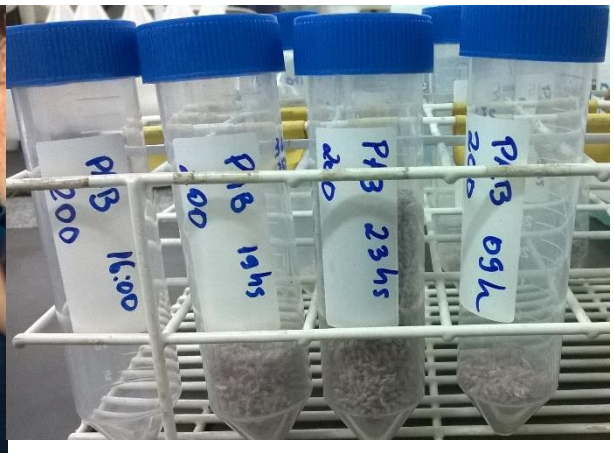

h) Zooplankton biomass

Fig.1S Colonies of *Favia gravida* and *Mussismilia braziliensis* in Abrolhos (a,b,c,d,) ;Tissue removal for isotopic and physiological analyses (e,f,g,); dried biomass of zooplankton (h)

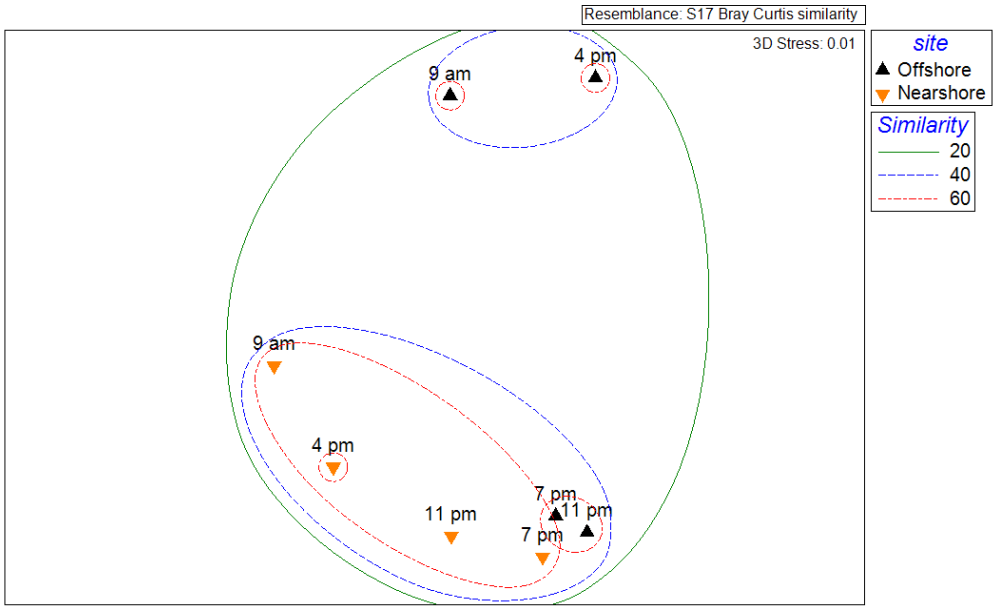

Fig. 2S Ordination of the non-Metric Multidimensional Scaling based on the Bray-Curtis distance matrix representing zooplankton communities from nearshore and offshore reefs at different hours of the day (9 am, 4 pm, 7 pm, 11 pm)

6.2 Tables

Table 1S Water parameters on nearshore and offshore reefs and results from Welch's t-test. Significant differences ($p < 0.05$) are shown in bold; N = number of samples.

		Mean nearshore	Mean offshore	t-value	df	p	N nearshore	N offshore
water parameters	**pH**	**7.51**	**8.26**	**10.63**	**6.1**	**0.000**	6	4
	Turbidity (NTU)	**3.89**	**2.47**	**-15.16**	**7.1**	**0.000**	6	4
	SPM (mg/L)	6.00	9.55	-2.40	4.3	0.071	6	4
	DOC (mg/L)	2.67	2.11	1.61	7.6	0.149	6	4
	TDN (mg/L)	0.31	0.24	0.60	7.8	0.570	6	4

Table 2S Two-Factorial ANOVA results showing differences in biogeochemical parameters of host and symbiont between sites (nearshore and offshore reefs) and species (*Favia gravida* and *Mussismilia braziliensis*). Significant differences ($p < 0.05$) are shown in bold.

Source of variation	*df*	MS	F	p-value	p
$\delta^{15}N_{symbiont}$					
ssp	**1**	**0.84**	**6.54**	**0.014**	*
site	1	0.46	3.59	0.063	ns
ssp*site	**1**	**1.69**	**13.16**	**0.000**	***
Residuals	52	0.12			
$\delta^{15}N_{host\ tissue}$					
ssp	**1**	**34.43**	**115.87**	**0.000**	***
site	**1**	**9.74**	**32.78**	**0.002**	**
ssp*site	1	0.19	0.64	0.237	ns
Residuals	52	0.30			
$\delta^{15}N_{host\text{-}symbiont}$					
ssp	**1**	**0.60**	**44.32**	**0.000**	***
site	1	0.01	0.52	0.470	ns
ssp*site	1	0.00	0.02	0.890	ns
Residuals	52	0.01			
$\delta^{13}C_{symbiont}$					
ssp	**1**	**0.04**	**30.84**	**0.000**	***
site	1	0.00	1.97	0.167	ns
ssp*site	1	0.00	0.89	0.351	ns
Residuals	46	0.00			
$\delta^{13}C_{host\ tissue}$					
ssp	**1**	**0.03**	**52.45**	**0.000**	***
site	1	0.00	0.02	0.896	ns
ssp*site	1	0.00	2.38	0.129	ns
Residuals	53	0.00			
$\delta^{13}C_{host\text{-}symbiont}$					

ssp	1	1.19	0.76	0.387	ns
site	1	2.38	1.53	0.220	ns
ssp*site	1	0.41	0.26	0.610	ns
Residuals	45	1.56			
$C:N_{a\ symbiont}$					
ssp	**1**	**65.85**	**28.64**	**0.000**	***
site	1	0.61	0.26	0.611	ns
ssp*site	**1**	**10.87**	**4.73**	**0.035**	*
Residuals	44				
$C:N_{a\ host\ tissue}$					
ssp	1	0.14	0.07	0.788	ns
site	1	0.37	0.19	0.667	ns
ssp*site	1	0.68	0.35	0.558	ns
Residuals	53	1.96			
$C:N_{a\ host\text{-}symbiont}$					
ssp	**1**	**76.78**	**21.63**	**0.000**	***
site	1	3.39	0.96	0.333	ns
ssp*site	**1**	**18.86**	**5.31**	**0.026**	*
Residuals	44				

Table 3S Two-Factorial ANOVA results showing differences in physiological parameters between sites (nearshore and offshore reefs) and species (*Favia gravida* and *Mussismilia braziliensis*). Significant differences ($p < 0.05$) are shown in bold.

Source of variation	*df*	MS	F	p-value	p
Density/cm²					
ssp	**1**	**1.08**	**33.88**	**0.000**	***
site	1	0.06	1.95	0.177	ns
ssp*site	**1**	**0.43**	**13.37**	**0.001**	**
Residuals	21	0.03			
Biovolume/cm²					
ssp	**1**	**0.86**	**32.58**	**0.000**	***
site	1	0.08	3.20	0.088	ns
ssp*site	**1**	**0.53**	**19.97**	**0.000**	***
Residuals	21	0.03			
Biovolume/cell					
ssp	1	285.91	0.17	0.687	ns
site	1	720.36	0.42	0.523	ns
ssp*site	1	957.42	0.56	0.462	ns
Residuals	26	1718.72			
Chl a/cm²					
ssp	1	1.08	0.63	0.430	ns
site	**1**	**36.37**	**21.35**	**0.000**	***
ssp*site	**1**	**29.26**	**17.18**	**0.000**	***
Residuals	31	1.70			
Chl a/cell					
ssp	**1**	**12.52**	**30.95**	**0.000**	***
site	1	0.53	1.32	0.250	ns

ssp*site	1	0.04	0.09	0.760	ns
Residuals	19	0.40			
Margalef index					
ssp	1	0.72	2.43	0.130	ns
site	**1**	**4.14**	**13.89**	**0.001**	***
ssp*site	1	0.11	0.35	0.556	ns
Residuals	31	0.30			
FL3 H					
ssp	1	0.4 $x10^{10}$	0.15	0.700	ns
site	1	1.8 $x10^{10}$	0.71	0.410	ns
ssp*site	1	1.9$x10^{10}$	0.75	0.390	ns
Residuals	27	2.5 $x10^{10}$			
CV FL3 H					
ssp	**1**	**0.06**	**5.12**	**0.031**	*
site	1	0.04	3.74	0.063	ns
ssp*site	1	0.00	0.28	0.599	ns
Residuals	27	0.01			
CV FSC H					
ssp	**1**	**0.75**	**9.10**	**0.005**	**
site	1	0.00	0.00	0.960	ns
ssp*site	1	0.00	0.05	0.830	ns
Residuals	27				

6.3 Stable isotopes ($\delta^{13}C$ and $\delta^{15}N$) of Symbiodinium in culture

In addition to field measurements, we investigated the isotopic composition ($\delta^{15}N$ and $\delta^{13}C$) and C:N ratio of cultured *Symbiodinium* strain 043D10 (clade D), lineage A4 (ITS2), isolated from *Mussismilia braziliensis* aiming to have a reference for free living *Symbiodinium* in different growth stages of

population. Culture was grown in sterile F/2 medium under the conditions 100 µE/m^2/s; 14 light/10 dark at 24±1 °C. Growth was monitored every two days by counting Symbiodinium cells using microscope and bacteria load. Samples for isotopes analyses were taken at culture 1, culture 2 and matrix: 1) exponential phase (after ca. 1 week of the inoculum); and 2) Stationary phase (ca. 3-4 weeks after inoculum). *Symbiodinium* counts were conducted every two days using a microscope, after fixing samples in formalin (20%). To determine the bacterial load 1.5mL sample were fixed in glutaraldehyde (1%) fixed cryotubes for 10 min at room temperature in the dark, frozen in liquid nitrogen and kept at -80°C. Bacterial counts were performed using the cytometer after coloring samples with SYBR™ green. For isotope samples, 50-100 mL of *Symbiodinium* in culture were filtered on precombusted (350°C/4h) and pre-weighed GF/C filters (Whatman, nominal pore size 1.2 µm) in triplicate and rinsed with 10 mL of MilliQ water to remove salt and excess bacteria.

The isotopic composition of free living *Symbiodinium* (type A4 from *M. braziliensis*) in culture showed values ranging from -20 to -22‰ for δ^{13}C, 1.8 to 9.2‰ for δ^{15}N, 7:1 to 16:1 for C:N ratio according to the time after inoculation development stage of the culture (Table 4S). In free living *Symbiodinium* cells, values of δ^{13}C was closer to phytoplankton references (Manuscript 2) compared to symbionts in coral host tissue, as inorganic carbon fractionation in culture was not mediated by the host. Symbionts were most enriched in ^{15}N in the *Symbiodinium* matrix stationary phase, showing the same isotopic composition of nitrate source (δ^{15}N= 9.2%) after 52 days of inoculation. Although hosting the highest load of bacterial material (623x10^5) higher enrichment by nitrogen cycling in the matrix was not observed.

Table 4S References and variation in the elemental and natural abundance of isotope in free living *Symbiodinium* clade D cells in culture according to time after inoculation, cell densities and bacterial load.

Sample/growth phase	**Time after inoculation (days)**	***Symbiodinium* density (cell/mL)**	**Bacterial load (events/mL)**	**C (%)**	**δ^{13}C (‰)**	**N (%)**	**δ^{15}N (‰)**	**C:N**
Culture 1/ late exponential	10	9x10^3	55x10^5	6.96	-22.2	0.51	3.0	16
Culture 1/ stationary	20	7x10^3	71x10^5	15.2	-22.3	1.09	1.8	16
Culture 2	0	24x10^3	75x10^5	29.9	-20.0	3.49	7.2	10
Culture 2/ stationary	7	33x10^3	130x10^5	20.6	-20.3	3.42	7.4	7
Matrix/ stationary	52	143x10^3	623x10^5	24.0	-20.2	3.39	9.2	8
Matrix/ stationary	56	223x10^3	430x10^5	16.8	-20.2	2.59	9.2	8
Nutrient $NaNO_3$				-	-	16.01	9.2	-

Chapter 4

Conclusions

1 *Implications for Biodiversity Conservation*

This is the first study to address resource partitioning and nutritional status of shallow corals from South Western Atlantic under natural conditions. Corals closer to the coast of Abrolhos are subjected to a higher degree of environmental disturbance, such as temperature variability, turbidity levels, and to a higher degree of anthropogenic impacts. The interaction of anthropogenic local impacts observed in Abrolhos, such as lower fish biomass (FRANCINI-FILHO et al., 2013), can drive changes in different levels of the ecosystem and other subsequent disturbances, such as higher microalgae cover. However, finding appropriate response variables to measure the effect of fisheries management on corals is typically challenging because ecological cascades processes are attenuated from one trophic level to another (STENECK et al., 2018). Past studies demonstrated when significant differences are observed in benthic cover, at the community level, a completely phase shift to algal-dominated state may have been already taken over, and will probably be late to take action to recover the system (ARONSON et al., 2004; BELLWOOD et al., 2004; BRUNO et al., 2009; HUGHES, 1994). For coral reef managers, the coral response is most important to be observed before they decline. Thus, at the physiological level, corals may offer efficient clues to evaluate small changes in ecosystem health in areas subjected to different fisheries management measures.

The study provided feedback information of 35 years' efforts protecting offshore reefs from fishing in the Abrolhos Marine National Park. Based on a 15 years monitoring program of fish abundance, protected reefs offshore it is estimated to have ~3 times higher biomass. The observation of nutritional sources, environmental conditions and metabolic and physiological aspects of corals allowed a holistic understanding of the effect from contrasting areas in Abrolhos. The results highlight that nutrition (given by nitrogen status and symbionts parameters) of *Mussismilia braziliensis* was favored in offshore reefs (where fishing is banned and anthropogenic impacts are lower). Our sampling effort was sufficient for a snapshot assessment of the nitrogen (^{15}N) enrichment in the potential resource (nutritional sources: POM, plankton and symbiont), and corals (consumers), the latter reflecting the sources assimilated ~3 weeks earlier.

It is important to note that coralline reefs of South Western Atlantic (SWA) are represented by a small number (~18) of highly endemic (> 50%) species (with respect to the Pacific and Caribbean). Some of them are widely distributed in the Atlantic Ocean, such as *F. gravida,* recently registered in extreme conditions off the Amazon River mouth) (see Attachments), showing to adapt to high turbidity levels and low light conditions (MOURA et al., 2016). However, other species, such as, *Mussismilia braziliensis* has a narrower distribution, limited to the coast of Bahia State (Brazil). Trophic plasticity was species specific: the broader geographically distributed *F. gravida* was accompanied by broader isotopic niche and higher trophic plasticity in the scale of 50 Km. The endemic and more geographically restricted species *M. braziliensis* showed lower trophic plasticity compared to *F. gravida*, given by its isotopic niche width and by the significant changes observed in symbionts populations between nearshore and offshore reefs. The endemic *M. braziliensis* presented higher contribution from symbionts in its nutrition, in relation to the weedy coral *Favia gravida*. Recent research using fatty acids profiles concludes *Mussismilia hispida* is also highly autotrophic (Tenório, 2016).

Although we must interpret SIAR model results with caution as they were built based on heterotrophy pathway (here adapted for mixotrophic corals), we suggest that groups of corals with similar nutritional strategies to *M. braziliensis* tend to be more susceptible to coastal disturbances (e.g. high temperature fluctuation) than groups of corals similar to *F. gravida.* The latter show higher trophic

plasticity, feed on wider variety of sources of particles, while keeping physiological parameters of symbionts stable. The low nitrogen internal pool of *F. gravida* may force symbionts to assimilate DIN from seawater suggesting lower exchange with the host. Future researches can further explore the potential and limitation of these two species of distinct isotopic niche.

Both species inhabit similar depth and location on the reefs of Abrolhos, adopt the same feeding strategies / mechanism, and are morphologically and genetically related (NUNES et al., 2008). However, the study suggests they belong to distinct trophic groups, differing in nitrogen requirements, and possibly differing in exchange and retention between fractions. Tanaka et al. (2015) argue that a larger N pool in the coral tissue play an important role in supporting symbiont's function, photosynthesis (as also observed in our data), and consequent coral reef growth. In fact, the nitrogen status seem to be the driver of *Symbiodinium* population in *M. braziliensis* but this characteristics may also turn them more vulnerable in case of being affected by bleaching events.

Temperature showed greater fluctuations nearshore where 28°C was often reached (Fig. 2). When the water temperature exceeds 28 ° C for a certain period of time (one to two weeks) the disruption of coral symbiosis (as observed in 2016 for *M. braziliensis* in Abrolhos). Given the higher bleaching probability of *M. braziliensis* nearshore, we propose this species is more vulnerable when in coastal areas. The results bring new arguments to support the selection of future Marine Protected Areas towards offshore reefs rather than nearshore reefs. The combined results of multiple variables (chlorophyll, symbionts' density, stable isotopes, C:N atomic ratio), assessed with different methods strengthen reliability of the results. The effect of site influenced potential nutritional sources, but differences between sites were amplified in the compartments of coral tissue.

In addition, the parameters measured revealed when *Mussismilia braziliensis* became more ^{15}N enriched in offshore reefs, the population of endosymbionts was significant enlarged. With higher densities of symbionts offshore, the relative proportion of autotrophy was increased. Ultimately, the increase assimilation of carbon and nitrogen (HEIKOOP et al., 1998) offshore will produce skeleton more rapidly, and will provide higher contribution to reef growth (DUBINSKY; STAMBLER, 2011).

References

ALVAREZ-FILIP, L. et al. Flattening of Caribbean coral reefs : region-wide declines in architectural complexity. **Proceedings of The Royal Society/Biological sciences**, p. 1–7, 2009.

ANTHONY, K. Enhanced energy status of corals on coastal, high-turbidity reefs. **Marine Ecology Progress Series**, v. 319, p. 111–116, 18 ago. 2006.

ANTHONY, K.; FABRICIUS, K. Shifting roles of heterotrophy and autotrophy in coral energetics under varying turbidity. **Journal of Experimental Marine Biology and Ecology**, v. 252, n. 2, p. 221–253, 20 set. 2000.

ANTHONY, K. R. . Coral suspension feeding on fine particulate matter. **Journal of Experimental Marine Biology and Ecology**, v. 232, n. 1, p. 85–106, jan. 1999.

ARONSON, R. B. et al. Phase shifts, alternative states, and the unprecedented convergence of two reef systems. **Ecology**, v. 85, n. 7, p. 1876–1891, 2004.

BAKER, A. C.; GLYNN, P. W.; RIEGL, B. Climate change and coral reef bleaching: An ecological assessment of long-term impacts, recovery trends and future outlook. **Estuarine, Coastal and Shelf Science**, v. 80, n. 4, p. 435–471, dez. 2008.

BELLWOOD, D. et al. Confronting the coral reef crisis ¨. **Nature**, v. 429, n. June, p. 827–833, 2004.

BROWN, B. E. Disturbances to Reefs in Recent Times. p. 1–24, 1997.

BROWNE, N. K. Spatial and temporal variations in coral growth on an inshore turbid reef subjected to multiple disturbances. **Marine environmental research**, v. 77, p. 71–83, jun. 2012.

BRUCE, T. et al. Abrolhos bank reef health evaluated by means of water quality, microbial diversity, benthic cover, and fish biomass data. **PloS one**, v. 7, n. 6, p. e36687, jan. 2012.

BRUNO, J. F. et al. Assessing evidence of phase shifts from coral to macroalgal dominance on coral reefs. **Ecology**, v. 90, n. 6, p. 1478–1484, 2009.

CHISHOLM, B. S.; NELSON, D. E.; SCHWARCZ, H. P. Stable-carbon isotope ratios as a measure of marine versus terrestrial protein in ancient diets. **Science (New York, N.Y.)**, v. 216, n. 4550, p. 1131–2, 4 jun. 1982.

CONNELL, J. H. Diversity in Tropical Rain Forests and Coral Reefs. **Science**, v. 199, n. 4335, p. 1302–1310, 2008.

COSTA, O. S.; NIMMO, M.; ATTRILL, M. J. Coastal nutrification in Brazil: A review of the role of nutrient excess on coral reef demise. **Journal of South American Earth Sciences**, v. 25, n. 2, p. 257–270, mar. 2008.

COSTANZA, R. et al. Changes in the global value of ecosystem services. **Global Environmental Change**, v. 26, n. 1, p. 152–158, 2014.

DAVY, S. K.; ALLEMAND, D.; WEIS, V. M. Cell Biology of Cnidarian-Dinoflagellate Symbiosis. **Microbiology and Molecular Biology Reviews**, v. 76, n. 2, p. 229–261, 2012.

DUBINSKY, Z.; STAMBLER, N. **Coral Reefs: An Ecosystem in Transition**. [s.l: s.n.].

ESTES, J. A. et al. Trophic Downgrading of Planet Earth. **Science**, v. 333, n. 6040, p. 301–306, 14 jul. 2011.

FERRIER-PAGÈS, C. et al. Microheterotrophy in the zooxanthellate coral Stylophora pistillata: efects of light and ciliate density. **Limnology and Oceanography**, v. 43, n. 7, p. 1639–1648, 1998.

FERRIER-PAGÈS, C. et al. Summer autotrophy and winter heterotrophy in the temperate symbiotic coral Cladocora caespitosa. **Limnology and Oceanography**, v. 56, n. 4, p. 1429–1438, 2011.

FERRIER-PAGÈS, C.; SAUZÉAT, L.; BALTER, V. Coral bleaching is linked to the capacity of the animal host to supply essential metals to the symbionts. **Global Change Biology**, p. 0–2, 2018.

FRANCINI-FILHO, R. B. et al. Dynamics of coral reef benthic assemblages of the Abrolhos Bank, Eastern Brazil: inferences on natural and anthropogenic drivers. **PLoS ONE**, v. 8, n. 1, p. e54260, 24 jan. 2013.

FRY, B.; BRAND, W. Automated Analysis System for Coupled d13C and d15N Measurements. **Analytical Chemistry**, v. 64, p. 288–291, 1992.

FRY, B.; DAVIS, J. Rescaling stable isotope data for standardized evaluations of food webs and species niches. **Marine Ecology Progress Series**, v. 528, n. Phillips 2012, p. 7–17, 2015.

GARDNER, T. A. et al. Long-term region-wide declines in Caribbean corals. **Science**, v. 301, n. 5635, p. 958–960, 2003.

GOREAU, T. F.; GOREAU, N. I.; YONGE, C. M. Reef corals: autotrophs or heterotrophs? **Biological Bulletin**, v. 141, p. 247–260, 1971.

GROTTOLI, A. G.; WELLINGTON, G. M. Effect of light and zooplankton on skeletal δ13C values in the

eastern Pacific corals Pavona clavus and Pavona gigantea. **Coral Reefs**, v. 18, p. 29–41, 1999.

GROTTOLI, G.; RODRIGUES, L. J.; PALARDY, J. E. Heterotrophic plasticity and resilience in bleached corals. **Nature**, v. 440, n. April, p. 10–13, 2006.

HARTMANN, A. C. et al. Stable isotopic records of bleaching and endolithic algae blooms in the skeleton of the boulder forming coral Montastraea faveolata. **Coral Reefs**, v. 29, p. 1079–1089, 2010.

HEIKOOP, J. M. et al. Relationship between light and delta 15N of coral tissue: Examples from Jamaica and Zanzibar. **Limnology and Oceanography**, v. 43, n. 5, p. 909–920, 1998.

HOEGH-GULDBERG, O. Climate change, coral bleaching and the future of the world's coral reefs. **Marine Freshwater Research**, v. 50, p. 839–66, 1999.

HOEGH-GULDBERG, O.; BRUNO, J. F. The impact of climate change on the world's marine ecosystems. **Science (New York, N.Y.)**, v. 328, n. 5985, p. 1523–8, 18 jun. 2010.

HOOGENBOOM, M. O. et al. Effects of Light , Food Availability and Temperature Stress on the Function of Photosystem II and Photosystem I of Coral Symbionts. **PLoS biology**, v. 7, n. 1, p. e30167, 2012.

HOULBRÈQUE, F.; FERRIER-PAGÈS, C. Heterotrophy in tropical scleractinian corals. **Biological reviews of the Cambridge Philosophical Society**, v. 84, n. 1, p. 1–17, fev. 2009.

HUGHES, A. D.; GROTTOLI, A. G. Heterotrophic Compensation: A Possible Mechanism for Resilience of Coral Reefs to Global Warming or a Sign of Prolonged Stress? **PLoS ONE**, v. 8, n. 11, p. e81172, 21 nov. 2013.

HUGHES, T. P. Community structure and diversity of coral reefs : The role of history. **Ecology**, v. 70, n. 1, p. 275–279, 1989.

HUGHES, T. P. Catastrophes, phase shifts , and large-scale degradation of a Caribbean coral reef. **Science**, v. 265, n. September 1994, p. 1547–1551, 1994.

HUGHES, T. P. et al. Climate Change, human impacts , and the resilience of coral reefs. **Science**, v. 301, n. August, p. 929–933, 2003.

HUGHES, T. P. et al. Phase shifts, herbivory, and the resilience of coral reefs to climate change. **Current Biology**, v. 17, n. 4, p. 360–365, 2007.

HUGHES, T. P. et al. Global warming and recurrent mass bleaching of corals. **Nature**, v. 543, n. 7645, p. 373–377, 2017.

HUGHES, T. P. et al. Spatial and temporal patterns of mass bleaching of corals in the Anthropocene. **Science**, v. 359, n. 6371, p. 80–83, 2018a.

HUGHES, T. P. et al. Global warming transforms coral reef assemblages. **Nature**, p. 1–5, 2018b.

HUGHES, T. P.; CONNELL, J. H. Multiple stressors on coral reefs: A long-term perspective. **Limnology and Oceanography**, v. 44, n. 3_part_2, p. 932–940, 1999.

ILUZ, D.; DUBINSKY, Z. Coral photobiology: new light on old views. **Zoology**, v. 118, n. 2, p. 71–78, 2015.

JACKSON, A. L. et al. Comparing isotopic niche widths among and within communities: SIBER - Stable Isotope Bayesian Ellipses in R. **Journal of Animal Ecology**, v. 80, n. 3, p. 595–602, 2011.

JOMPA, J.; MCCOOK, L. J. The effects of nutrients and herbivory on competition between a hard coral (Porites cylindrica) and a brown alga (Lobophora variegata). **Limnology and Oceanography**, v. 47, n. 2, p. 527–534, 2002.

LAYMAN, C. A. et al. Can stable isotope ratios provide for community-wide measures of trphic structure? **Ecology**, v. 88, n. 1, p. 42–48, 2007.

LAYMAN, C. A. et al. Applying stable isotopes to examine food-web structure : an overview of analytical tools. **Biological reviews of the Cambridge Philosophical Society**, 2011.

LEWIS, J. B.; PRICE, W. S. Feeding mechanisms and feeding strategies of Atlantic reef corals. **Journal of Zoology (London)**, v. 176, p. 527–544, 1975.

MILLS, M. M.; LIPSCHULTZ, Æ. F.; SEBENS, K. P. Particulate matter ingestion and associated nitrogen uptake by four species of scleractinian corals. **Coral Reefs**, v. 23, p. 311–323, 2004.

MINAGAWA, M.; WADA, E. Stepwise enrichment of 15N along food chains: Further evidence and the relation between δ15N and animal age. **Geochimica et Cosmochimica Acta**, v. 48, n. 5, p. 1135–1140, 1984.

MINDELL, D. P. Phylogenetic consequences of symbioses: Eukarya and eubacteria are not monophyletic taxa. **BioSystems**, v. 27, n. 1, p. 53–62, 1992.

MOURA, R. L. Brazilian reefs as priority areas for biodiversity conservation in the Atlantic Ocean. **Proceedings 9th International Coral Reef Symposium- Bali, Indonesia**, v. 2, n. October, 2000.

MOURA, R. L. et al. An extensive reef system at the Amazon River mouth. **Science Advances**, v. 2, n. 4, p. e1501252–e1501252, 2016.

MUSCATINE, L. The role of symbiotic algae in carbon and energy flux in reef corals. **Coral Reefs**, v. 25, p. 1–29, 1990.

MUSCATINE, L.; CERNICHIARI, E. Assimilation of photosynthetic products of zooxathellae by a reef coral. **The Biological Bulletin**, v. 137, p. 506–523, 1969a.

MUSCATINE, L.; CERNICHIARI, E. Assimilation of photosynthetic products of zooxathellae by a reef coral. **Biological Bulletin**, v. 137, p. 506–523, 1969b.

MUSCATINE, L.; KAPLAN, I. R. Resource Partitioning by Reef Corals as Determined from Stable Isotope Composition II. δ l5N of Zooxanthellae and Animal Tissue versus Depth. **Pacific Science**, v. 48, n. 3, p. 304–312, 1994.

MUSCATINE, L.; MCCLOSKEY, L. R.; MARIAN, R. E. Estimating the daily contribution of carbon from zooxanthellae to coral animal respiration. **Limnology and Oceanography**, v. 26, n. 4, p. 601–611, 1981.

MUSCATINE, L.; PORTER, J. W.; KAPLAN, I. R. Resource partitioning by reef corals as determined from stable isotope composition - I. 13C of zooxanthellae and animal tissue vs depth. **Marine Biology**, v. 100, p. 185–193, 1989.

NEWSOME, S. D. et al. A niche for isotopic ecology. **Frontiers in Ecology and the Environment**, v. 5, p. 429–436, 2007.

NUNES, F. et al. Re-evaluation of the systematics of the endemic corals of Brazil by molecular data. **Coral Reefs**, v. 27, n. 2, p. 423–432, 23 jan. 2008.

ODUM, H. T.; ODUM, E. P. Trophic structure and productivity of a windward coral reef community on Eniwetok Atoll. **Ecological Monographs**, v. 25, n. 3, p. 291–320, 1955.

PALARDY, J. E.; RODRIGUES, L. J.; GROTTOLI, A. G. The importance of zooplankton to the daily metabolic carbon requirements of healthy and bleached corals at two depths. **Journal of Experimental Marine Biology and Ecology**, v. 367, n. 2, p. 180–188, 2008.

PANDOLFI, J. M. et al. Global trajectories of the long-term decline of coral reef ecosystems. **Science (New York, N.Y.)**, v. 301, n. 5635, p. 955–8, 15 ago. 2003.

PARNELL, A. C. et al. Bayesian stable isotope mixing models. **Environmetrics**, v. 24, n. 6, p. 387–399, 2013.

PARNELL, A.; JACKSON, A. Package 'siar': Stable Isotope Analysis in R. **R Found. Stat. Comput., Vienna**,

p. 34, 2015.

PETERSON, B. J.; FRY, B. Stable isotopes in ecosystem studies. **Annual Review of Ecology and Systematics**, v. 18, p. 293–320, 1987.

POGOREUTZ, C. et al. Nitrogen fixation aligns with nifH abundance and expression in two coral trophic functional groups. **Frontiers in Microbiology**, v. 8, n. JUN, p. 1–7, 2017.

PORTER, J. W. Autotrophy, heterotrophy and resource partitioning in Caribbean reef-building corals. **The American Naturalist**, v. 110, n. 975, p. 731–742, 1976.

PORTER, J. W. et al. Bleaching in reef corals : Physiological and stable isotopic responses. **Procedings of National Academy of Science**, v. 86, n. December, p. 9342–9346, 1989.

POST, D. M. Using stable isotopes to estimate trophic position: models, methods, and assumptions. **Ecology**, v. 83, n. 3, p. 703–718, 2002.

ROHWER, F. et al. Diversity and distribution of coral-associated bacteria. **Marine Ecology Progress Series**, v. 243, p. 1–10, 2002.

ROWAN, R.; POWERS, D. A. Molecular genetic identification of symbiotic dinoflagellates (zooxanthellae). **Marine Ecology Progress Series**, v. 71, p. 65–73, 1991.

SANDERS, D.; BARON-SZABO, R. C. Scleractinian assemblages under sediment input: their characteristics and relation to the nutrient input concept. **Palaeogeography, Palaeoclimatology, Palaeoecology**, v. 216, n. 1–2, p. 139–181, jan. 2005.

SCHLICHTER, D.; BRENDELBERGER, H. Plasticity of the scleractinian body plan: Functional morphology and trophic specialization of Mycedium elephantotus (Pallas, 1766). **Facies**, v. 39, p. 227–241, 1998.

SCHLICHTER, D.; KAMPMANN, H.; CONRADY, S. Trophic potential and photoecology of endolithic algae living within coral skeletons. **Marine Ecology**, v. 18, n. 4, p. 299–317, 1997.

SCHOENER, T. W. Resource partitioning in ecological communities. **Science**, v. 185, n. 1, p. 27–39, 1974.

SILVA, A. S. et al. Sedimentation in the coastal reefs of Abrolhos over the last decades. **Continental Shelf Research**, v. 70, p. 159–167, nov. 2013.

SMITH, L. D.; GILMOUR, J. P.; HEYWARD, A. J. Resilience of coral communities on an isolated system of reefs following catastrophic mass-bleaching. **Coral Reefs**, v. 27, n. 1, p. 197–205, 18 out. 2007.

SOROKIN, Y. I. On the feeding of some scleractinian coral with bacteria and dissolved organic matter.

Limnology and Oceanography, v. 18, n. 3, p. 380–385, 1973.

STENECK, R. S. et al. Attenuating effects of ecosystem management on coral reefs. n. May, p. 1–12, 2018.

TANAKA, Y.; SUZUKI, A.; SAKAI, K. The stoichiometry of coral-dinoflagellate symbiosis: carbon and nitrogen cycles are balanced in the recycling and double translocation system. **ISME Journal**, p. 1–9, 2018.

TITLYANOV, E. A.; TITLYANOVA, T. V. Reef-building corals - Symbiotic autotrophic organisms: 1. General structure, feeding pattern, and light-dependent distribution in the shelf. **Russian Journal of Marine Biology**, v. 28, n. SUPPL., 2002.

TITLYANOV, E. A.; TITLYANOVA, T. V. Marine plants in a coral reef ecosystem. **Russian Journal of Marine Biology**, v. 38, n. 3, p. 201–210, 4 jul. 2012.

TREMBLAY, P. et al. Autotrophic carbon budget in coral tissue: a new 13C-based model of photosynthate translocation. **The Journal of experimental biology**, v. 215, n. Pt 8, p. 1384–93, 2012.

TREMBLAY, P. et al. Trophic dynamics of scleractinian corals: A stable isotope evidence. **Journal of Experimental Biology**, p. 1223–1234, 2015.

TREMBLAY, P. et al. Heterotrophy promotes the re-establishment of photosynthate translocation in a symbiotic coral after heat stress. **Scientific Reports**, v. 6, n. June, p. 1–14, 2016.

TURNER, T. F.; COLLYER, M. L.; J, K. T. A general hypothesis-testing framework for stable isotope ratios in ecological studies. **Ecology**, v. 91, n. 8, p. 2227–2233, 2010.

VAN WOESIK, R. et al. Revisiting the winners and the losers a decade after coral bleaching. **Marine Ecology Progress Series**, v. 434, p. 67–76, 28 jul. 2011.

WALTHER, G.-R. et al. Ecological responses to recent climate change. **Nature**, v. 416, p. 389–395, 2002.

WILKINSON, C. R. **Status of coral reefs of the world: 2008Global Coral Reef Monitoring Network and Reef and Rainforest Research Centre, Townsville, Australia**. [s.l: s.n.].

WOOLDRIDGE, S. A. Differential thermal bleaching susceptibilities amongst coral taxa : re-posing the role of the host. **Coral Reefs**, v. 33, p. 15–27, 2014.

WOOLDRIDGE, S. A. et al. Excess seawater nutrients, enlarged algal symbiont densities and bleaching sensitive reef locations: 2. A regional-scale predictive model for the Great Barrier Reef, Australia.

Marine Pollution Bulletin, n. April, 2016.

YONGE, C. M. The significance of the relationship between corals and zooxanthellae. **Nature**, v. 128, p. 309–311, 1931.

Appendix

.....

Published Article

An Extensive Reef System at the Amazon River mouth

This article contributes to broaden the understanding of trophic niche, trophic potential and geographic distribution of twelve species of scleractinian corals and one species of hydrocoral. The species were found under high continental load conditions under the plume of the Amazon river mouth, from 30 to 300 m depth. I took part in the first expedition and contributed with planning the trip, data collection and the article revision.

MARINE ECOSYSTEMS

10.1126/sciadv.1501252

An extensive reef system at the Amazon River mouth

Rodrigo L. Moura,[1,2] Gilberto M. Amado-Filho,[3] Fernando C. Moraes,[3,9] Poliana S. Brasileiro,[3] Paulo S. Salomon,[1,2] Michel M. Mahiques,[4] Alex C. Bastos,[5] Marcelo G. Almeida,[6] Jomar M. Silva Jr.,[6] Beatriz F. Araujo,[6] Frederico P. Brito,[6] Thiago P. Rangel,[6] Braulio C. V. Oliveira,[6] Ricardo G. Bahia,[3] Rodolfo P. Paranhos,[1] Rodolfo J. S. Dias,[4] Eduardo Siegle,[4] Alberto G. Figueiredo Jr.,[7] Renato C. Pereira,[8] Camille V. Leal,[1,9] Eduardo Hajdu,[9] Nils E. Asp,[10] Gustavo B. Gregoracci,[11] Sigrid Neumann-Leitão,[12] Patricia L. Yager,[13] Ronaldo B. Francini-Filho,[14] Adriana Fróes,[1] Mariana Campeão,[1] Bruno S. Silva,[1] Ana P. B. Moreira,[1] Louisi Oliveira,[1] Ana C. Soares,[1] Lais Araujo,[1] Nara L. Oliveira,[15] João B. Teixeira,[15] Rogerio A. B. Valle,[2] Cristiane C. Thompson,[1] Carlos E. Rezende,[6]* Fabiano L. Thompson[1,2]*

Large rivers create major gaps in reef distribution along tropical shelves. The Amazon River represents 20% of the global riverine discharge to the ocean, generating up to a 1.3 × 10^6–km^2 plume, and extensive muddy bottoms in the equatorial margin of South America. As a result, a wide area of the tropical North Atlantic is heavily affected in terms of salinity, pH, light penetration, and sedimentation. Such unfavorable conditions were thought to imprint a major gap in Western Atlantic reefs. We present an extensive carbonate system off the Amazon mouth, underneath the river plume. Significant carbonate sedimentation occurred during lowstand sea level, and still occurs in the outer shelf, resulting in complex hard-bottom topography. A permanent near-bottom wedge of ocean water, together with the seasonal nature of the plume's eastward retroflection, conditions the existence of this extensive (~9500 km^2) hard-bottom mosaic. The Amazon reefs transition from accretive to erosional structures and encompass extensive rhodolith beds. Carbonate structures function as a connectivity corridor for wide depth–ranging reef-associated species, being heavily colonized by large sponges and other structure-forming filter feeders that dwell under low light and high levels of particulates. The oxycline between the plume and subplume is associated with chemoautotrophic and anaerobic microbial metabolisms. The system described here provides several insights about the responses of tropical reefs to suboptimal and marginal reef-building conditions, which are accelerating worldwide due to global changes.

INTRODUCTION

Biogenic reefs are topographically significant structures built by benthic animals, plants, and microbes that mineralize carbonate or siliceous skeletons and/or induce carbonate precipitation (*1*). The most conspicuous biogenic reefs are the highly biodiverse coral reefs that occur in shallow, warm, and oligotrophic waters with a higher saturation state of calcium carbonate (Ω $CaCO_3$). Under such optimal mineralization conditions, carbonate accumulation reaches up to 10 kg m^{-2} $year^{-1}$, and structures may extend for thousands of kilometers (*2*). However, biogenic reefs develop under a much wider array of conditions that constrain mineralization and other core ecosystem processes typical of tropical coral reefs (for example, grazing by metazoans) (*3*, *4*). The main controls over reef ecosystems interact and vary in a wide range of spatial and temporal scales. As a result, many types of reefs have been subjected to fruitless nomenclatural controversies since the 19th century (*3*).

Because of their impact on salinity, pH, light penetration, sedimentation, and nutrients, large tropical rivers typically exclude carbonate reef builders from continental shelves. The Amazon-Orinoco and the Ganges-Brahmaputra mouths are textbook examples of such major reef gaps (*2*). The wide (~300 km) Amazon continental shelf evolved from a carbonate to a siliciclastic system during the early Late Miocene (9.5 to 8.3 million years ago) (*5*, *6*). By this time, under lowstand sea level, an incised canyon system directed sediment influx toward the slope and basin floor (*7*). Shelf edge reef buildups occurred peripherally to this deep Amazon Fan and were gradually overlain by siliciclasts during Neogene and Quaternary highstands (*7*, *8*). At present, the high sediment load from the river settles relatively quickly in the inner and mid shelves, conditioning an unstable muddy benthic habitat with high bacterial biomass and low diversity and abundance of epifauna and meiofauna (*9*, *10*). The region is also subjected to a highly energetic physical regime because of the fast-flowing North Brazil Current (NBC), strong wind stress, and high semidiurnal tidal ranges. Such conditions create a stressful habitat for benthic megafauna, especially in the areas with

[1]Instituto de Biologia, Universidade Federal do Rio de Janeiro (UFRJ), Rio de Janeiro RJ CEP 21941-599, Brazil. [2]Laboratório de Sistemas Avançados de Gestão da Produção, Instituto Alberto Luiz Coimbra de Pós-Graduação e Pesquisa de Engenharia, COPPE, UFRJ, Rio de Janeiro RJ CEP 21941-972, Brazil. [3]Instituto de Pesquisas Jardim Botânico do Rio de Janeiro, Rio de Janeiro RJ CEP 22460-030, Brazil. [4]Instituto Oceanográfico, Universidade de São Paulo, São Paulo SP CEP 05508-120, Brazil. [5]Departamento de Oceanografia, Universidade Federal do Espírito Santo, Vitória ES CEP 29199-970, Brazil. [6]Laboratório de Ciências Ambientais, Centro de Biociências e Biotecnologia, Universidade Estadual do Norte Fluminense, Campos dos Goytacazes RJ CEP 28013-602, Brazil. [7]Instituto de Geociências, Universidade Federal Fluminense, Niterói RJ CEP 24210-346, Brazil. [8]Instituto de Biologia, Universidade Federal Fluminense, Niterói RJ CEP 24210-130, Brazil. [9]Museu Nacional, Universidade Federal do Rio de Janeiro, Rio de Janeiro RJ 20940-040, Brazil. [10]Instituto de Estudos Costeiros, Universidade Federal do Pará, Bragança PA CEP 68600-000, Brazil. [11]Departamento de Ciências do Mar, Universidade Federal de São Paulo, Santos SP CEP 11070-100, Brazil. [12]Departamento de Oceanografia, Universidade Federal de Pernambuco, Recife PE CEP 50670-901, Brazil. [13]Department of Marine Sciences, University of Georgia, Athens, GA 30602–2626, USA. [14]Universidade Federal da Paraiba, Rio Tinto PB CEP 58297000, Brazil. [15]Departamento de Ciências Biológicas, Universidade Estadual de Santa Cruz, Ilhéus, BA CEP 45650-000, Brazil. *Corresponding author: E-mail: fabianothompson1@gmail.com (F.L.T.); crezendeuenf@yahoo.com.br (C.E.R.)

soft, fluid sediments. The massive sedimentation and sediment reworking in the inner and mid shelves have been comprehensively surveyed in the last decades, including the core river-ocean biogeochemical processes (*9*). On the other hand, the "relict magnesian calcite ooids" (*11*) and other carbonate sediments recorded along the outer shelf (*5*, *8*) have received much less attention. For instance, it is unknown whether this surficial carbonate layer comprises living biomineralizers and other reef-associated organisms and how this benthic system may be coupled to the pelagic compartments. The only noteworthy exceptions to such knowledge gap about the outer shelf is a brief description of reef fishes associated with sponge bottoms (*12*) and a checklist of corals produced from specimens deposited in museums (*13*), both of which fail to report the presence of carbonate structures and rhodolith beds.

The Amazon River represents ~20% of the global riverine discharge to the ocean [$\sim 120 \times 10^3$ m^3 s^{-1} in December to $\sim 300 \times 10^3$ m^3 s^{-1} in May; (*14*)], generating an up to 1.3×10^6–km^2 offshore plume enriched with chromophoric dissolved organic matter (*15*, *16*). This relatively shallow (5 to 25 m deep) and hyposaline layer is driven by seasonal winds and currents, flowing northward into the Caribbean and retroflecting eastward during September and October. Phytoplankton productivity is limited by low light penetration in the inner shelf, increasing only once sediments have cleared (*16*, *17*). The resulting downward particle flow occurs away from the continental shelf (*18*). On the shelf break, sedimentation under the plume is limited by a permanent frontal process that draws near-bottom seawater landwards, coupled with Ekman veering (*9*). Oxygen levels are lowered in the subplume and near the bottom because of the high rates of organic matter mineralization in the inner and mid-shelf (*10*, *19*). Although the plume has been the focus of recent studies (*16*, *17*, *20*), the subplume and the coupling between the plume, subplume, and outer-shelf benthic systems have been largely ignored.

The Amazon River mouth represents the distribution boundary for several sponges, scleractinian corals, and shallow water fishes, among other groups of coastal and reef-associated organisms, as a consequence of the massive oceanographic discontinuities that it imprints in the West Atlantic continental margin (*21*). On the other hand, many reef-associated species occur at both sides of the river mouth, with possible connectivity mechanisms related to long-range larval dispersal, rafting, or demersal migration through stepping stones (*22*). The operation of the Amazon mouth biogeographic filter is not completely known because information about the nature and extension of reef habitats off the Amazon mouth is still limited (*11*–*13*, *23*, *24*).

Here, we present the results of a multidisciplinary assessment of the outer Amazon shelf, where we found a unique carbonate reef system of ~9500 km^2, between the French Guiana–Brazil border and the Maranhão State in Brazil (~1000 km). Our survey was carried out near the shelf edge and in the upper slope (25 to 120 m), and included geophysical and physical-chemical surveys, radiocarbon dating and petrographic characterization of reef samples, biogeochemical tracers, and microbial metagenomics. We provide a description of macrobenthic and demersal assemblages, including extensive rhodolith beds built by coralline algae and sponge-dominated hard bottom, and also adding primary and gray literature data about the large reef fisheries that operate off the Amazon mouth [for example, CREOCEAN (*25*) and IBAMA (*26*)]. The novel system presented here adds to the repertoire of "marginal" reef types shaped by conditions deviating from those of the archetypal tropical coral reefs. The ubiquity of large sponges and other filter feeders, as well as the increase of chemoautotrophic and anaerobic microbial metabolisms recorded in the subplume, provides insights about ecosystem-level responses to the globally accelerating conditions that select against photosymbiotic biocalcifiers (for example, scleractinian corals).

RESULTS

Structure, composition, and age of reef structures

An extensive carbonate reef system of ~9500 km^2, spanning from 5°N to 1°S and 44° to 51°W, was recorded between the Brazil–French Guiana border and Maranhão State, Brazil (Fig. 1). Rhodolith beds and higher-relief structures were recorded across a relatively long (~1000 km) and narrow (~50 km) stretch in the outer shelf and upper slope, in depths ranging from 30 m to the shelf break at 90 to 120 m. This extensive submerged carbonate system extends from French Guiana southward to the Manuel Luis reef, the northernmost emerging reef within the Brazilian Biogeographic Province.

In the Northern Sector of the study region, structures were recorded near the shelf edge, comprising widely spaced (hundreds to thousands of meters) patches with lengths of up to 300 m and heights of up to 30 m. These irregularly shaped reefs tended to be elongated with a parallel shelf edge orientation, resembling erosive structures (Fig. 1B). Dredged materials consist of carbonate fragments with incipient living cover of crustose coralline algae (<5%) and low-vitality rhodoliths recovered in the vicinity of the larger reef patches, and also include lateritic crusts. The dated sample (surficial carbonate fragment) presented a 2σ radiocarbon calibrated age of 13,382 to 13,749 years before present (BP), with microfacies typical of grainstone composed of skeleton fragments of tube worms, foraminifera, barnacles, bryozoans, and molluscs (Fig. 2, A and B). Dredge casts that did not hit structures recovered large sponges among soft sediments (fig. S1). In the Central Sector, the bottom was dominated by rhodoliths with high vitality (>50% of live coralline algae cover), as well as by complex sandwaves and gravel ripples between 20- and 100-m depths (Fig. 1C). Patches of carbonate blocks were small (<10 m^2) and sparsely distributed. The core and surface of a ~70 × 40–cm block collected in this sector presented 2σ radiocarbon calibrated ages of 4487 to 4846 and 4157 to 4562 years BP, respectively. Microfacies is typical of boundstone and is mainly composed of crustose coralline algae and bryozoans (Fig. 2, C and D). The surface of this block presented small and sparse patches of living coralline algae. In the Southern Sector, structures were widespread and occurred between 30- and 90-m depths. Reef morphology consists of ridge-like features <5 m in height and irregular and low-relief patch reefs (<5 m in height) (Fig. 1D). Structures are surrounded by a high backscatter and flat hardground (fig. S2) dominated by high-vitality rhodoliths and carbonate sand. The dated sample (surficial carbonate fragment) presented a modern radiocarbon age (<150 years), with microfacies typical of boundstone composed of hydrocorals, crustose coralline algae, and corals (Fig. 2, E and F). The southern part of this sector encompasses one relatively shallow (<10-m depth) submerged reef (Banco do Álvaro reef) and the emerging Manoel Luís reef (~450 km^2), both consisting of isolated and coalesced coralline pinnacles. None of the benthic casts in the Central and Southern Sectors recovered mud.

Macrobenthos, demersal fish, and reef fisheries

Red algae (Rhodophyta, 25 species) were the predominant benthic plant group, followed by green (Chlorophyta, 6 species) and brown algae

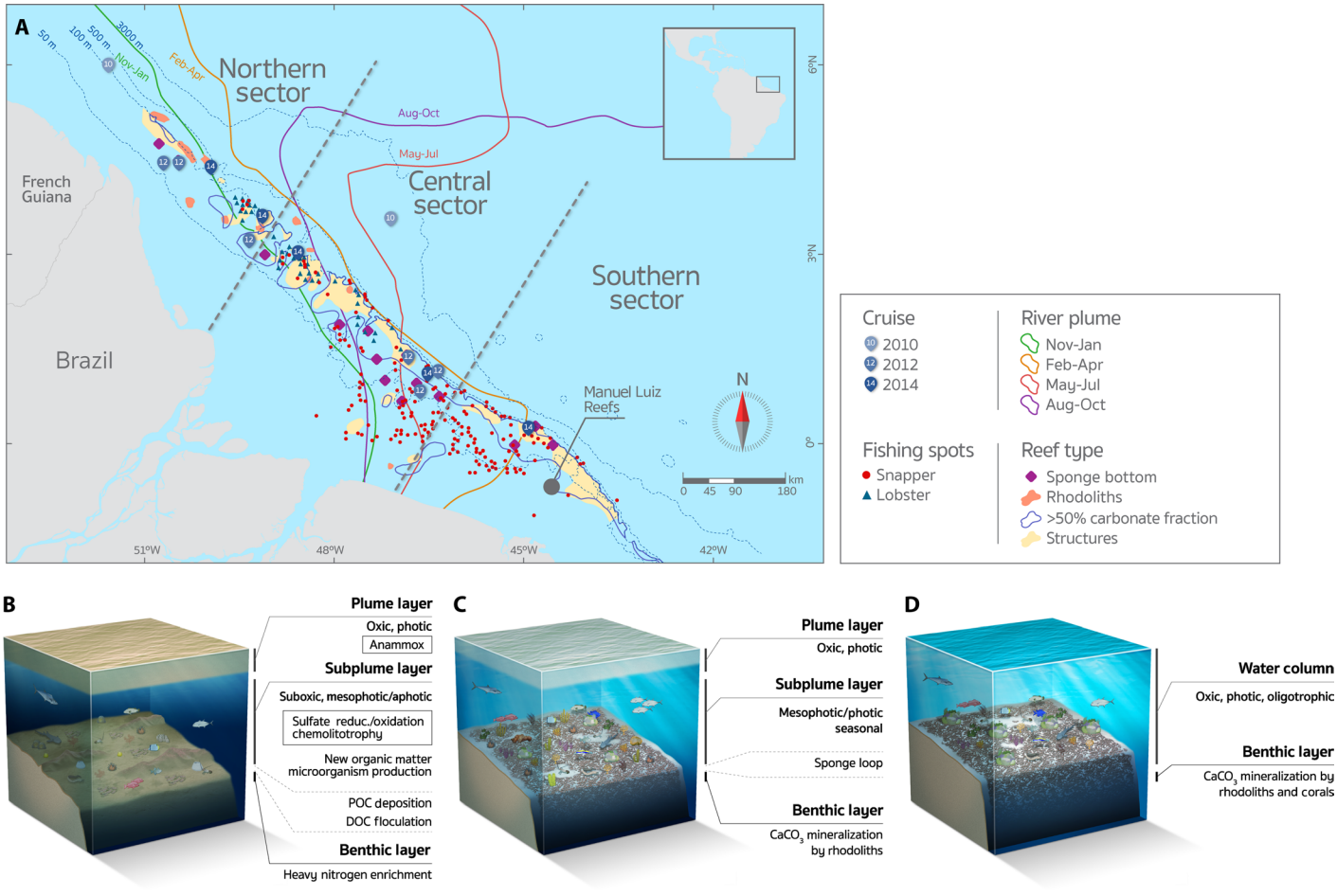

Fig. 1. Map of the Amazon shelf showing the benthic megahabitats and seasonal influence of the river plume. (**A**) Distribution of reef fisheries and oceanographic stations. Manuel Luis reefs are the northernmost emerging reefs in Brazil. (**B** to **D**) Main structural and functional traits of the reefs in the Northern (120 m), Central (55 m), and Southern Sectors (25 m), respectively. Plume POC $\delta^{13}C = -22.9 \pm 0.7$, $\delta^{15}N = 4.0 \pm 1.2$; Plume DOC $\delta^{13}C = -27.7 \pm 1.0$, $\delta^{15}N = 1.3 \pm 0.3$. Subplume POC $\delta^{13}C = -24.2 \pm 1.3$, $\delta^{15}N = 5.1 \pm 1.7$; Subplume DOC $\delta^{13}C = -26.6 \pm 1.7$, $\delta^{15}N = 0.1 \pm 1.8$. Benthic (sediment) δ13C = −26.2 ± 0.6, δ15N = 2.2 ± 0.5. Some graphic elements are courtesy of the Integration and Application Network, University of Maryland Center for Environmental Science (http://ian.umces.edu/symbols/). The plume lines represent the outer edge of the plume during that season, according to satellite climatology (*80*).

(Ochrophyta, 4 species) (table S1). Calcareous algae were ubiquitous (fig. S3), with a clear impoverishment gradient northward. Five encrusting calcareous algae taxa were identified in the surface of rhodoliths and carbonate blocks, with living *Lithothamnion crispatum* and *Sporolithon ptychoides* distributed across the entire outer shelf, including the subplume environment of the Northern Sector. A low-diversity assemblage (34 species) of typically tropical-subtropical and wide depth–ranging seaweeds was recorded in association with the rhodoliths in the Central and Southern Sector. These assemblages included greater functional diversity than those of the Northern Sector (table S1). Seaweeds recovered from the Northern Sector (for example, *Gelidium* and *Anadyomene*) consisted of detached and low-vitality fragments. With the exception of *Anadyomene*, green and brown algae were restricted to the South Sector.

The sponge assemblage comprised 61 species and was dominated by massive forms that were wide depth–ranging within the photic and mesophotic zones, but also included a few deep-water species (table S2 and fig. S4). Three Northern Sector stations were remarkable as they recovered sponges among soft sediments, including large-sized *Xestospongia muta* with unusual pale coloration and narrow atria and *Tribrachium schmidtii* with a buried bulbous base and an upward long papilla (fig. S4). The highest sponge diversity and biomass was recorded on the flatter rhodolith beds of the Central Sector. For instance, a single 20 minutes trawl (station 2014-6; 55-m depth) recovered about 30 species (150 specimens, ~900 kg), most of which exhibited large, erect, cup-like, and massive forms, growing attached to rhodoliths (table S2, fig. S4, and movie S1). The most common sponge species in the Central Sector were *Agelas* spp., *Aplysina* spp., *Callyspongia vaginalis*, *Clathria nicoleae Geodia* spp., *Monanchora arbuscula*, and *Oceanapia bartschi*. Encrusting species (for example, *Clathria* cf. *calla*) were overall rare and restricted to grow on other sponges. *Lissodendoryx* sp. and *O. bartschi* were heavily colonized by epibionts (ascidians, hydroids, and other sponges). Two excavating species of genus *Cliona* were found associated

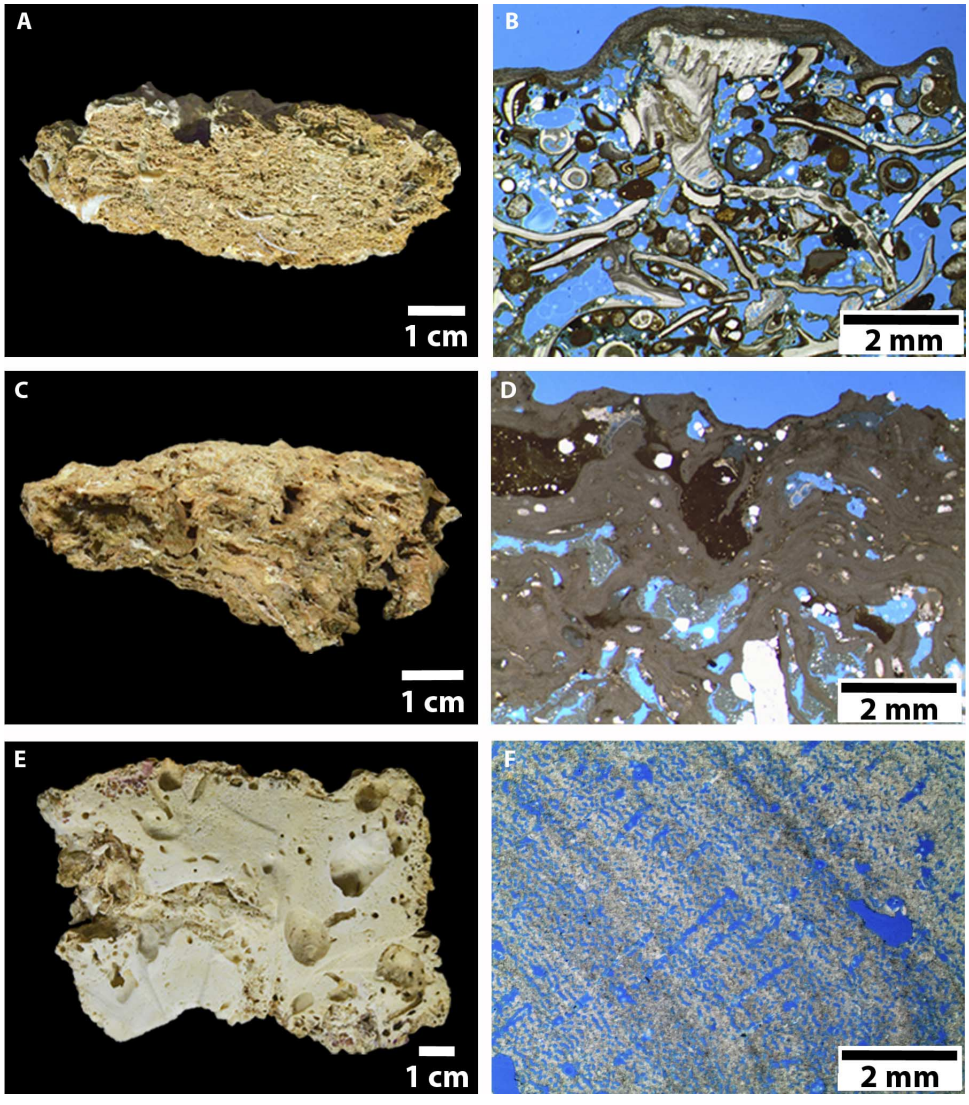

Fig. 2. Surficial reef fragments (left) and corresponding petrographic images (right) from the Northern (A and B, 120-m depth), Central (C and D, 60 m), and Southern Sectors (E and F, 23 m). Microfacies transition from an older grainstone (12,100 ± 30 thousand years BP) composed of filter feeders (polychaetes, foraminifera, barnacles, bryozoans, and molluscs) under a thin veener of coralline algae in the Northern Sector (A and B) to a more recently turned-off (5220 ± 110 thousand years BP) boundstone composed of photosynthesizers (crustose coralline algae) and filter feeders (bryozoans) in the Central Sector (C and D) and, finally, to a recent boundstone typical of turbid zone reefs (hydrocorals, crustose coralline algae, and corals) in the Southern Sector (E and F).

with scleractinian corals in the Southern Sector (table S2 and figs. S4 and S5), whereas no boring sponges were recorded in the Northern Sector.

Cnidarians were present at all stations, with hydroids (benthic colonial life stage of hydrozoans) being particularly abundant across the region. Two black coral species (Antipatharia), *Antipathes furcata* and *Tanacetipathes tanacetum*, typical of mesophotic zone reefs, were recorded at the Northern Sector (table S3). Octocorallia was the most speciose group (26 species), but most records are from sparse museum specimens without precise locality records (*13*). Scleractinians with symbiotic dinoflagellates (*Symbiodinium* spp.) were largely restricted to the Central and Southern Sectors. Where present (Central and Southern Sectors), scleractinians comprised impoverished (12 species, table S3) and low-density/cover assemblages (fig. S5) encompassing encrusting colonies of small-sized species (*Meandrina braziliensis*, *Agaricia* spp., *Scolymia wellsii*, and *Favia gravida*), small colonies of massive species (*Montastraea cavernosa* and *Madracis decactis*), and branching colonies of *Millepora* cf. *alcicornis*. With the exception of *F. gravida* and *Millepora* cf. *alcicornis*, all corals recorded off the Amazon mouth were wide depth–ranging species, occurring in photic and mesophotic habitats. An alien brittle star from the Pacific Ocean, *Ophiothela mirabilis*, was recorded in association with *Leptogorgia miniata*.

We recorded 73 reef fish species in the study region, most of them with wide depth and geographic ranges (table S4 and fig. S6). Most fish species were carnivores (86%), including piscivores and invertivores,

whereas a few were planktivores or herbivore/detritivores (two species, 3% each). Four species (5.5%) of sponge-eating fishes of family Pomacanthidae (angelfishes) were recorded across the region. Significant fisheries for the Southern red snapper, *Lutjanus purpureus* (2900 metric tons year^{-1}), and spiny lobsters, *Palinurus* spp. (1360 metric tons year^{-1}), were recorded across the region, the latter being concentrated in the Northern and Central Sectors (Fig. 1). Reef fisheries are carried out by small- to medium-sized boats (8 to 20 m lengths) operating with traps (for lobsters) and hand lines or long lines (for reef fishes) in the outer shelf. Smaller dinghies with one to two crew (fig. S7) operating hand lines are also regularly spotted, and are used to increase fishing area and the chance of finding reef structures where fishes aggregate. At least 131 boats are currently registered to fish lobsters with traps (~3 boats per 10 km of the linear extension of the reef system), but a larger number of unregistered boats target reef fishes. Targeted species include a diverse assemblage of groupers (Serranidae, 321 metric tons year^{-1}) and snappers (Lutjanidae, 4220 metric tons year^{-1}), which are landed mainly in Pará and Amapá (*26*). Such intense reef fisheries (fig. S8) represent additional evidence for the wide distribution and importance of the reefs close to the Amazon mouth. In the inner shelf, fisheries are carried out over soft sediments, mostly with gillnets, trawls, and long lines.

Biogeographic patterns. All macroalgae recorded off the Amazon mouth are wide-ranging species that are distributed across large expanses of the Atlantic and Pacific basins. The sponge fauna was a typical tropical West Atlantic reef assemblage, with only three Brazilian endemics and two species that also occur in West Africa. Three new records were added to the Brazilian sponge fauna: *Theonella atlantica*, a typical deep-water species previously recorded in the Southern Caribbean; *Clathria echinata*, previously known from the Caribbean; and *Didiscus verdensis*, previously known from shallow waters in the Cape Verde Archipelago (*27*). The octocoral fauna (26 species) included typically mesophotic species, with 18 species that are wide-ranging in the West Atlantic, 7 Brazilian endemics, and 1 circum-globally distributed gorgonian. Anthipatarians included only three species that are widely distributed in the West Atlantic, including the black coral *Anthipathes furcate*, which is a new record to Brazilian tropical waters (previously known from the Caribbean and Southeastern Brazil). Of the 6 recorded scleractinians, 2 are Brazilian endemics and the remaining 4 are wide-ranging in the Atlantic Ocean. Brazilian-endemic scleractinians were restricted to the Central and Southern Sectors. The reef fish assemblage was also dominated by wide-ranging species (63% are widely distributed in the West Atlantic, 22% occur in the West and East Atlantic, and 11% occur in the Atlantic and Pacific), with the exception of *Stegastes pictus*, *Halichoeres dimidiatus*, and *Sparisoma frondosum*, which are Brazilian endemics with occasional records northward into the Caribbean and West Africa (*S. frondosum*). Pelagic spawners with high dispersal capabilities (80%) dominated the reef fish assemblage. Most recorded species (algae, sponges, cnidarians, and fishes) are wide depth–ranging, with a few exceptions restricted to the Southern Sector (tables S1 to S4).

Plume and nonplume water column. Water column profiles under nonplume conditions encompassed outer shelf, slope, and open-ocean/deep-sea stations (Fig. 3 and fig. S9). These profiles were well mixed to about 100 m, with near constant salinity at ~35.5 to 36. Temperatures near the surface were consistently ~28°C, cooling rapidly below 50 m, with 1% light level [photosynthetically active radiation (PAR)] reaching ~100 m. Dissolved inorganic nitrogen (DIN), a limiting nutrient, was near the detection limit in the upper 70 m, and particulate organic carbon (POC) and dissolved organic carbon (DOC) concentrations were generally low throughout the upper water column (Fig. 3). Oxygen was uniform at around 4 ml liter^{-1} throughout the upper 100 m (Fig. 3). Conversely, in profiles associated with the plume (Fig. 3 and fig. S9), the water column was strongly stratified with an evident lower salinity and higher temperature signal in the upper 10 to 15 m. Light attenuation was much stronger in plume profiles, with 1% levels no deeper than 50 m (Fig. 3), and nutrient concentrations (such as DIN) were consistently >0, with values depending on proximity to river mouth. Concentrations of POC and DOC were higher in the plume (Fig. 3), reflecting both riverine and marine organic inputs. Oxyclines were detectable at depths of ~5 to 10 m across the plume interface and 35 to 50 m within the subplume. Dissolved oxygen (DO) levels dropped to $\leq$ 3.5 ml liter^{-1} near the bottom at some stations on the outer shelf (fig. S9).

Isotopic analysis. The isotopic composition of POC was heavier in the plume (−22.9 ± 0.7‰) than in the subplume (−24.2 ± 1.3‰) and benthic (sediment) layers (−26.2 ± 0.6‰), whereas DOC showed a slight but not significant difference between the plume (−27.7 ± 1.0‰) and subplume (−26.6 ± 1.7‰) layers. The same trend was observed for nitrogen isotopic composition of particulate organic nitrogen (PON) in the plume (4.0 ± 1.2‰) and subplume (5.1 ± 0.7‰) layers, respectively, but significantly lower values were found in the benthic layer (2.2 ± 0.5‰) (Fig. 1). Dissolved organic nitrogen showed an opposite trend when compared with PON, with higher values in the plume (1.3 ± 0.3‰) than in the subplume (−0.1 ± 1.8‰) layer.

Transcriptome analysis. Compared to nonplume (oceanic) metatranscriptomes, more gene transcripts related to anaerobic metabolism were detected in the plume and subplume layers (fig. S10), corroborating the water column physical-chemical features. An opposite trend was observed for photosynthesis gene transcripts, except for the particle-associated fraction of the plume, reinforcing the increased contribution of chemosynthesis in the subplume. The adenylyl sulfate reductase subunits α and β (*aprAB*; responsible for dissimilatory sulfate reduction) and sulfur (thiosulfate and sulfide) oxidation (*soxB*) transcripts from free-living microbes were more abundant in the subplume layer. Anammox gene transcripts and respiratory nitrate/nitrite reductase (*narB* and *nirB*; responsible for nitrate respiration) transcripts were more abundant in the plume layer, from both free-living and particle-attached microbes in the plume.

DISCUSSION

Despite the iconic depiction of reefs as megadiverse systems thriving in warm, shallow, and oligotrophic waters, biogenic reefs develop under a much wider range of conditions. The benthic production by efficient mixotrophic holobionts that build carbonate structures (for example, scleractinian corals), together with the grazing by fish and macroinvertebrates, have been important drivers in the evolution of coral reef ecosystems (*28*, *29*). However, these processes are constrained in the so-called marginal reef systems (*4*), which may share parts of their taxonomic structure and some functional properties with tropical coral reefs (*29*). Marginal reefs are subjected to environmental forcing that depart from the optimal mineralization conditions for corals, such as the rhodolith beds that occur at great depths and latitudes (*30*, *31*), aphotic zone coralline and sponge reefs (*32*), and stromatolites that

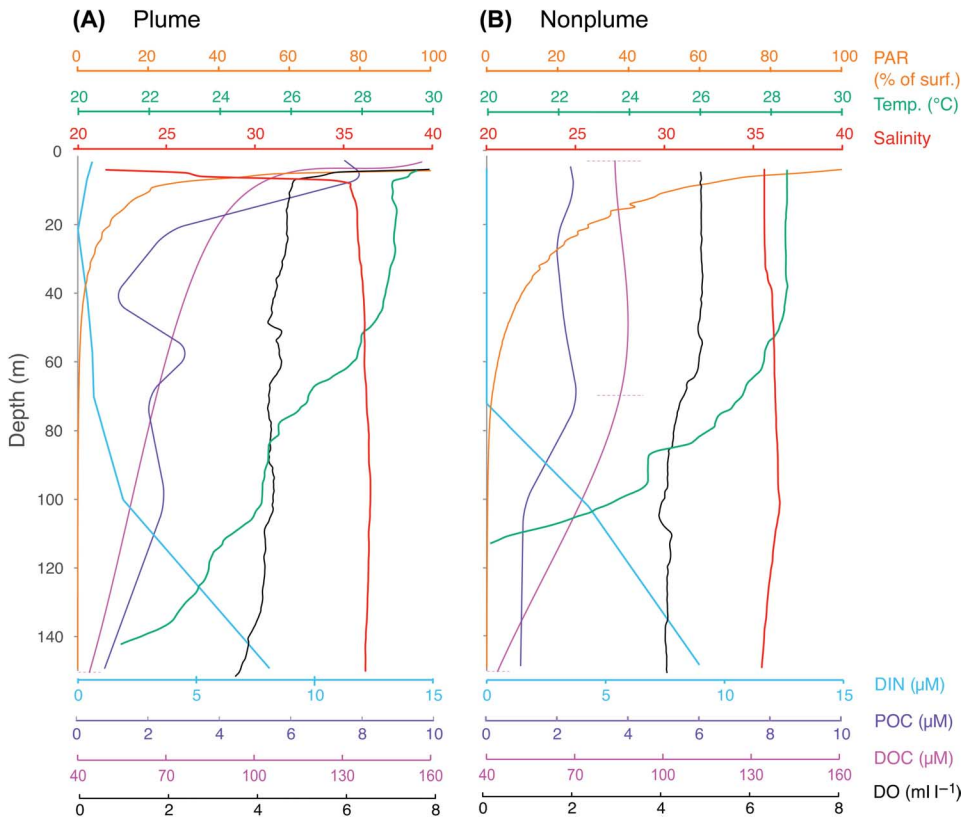

Fig. 3. Water column profiles under plume (A) and nonplume (B) conditions. (A) Station 2010-04 (5.495°N, 51.488°W), under intense plume influence, Northern Sector. (B) Station 2010-08 (4.349°N, 46.852°W) under nonplume condition, Central Sector.

develop under extreme physicochemical conditions (*3*). These marginal reef systems share some common trends such as a lowered importance of photosymbioses, reduced diversity of macroorganisms (macroalgae and metazoans), reduced grazing, and increased microbial diversity. With a greater areal extent, depth range, and latitudinal extent than that of coral reefs, marginal reefs have been relatively neglected by science, especially because of the logistical constrains for direct observation and mapping with remote sensing in turbid waters (*33*). Here, we presented a major carbonate system that occurs off the Amazon River mouth, adding to the wide repertoire of marginal reefs that includes large megahabitats (thousands of square kilometers) that were only recently mapped (*31*, *34*), despite occurring in continental shelves.

The extensive reef system off the Amazon River mouth presents erosive structures that ceased to grow during the late stages of the last post-glacial maximum transgression, as revealed by the carbonate rocks dated in the Northern (13,382 to 12,749 calibrated years BP) and Central Sectors (4487 to 4846 and 4157 to 4562 calibrated years BP). Dead rhodolith beds and relict magnesium calcite ooids (*11*) are recorded in the Northern Sector, extending into southern French Guiana (*25*), and their ages are compatible to the surface of the dated structure from this sector. The age of this structure also corresponds to the transitional period of the last turn off of the Amazon Fan because of widespread shelf flooding (sea level reaching 40 to 50 m below present-day sea level) (*7*). Besides the last post-glacial transgression and shifts in the sediment budget because of fluvial, oceanographic, and meteorological processes (*35*), the reef building turnoff (*36*) in the Northern Sector also seems related to shelf subsidence, which reached more than 100 m between 16 and 21 thousand years BP (*35*). Despite encompassing assemblages adapted to low light penetration, turbid zone reefs develop under narrow depth ranges and can be especially vulnerable to relative sea level changes (*4*).

Turbidity is elevated across the entire Equatorial Margin, but deposition is low in the outer shelf, especially in the Northern Sector, where the NBC reaches maximum speed (*9*) and prevents the burial of reefs by terrigenous sediments. Such high turbidity–low net sediment accumulation is also associated with the permanent frontal processes and Ekman pumping into the platform (*9*). From the Central Sector southward, turbidity decreases and the plume influence becomes more seasonal. The carbonate balance becomes positive from the Central Sector southward, mainly due to the high density of living rhodoliths covered by red algae (Corallinales), which are able to mineralize under very low light levels.

Although reef framework building has been "turned off" (*35*) in a significant portion of the Amazon reef range, in all sectors, there is a living assemblage of reef-associated organisms typical of West Atlantic mesophotic and deep reefs (*37*–*39*). The benthic assemblage of the Northern Sector is dominated by filter feeders adapted to strong currents, high suspended sediment, and lowered light and oxygen, such as octocorals and black corals, and especially by massive sponges with long papilla (*O. bartschi*), ball-shaped sponges (*Cinachyrella kuekenthali*), barrels with narrow atrium and high pumping rates (*X. muta*), and bulbs (*T. schmidtii*) (*40*). Besides bearing narrower atria typical of high current settings, the large barrel sponges, *X. muta*, were remarkable for being pale, possibly due to the lack of photosymbionts (fig. S1). An even more diverse assemblage of large sponges develops in association

to the high-vitality rhodolith beds of the Central Sector, including growth forms adapted to steady currents, to light capture by photosynthetic symbionts, and to sediment resistance (for example, tubes—*A. lacunosa*; curled fan—*C. vaginalis*; branched—*C. nicoleae*; massive with long inhaling papillae and narrow elevated central oscule—*O. bartschi*) (table S2). There are few larger coalesced structures in the Central Sector, and the topography of the rhodolith beds is limited by the size of the nodules (centimeters to tens of centimeters). However, the great sponge abundance significantly increases habitat complexity and enhances nutrient supply to other organisms, reducing DOC concentration and providing significant benthic production (*41*). The high abundance of sponges in the outer shelf was recorded in an early survey targeting the discovery of shrimp-trawling beds (*12*), but it is now clear that sponge diversity and abundance peaks in the intermediary portion of the plume influence gradient. Turbidity and extreme limitations in light penetration may control the diversity and abundance of sponges in the Northern Sector, whereas competition with other benthic organisms (coralline algae, macroalgae, and corals) and predation by reef fishes may be the most important controls southward.

Large sponge reefs are well documented in aphotic areas in different oceans, but they are generally dominated by Hexactinellida (glass sponges), with a few exceptions in which Demospongiae dominate. Reefs dominated by few species of hexactinellids are well documented in the Northeast Canadian shelf, between 30- and 240-m depths (*32*). Deep-water aggregates of large Demospongiae are known as "sponge grounds" or "sponge gardens" and are widely distributed in the North Atlantic (*42*). These habitats may encompass up to 50 sponge species, including a strong contribution of *Geodia* spp. (*42*, *43*), which is a ubiquitous genus in the Amazon reefs (table S2). A sponge garden hotspot in West Australia (tropical Carnarvon Shelf) also has high richness and biomass concentrated between 40- and 100-m depths (*40*). The Central Sector of the Amazon reefs system is similar to such sponge gardens, presenting (i) high sponge diversity and biomass in the mesophotic zone; (ii) large, erect, cup-like, and massive forms adapted to sedimentation; and (iii) species with low inorganic content (with few or no spicules) concentrated where the shelf is wider and currents are weaker.

The shallower Southern Sector is an area with higher wave energy and episodic plume influence (*23*, *44*), resembling the typical turbid zone reefs [for example, Perry and Larcombe (*4*)] with few species and sparse corals and hydrocorals (Fig. 1C). When compared to other reefs within the Brazilian Province and the Caribbean [for example, Wilkinson (*45*)], coral and coralline algal diversity is still relatively low, but carbonate accumulation is positive, as indicated by the dating of the structures. Indeed, high coral diversity and framework accumulation are often uncoupled, and the former may not be a universal surrogate of reef health (*4*).

The Amazon reefs are also noteworthy for supporting considerable fisheries yields that span all sectors, especially lobsters (Crustacea: Palinuroidea) and snappers (Perciformes: Lutjanidae). Although extensive shrimp trawling and other fisheries (for example, gill nets and long lines) are well documented in the soft sediments of the inner and mid-shelf [for example, Pinheiro and Frédou (*46*)], hundreds of artisanal and commercial boats operate in the outer shelf with hand lines and traps. For instance, lobster yields in the Amazon reefs (mostly *Panulirus argus*, but also including five other species) (*47*) are equivalent to 5% of the total lobster capture in the 23 Caribbean countries that explore this resource (*48*, *49*). Because of Brazil incipient fisheries management, the exact number of boats that operate in the Amazon reefs remains undisclosed, but tracking data show that fishing effort with hand lines and traps is concentrated in the outer shelf (fig. S8). Although some typical reef fisheries resources are lacking from the Amazon reefs (for example, parrot fishes), lobsters and other species (for example, red snapper and large groupers) may benefit from plume-related resources and conditions, showing that low-diversity reefs with incipient coral cover may still provide relevant and valuable ecosystem services.

The Amazon River mouth is the distribution boundary for several reef-associated organisms. Southward, the reef biota of the Brazilian Biogeographic Province is less diverse than that of the Caribbean and presents high endemism levels (*24*, *50*). Although such lowered species richness seems to result from the relatively smaller area and suboptimal conditions for reef development (for example, high turbidity and river runoff), endemism seems to be largely driven by the partial isolation of the Southwestern Atlantic. The selective and intermittent nature of the Amazon mouth biogeographic filter may drive parapatric divergence (instead of allopatric speciation) because this model allows for restricted gene flow between diverging populations (*51*). Indeed, the novel information about the characteristics and extension of the Amazon mouth reef system provides additional support to the phylogeographic evidence for the operation of parapatric speciation, whereas our updated checklist of reef-associated organisms (tables S1 to S4) clarifies the selective nature of the biogeographic corridor.

The relatively low-diversity assemblage of algae, sponges, corals, and reef fishes is dominated by wide depth–ranging species that are broadly distributed in the Atlantic (or in the West Atlantic) (tables S1 to S4). Shallow-water dwellers, or species that depend on specific coralline microhabitats or resources, are not able to use the Amazon reef system as a stepping stone because reef structures and rhodolith beds are largely located in relatively deep areas (>40 m) with limited availability of habitat and food resources. At ecological time frames, such shallow-water dwellers must rely on larval dispersal or rafting (*22*) across the hyposaline plume within the unidirectional NBC, a fact that helps explain the higher Brazilian-endemism level within fish groups such as blennies (shallow-water dwellers) and parrot fishes (specialized herbivores) (*52*–*54*). Brazilian-endemic corals such as *Mussimilia* spp., which have expressive cover southward (*55*), are also shallow-water dwellers. These species only occur in deeper habitats in oceanic islands and offshore banks, where light penetration reaches greater depths. At larger time scales (thousands to tens of thousands years), lowered relative sea level (*7*) and other environmental fluctuations may "turn on" the Amazon Fan and widespread reef development in the Amazon reef system, providing a more permeable connectivity matrix between the Caribbean and the South Atlantic.

At least 29 sponge taxa are still identified only at supraspecific levels, indicating a source for new species. An alien brittle star from the Pacific Ocean, *O. mirabilis*, which was known from Brazil and French Guiana (*56*), was recorded in the Amazon reefs, showing that invasive species introduced in the Caribbean (for example, lionfishes) may reach the South Atlantic through this countercurrent dispersal route (*57*). Modeling of potential bioinvasions through this route may take depth range into account because of depth selectivity of the Amazon mouth biogeographic filter.

The inner Amazon shelf is known for high rates of benthic respiration, which is associated with the river-sourced terrestrial material (*19*). In the Amazon reefs, microbial metabolisms deviate from those commonly found in coralline reefs (*39*, *58*) because they include chemosynthesis and heterotrophy, particularly in the Northern and Central Sectors. This particular functional structure is better understood from

the layered structure comprising the plume, the subplume, and the benthic mosaic (Fig. 1 and fig. S2). Light reduction may condition heterotrophic and chemosynthetic microbial metabolisms (Fig. 3 and figs. S9 and S10). Whereas photosynthesis is the major carbon fixation process in nonplume waters, the subplume presents significant amounts of gene transcripts related to anaerobic respiration, resembling an oxygen minimum zone (OMZ), and corroborates the observed oxycline. Oxygen depletion in the subplume is not as drastic as in other OMZs (*54*), but oxygen levels near the bottom can be as low as 3 ml liter^{-1} and can potentially limit some benthic organisms.

At the Northern and Central Sectors, calcareous algae may photosynthesize at low light levels, and sponges may tolerate anoxic and suboxic conditions for several days (*59*). The sponge assemblage includes both high microbial abundance (HMA) and low microbial abundance (LMA) species (*60*); the former rely heavily on microbial symbionts, whereas the latter use water column microbes for nourishment. Symbiotic microbes associated with HMA sponges include chemosynthetic and fermenting taxa (for example, *Proteobacteria*, *Firmicutes*, *Actinobacteria*, *Planctomycetes*, and *Thaumarchaeota*) and *Cyanobacteria* (*60*) that help sponge metabolism. On the other hand, the high POC and DOC concentration in the Amazon mouth reefs may promote an intense development of LMA sponge loop (*61*, *62*).

Although the low-salinity plume stays well above the seafloor, the plume may interact dynamically with benthic organisms through particle flux, shear, and enhanced eddy stirring and mixing (*15*). The clear marked difference in isotopic composition can be related to increased anoxia, with heavier N increased in the subplume (higher subplume N_2 concentration). A significant fractionation in isotopic composition of N between suspended particles (plume and subplume layers) and surface sediment corroborates the presence of processes such as nitrogen fixation and denitrification/anammox (*63*). In addition, the isotopic analysis of plume and subplume DOC and POC indicates a strong contribution from terrestrial and mangrove-derived material, suggesting that the reefs in the Northern and Southern Sector are subjected to very specific biogeochemical conditions. Previous studies have suggested a rapid turnover of organic matter from terrestrial and mangrove origins, with a longer persistence of mangrove-derived DOC, with contribution to oceanic areas accounting for >10% of DOC (*64*, *65*). Our results are in agreement with these patterns, and the isotopic signatures for Amazon rivers [−26.8 to −30.4‰ (DOC) and −27.4 ± 0.8‰ (POC)], mangrove waters [−31.4‰ (DOC) and −28.1 ± 1.5‰ (POC)], surface Atlantic waters [−20.8 ± 1.1‰ (DOC)], and deep Atlantic waters [−23.7‰ (DOC)] reinforce the contribution from terrestrial and mangrove-derived material to the reefs' DOC and POC pools.

The rapid decline of coral reefs is drawing considerable attention because of the alarming forecasts of biodiversity losses from local (for example, pollution and overfishing) and global stressors (temperature anomalies and ocean acidification) (*66*, *67*). Understanding the distribution of the several reef subtypes and how their biodiversity and functional properties are associated with different environmental forcing is a major and basic step toward forecasting generalized trajectories for reef systems (*41*, *68*). In this regard, studies of marginal reef ecosystems have a major role to play in reef ecology because scleractinian-dominated communities may not be a universal baseline. The Amazon reef system comprises a gradient from marginal mineralization conditions (South Sector) to structures that are beyond $CaCO_3$ mineralization thresholds for thousands of years (North Sector) but still supports significant reef-associated biodiversity and relevant ecosystem services. For low trophic level fisheries resources, such as lobsters, the system seems to support higher yields than coral-dominated reefs (*49*). The $CaCO_3$ production by rhodolith beds (1.3 to 2.7 kg m^{-2} year^{-1}), the dominant megahabitat in vast expanses of tropical and temperate shelves (*30*), as well as in the Amazon mouth, is close to the mean global coral reef rate (1.5 kg m^{-2} year^{-1}) (*31*). Although the impoverished coral reefs in the Brazilian Province represent only 5% of the Atlantic reef area (*33*), the region's extensive rhodolith beds produce >0.025 gigatons year^{-1}, rivaling with the total $CaCO_3$ production by coral reefs in the Caribbean (0.04 to 0.08 gigatons year^{-1}). Although corals appear biologically fragile, they are geologically robust ("the most ingenious paradox") (*69*), and there is mounting evidence that peripheral areas with reef-associated organisms may be a key to the evolution and survival of coral reef biota through geological time (*70*, *71*).

The sponge dominance in the Central Sector provides support to the idea that coral domination may phase-shift to sponge domination as climate changes and some local stressors escalate (for example, nutrients) (*40*, *70*). Sponges, corals, and coralline algae respond differently to ocean chemistry and environmental conditions, with sponges benefitting from increased DOC and POC while having broader tolerance to acidification and temperature anomalies. Indeed, sponges are the oldest reef-associated organisms; they dominated reef building during various stages of the Paleozoic and Mesozoic when conditions to biomineralizers deteriorated (*28*).

In conclusion, the novel reef system off the Amazon River is extensive, is impoverished in terms of biodiversity, and presents unique functional attributes due to the plume influence. The system provides relevant ecosystem services and functions as a selective biogeographic corridor between the Caribbean and the South Atlantic Ocean, and may give important insights in terms of future scenarios for forecasting coralline reefs trajectories under acute climate changes. Remarkably, 125 exploratory blocks for oil drilling in the Amazon shelf were offered in an international auction in 2013, 35 of which were acquired by domestic and transnational companies. In the past decade, a total of 80 exploratory blocks have been acquired for oil drilling in the study region, 20 of which are already producing. These blocks will soon be producing oil in close proximity to the reefs, but the environmental baseline compiled by the companies and the Brazilian government is still incipient and largely based on sparse museum specimens (*13*). Such large-scale industrial activities present a major environmental challenge, and companies should catalyze a more complete social-ecological assessment of the system before impacts become extensive and conflicts among the stakeholders escalate. The feasibility of oil and gas operations may be assessed by considering environmental and social sensibilities, but even the extent of the overlap of exploratory blocks with sensitive areas remains unclear. The context of great proximity to international waters and to the French border adds complexity. It is relevant to consider further studies on regional marine spatial planning, the functioning of the new reef biome in face of global changes, and sensitivities related to the hydrologic cycle of the Amazon—where extreme droughts and floods are on the increase and will influence the functioning of this novel carbonate reef system.

MATERIALS AND METHODS

Experimental design

Sampling was carried out onboard R/V Knorr (May 2010), R/V Atlantis (July 2012), and NHo Cruzeiro do Sul (September 2014). A

complete station list of the three cruises is provided in table S5. To assess the effects of the dynamic river-ocean interface, sampling was stratified in (i) Northern Sector, representing the area under the strongest and permanent plume influence; (ii) Central Sector, under seasonal plume influence; and (iii) Southern Sector, under intermittent riverine influence (Fig. 1). Water column profiles were acquired with a conductivity-temperature-depth with a recorder (CTD), which was also equipped with sensors of PAR and DO at eight stations in 2010 and at nine stations in 2014 (table S5). Water was collected from near the surface, bottom, and in the chlorophyll maximum using Niskin bottles or surface pumps, and was analyzed for inorganic nutrients (*16*), DOC and POC (*16*, *72*), and microorganisms (*20*, *73*).

Bottom topography. We obtained 800 km of acoustic data with a Kongsberg EM122 Multibeam Echosounder in 2012. In 2014, we surveyed 500 km with two EdgeTech side scan sonars (model 4200, 100 to 400 kHz at stations 1 to 56; model 4100, 100 to 500 kHz at stations 67 to 100). Both surveys were carried out with ~300-m swath widths. Sonograms were processed with Sonar WizMap 5.03, converted into 1-m pixel images, and further vectored and submitted to supervised qualitative classification in a GIS environment. Classification was based on backscatter intensity and indirect topography (*74*).

Macrobenthic and demersal assemblages. We sampled 14 stations (5 in 2012 and 9 in 2014; Fig. 1) with heavy (150 kg) metal dredges with mouths of 100 to 150 by 40 to 80 cm and mesh nets of 1 cm^2 that were trawled at 1 to 1.5 knots for 5 to 20 min. Two box corer launches were done in six stations of the 2014 cruise, and a flat shrimp net (15-m mouth, 1.5-cm mesh in the cod end, and two 150-kg trawl doors) was trawled in three stations. Dredging, trawling, or box-coring covered stations in all three sectors. Specimens were washed in seawater, sorted, and photographed on board, and were further preserved in 80% ethanol or 5% formalin. Frozen or dried subsamples were kept for microbiological, genetic, and chemical analyses. Vouchers were deposited at the Museu Nacional, Universidade Federal do Rio de Janeiro, and at the Jardim Botânico do Rio de Janeiro. Crustose coralline algae, sponges, and fishes were identified with standard methods (*75*, *76*). Fisheries yields were obtained from unpublished governmental reports that refer to the last year during which Brazil monitored fisheries (2007). Only landings in Pará and Amapá were accounted for (Maranhão was excluded because its fleet extends southward to the Amazon River mouth).

Petrographic and isotopic analyses. Petrographic thin sections (30 μm) of carbonate rocks recovered in each sector were used to assess reef builders' identities and relative importance. Radiocarbon (^{14}C) ages were determined from the same samples, which included the surface and core of a larger carbonate block (~45 cm) from the Central Sector (80-m depth), and two superficial smaller (~20 cm) framework fragments from the North and Central Sector, obtained at depths of 120 and 23 m, respectively. Radiocarbon ages were derived from carbon reduction to graphite (100% C) after acid etch pretreatment, with subsequent detection in Accelerator Mass Spectrometry (Center for Applied Isotope Studies, University of Georgia). Dates were reported as 2σ calibrated (95% confidence) radiocarbon ages BP. Calibration was carried out using Calib 7.1 (available at http://calib.qub.ac.uk/calib/), Marine13 calibration curve, and assuming a global marine reservoir effect of 400 years (radiocarbon years before present, "present" = AD 1950). Organic matter samples were analyzed for C and N isotopes using an isotope ratio mass spectrometer (model DELTA V Advantage, Thermo Fisher Scientific) as described previously (*77*).

Secondary data sets. Literature data indicative of reefs and reef-associated biota were compiled and incorporated in the GIS (Fig. 2), including observations of high $CaCO_3$ sediments, magnesium calcite ooids [for example, Barreto *et al.* (*8*)], sponges and reef fish (*12*), and reef fisheries (*26*).

Metatranscriptomes from the plume and subplume. Microbial genes and transcripts were obtained from water samples obtained at six stations of the 2010 cruise (*73*) and two stations of the 2012 cruise, inside and outside the plume, and in the subplume. Data sets were generated by Illumina sequencing (150 × 150 base pairs overlapping paired-end reads) and were deposited in GenBank under accession number SRP037995 (*73*). Ribosomal sequences in RNA-seq data (complementary DNA sequencing) were identified and removed from metatranscriptome data sets using riboPicker tool (*73*). Identification of chemosynthesis-related genes (that is, sulfur oxidation, sulfate reduction, and anammox transcripts in the plume and subplume interface) was performed based on profile hidden Markov model (pHMM) approach. Full-length sulfur oxidation (SoxA, SoxB, SoxX, SoxY, and SoxZ), sulfate reduction (DsrA, DsrB, DsrJ, DsrK, DsrL, DsrM, DrsO, DrsP, AprA, and AprB), and anammox (NarB, NarG, NarH, NarI, NirA, NirB, NirK, and NirS) amino acid sequences obtained from the UniProtKB database (www.uniprot.org) were used as seed alignments. pHMM profiles of protein subunits families related to photosynthesis were also used for contrasting water layers, using both photosystem complexes: I (PsaF, PsaM, PsaN, and PsaAB) and II (PsbN, PsbI, PsbH, and PSII). Profiles were obtained directly from the Pfam database (PsaN-PF05479, PsaM-PF07465, PsaAB-PF00223, PsaF-PF02507, PsbN- PF02468, PsbI- PF02532, PSII- PF00421, and PsbH-PF00737). Multiple alignments were conducted using MAFFT (version 6.717b) (*78*, *79*) with the auto mode option, and pHMMs were built using hmmbuild functionality from HMMER package (version 3.0). Contigs assembled from metatranscriptomes were translated into six frames using the Transeq program from the EMBOSS package (v6.1.0) and used as the database for searching genes related to sulfur oxidation, sulfate reduction, and anammox metabolisms. Search was conducted using hmmersearch functionality from HMMER package of the pHMMs built against the plume database. Results were parsed and counted using Python, and shell scripts and relative abundance were calculated.

SUPPLEMENTARY MATERIALS

Supplementary material for this article is available at http://advances.sciencemag.org/cgi/content/full/2/4/e1501252/DC1

fig. S1. Trawl and dredge casts on ships' deck.
fig. S2. Sonographic images of the main reef megahabitats off the Amazon River mouth.
fig. S3. Carbonate fragments (A and B) and rhodoliths (C and D) sampled off the Amazon River mouth.
fig. S4. Representative species of sponges collected off the Amazon River mouth.
fig. S5. Representative species of corals and hydrocoral collected off the Amazon River mouth.
fig. S6. Representative reef fish species collected off the Amazon River mouth.
fig. S7. Fishing boat operating dinghies with hand lines and long lines near the shelf edge in the Northern Sector during the 2014 cruise.
fig. S8. Density of fishing operations targeting red snapper (*L. purpureus*) in 2010 off the Amazon mouth.
fig. S9. Depth profiles of salinity and DO measured during the R/V Cruzeiro do Sul cruise (September 2014).
fig. S10. Relative contribution of functions related to chemosynthesis and photosynthesis recorded outside, within, and underneath the Amazon River plume.

table S1. Algae recorded off the Amazon River mouth.
table S2. Sponges recorded off the Amazon River mouth.
table S3. Corals, hydrocorals, and gorgonians recorded off the Amazon River mouth.
table S4. Reef fish species recorded off the Amazon mouth [does not include species recorded at the Manuel Luis reefs; see de Moura *et al*. (*23*) and Rocha and Rosa (*44*)].
table S5. Oceanographic stations (primary data sources).
movie S1. Sampling the plume, subplume, and reefs off the Amazon river mouth during the NHo Cruzeiro do Sul cruise (2014).
Supplementary file. Shape files.
References (*81*–*85*)

REFERENCES AND NOTES

1. C. Birkeland, Ed. *Life and Death of Coral Reefs* (Chapman & Hall, New York, 1997).
2. W. N. Goldberg, *The Biology of Reefs and Reef Organisms* (The University of Chicago Press, Chicago, IL, 2013).
3. R. Riding, Structure and composition of organic reefs and carbonate mud mounds: Concepts and categories. *Earth Sci. Rev.* **58**, 163–231 (2002).
4. C. T. Perry, P. Larcombe, Marginal and non-reef-building coral environments. *Coral Reefs* **22**, 427–432 (2003).
5. J. D. Milliman, C. P. Summerhayes, H. T. Barreto, Quaternary sedimentation on the Amazon continental margin: A model. *Geol. Soc. Amer. Bull.* **86**, 610–614 (1975).
6. C. Gorini, B. U. Haq, A. T. dos Reis, C. G. Silva, A. Cruz, E. Soares, D. Grangeon, Late Neogene sequence stratigraphic evolution of the *Foz do Amazonas* Basin, Brazil. *Terra Nova* **26**, 179–185 (2014).
7. M. A. Maslin, E. Durham, S. J. Burns, E. Platzman, P. Grootes, S. E. J. Greig, M.-J. Nadeau, M. Schleicher, U. Pflaumann, B. Lomax, N. Rimington, Paleoreconstruction of the Amazon River freshwater and sediment discharge using sediments recovered at site 942 on the Amazon Fan. *J. Quaternary Sci.* **15**, 419–434 (2000).
8. L. A. Barreto, J. D. Milliman, C. A. B. Amaral, O. Francisconi, Upper continental margin sedimentation off Brazil, northern Brazil. *Contr. Sedimentol.* **4**, 11–43 (1975).
9. C. A. Nittrouer, D. J. DeMaster, The Amazon shelf setting: Tropical, energetic, and influenced by a large river. *Cont. Shelf Res.* **16**, 553–573 (1996).
10. J. Y. Aller, I. Stupakoff, The distribution and seasonal characteristics of benthic communities on the Amazon shelf as indicators of physical processes. *Cont. Shelf Res.* **16**, 717–751 (1996).
11. J. D. Milliman, H. T. Barretto, Relict magnesian calcite oolite on the Amazon shelf. *Sedimentology* **22**, 137–145 (1975).
12. B. B. Collette, K. Rützler, Reef fishes over sponge bottoms off the mouth of the Amazon river. *Proceedings of the 3rd International Coral Reef Symposium*, Miami, FL, 1977 May.
13. R. T. S. Cordeiro, B. M. Neves, J. S. Rosa-Filho, C. D. Pérez, Mesophotic coral ecosystems occur offshore and north of the Amazon River. *Bull. Mar. Sci.* **91**, 491–510 (2015).
14. N. D. Ward, A. V. Krusche, H. O. Sawakuchi, D. C. Brito, A. C. Cunha, J. M. S. Moura, R. da Silva, P. L. Yager, R. G. Keil, J. E. Richey, The compositional evolution of dissolved and particulate organic matter along the lower Amazon River—Óbidos to the ocean. *Mar. Chem.* **177**, 244–256 (2015).
15. V. J. Coles, M. T. Brooks, J. Hopkins, M. R. Stukel, P. L. Yager, R. R. Hood, The pathways and properties of the Amazon River plume in the tropical North Atlantic Ocean. *J. Geophys. Res.* **118**, 6894–6913 (2013).
16. J. I. Goes, H. do Rosario Gomes, A. M. Chekalyuk, E. J. Carpenter, J. P. Montoya , V. J. Coles, P. L. Yager, W. M. Berelson, D. G. Capone, R. A. Foster, D. K. Steinberg, A. Subramaniam, M. A. Hafez, Influence of the Amazon River discharge on the biogeography of phytoplankton communities in the western tropical north Atlantic. *Prog. Oceanogr.* **120**, 29–40 (2014).
17. A. Subramaniam, P. L. Yager, E. J. Carpenter, C. Mahaffey, K. Björkman, S. Cooley, A. B. Kustka, J. P. Montoya, S. A. Sañudo-Wilhelmy, R. Shipe, D. G. Capone, Amazon River enhances diazotrophy and carbon sequestration in the tropical North Atlantic Ocean. *Proc. Natl. Acad. Sci. U.S.A.* **105**, 10460–10465 (2008).
18. L. S. Chong, W. M. Berelson, J. McManus, D. E. Hammond, N. E. Rollins, P. L. Yager, Carbon and biogenic silica export influenced by the Amazon River Plume: Patterns of remineralization in deep-sea sediments. *Deep Sea Res. Pt. I* **85**, 124–137 (2014).
19. N. E. Blair, R. C. Aller, Anaerobic methane oxidation on the Amazon shelf. *Geochim. Cosmochim. Acta* **59**, 3707–3715(1995).
20. B. M. Satinsky, B. C. Crump, C. B. Smith, S. Sharma, B. L. Zielinski, M. Doherty, J. Meng, S. Sun, P. M. Medeiros, J. H. Paul, V. J. Coles, P. L. Yager, M. A. Moran, Microspatial gene expression patterns in the Amazon River Plume. *Proc. Natl. Acad. Sci. U.S.A.* **111**, 11085–11090 (2014).
21. P. Miloslavich, E. Klein, J. M. Díaz, C. E. Hernández, G. Bigatti, L. Campos, F. Artigas, J. Castillo, P. E. Penchaszadeh, P. E. Neill, A. Carranza, M. V. Retana, J. M. Díaz de Astarloa, M. Lewis, P. Yorio, M. L. Piriz, D. Rodríguez, Y. Yoneshigue-Valentin, L. Gamboa, A. Martín, Marine biodiversity in the Atlantic and Pacific coasts of South America: Knowledge and gaps. *PLOS One* **6**, e14631 (2011).
22. O. J. Luiz, J. S. Madin, D. R. Robertson, L. A. Rocha, P. Wirtz, S. R. Floeter, Ecological traits influencing range expansion across large oceanic dispersal barriers: Insights from tropical Atlantic reef fishes. *Proc. R. Soc. B* **279**, 1033–1040 (2011).
23. R. L. de Moura, M. C. Martins Rodrigues, R. B. Francini-Filho, I. Sazima, Unexpected richness of reef corals near the southern Amazon River mouth. *Coral Reefs* **18**, 170 (1999).
24. L. A. Rocha, Patterns of distribution and processes of speciation in Brazilian reef fishes. *J. Biogeogr.* **30**, 1161–1171 (2003).
25. CREOCEAN, Évaluation de l'évolution des peuplementshalieutiques des zones adjacente-setéloignées au site. Première campagne–avant acquisition sismique (Shell E&P France, Le Lamentin, Martinique, 2012).
26. IBAMA, *Instituto Brasileiro do Meio Ambiente e dos Recursos Naturais Renováveis. Estatística da Pesca no Brasil. Grandesregiões e unidades da federação* (Ministério do Meio Ambiente, Brasília, Brasil, 2007); http://www.ibama.gov.br/documentos-recursos-pesqueiros/estatistica-pesqueira.
27. F. Hiemstra, R. W. M. van Soest, *Didiscus verdensis* spec. nov. (Porifera: Halichondrida) from the Cape Verde Islands, with a revision and phylogenetic classification of the genus *Didiscus*. *Zoölogische Mededelingen* **65**, 39–52 (1991).
28. W. Kiessling, Geologic and biologic controls on the evolution of reefs. *Annu. Rev. Ecol. Evol. Syst.* **40**, 173–192 (2009).
29. D. R. Bellwood, C. H. R. Goatley, S. J. Brandl, O. Bellwood, Fifty million years of herbivory on coral reefs: Fossils, fish and functional innovations. *Proc. R. Soc. B.* **281**, 20133046 (2014).
30. M. S. Foster, Rhodoliths: Between rocks and soft places. *J. Geophys. Res.* **37**, 659–667(2001).
31. G. M. Amado-Filho, R. L. Moura , A. C. Bastos, L. T. Salgado, P. Y. Sumida, A. Z. Guth, R. B. Francini-Filho, G. H. Pereira-Filho, D. P. Abrantes, P. S. Brasileiro, R. G. Bahia, R. N. Leal, L. Kaufman, J. A. Kleypas, M. Farina, F. L. Thompson, Rhodolithbedsare beds are major $CaCO_3$bio-factories in the Tropical South West Atlantic. *PLOS One* **7**, e35171 (2012).
32. L. S. Eluik, Siliceous sponge communities, biological zonation, and recent sea-level change on the Arctic margin: Ice island results: Discussion. *Can. J. Earth Sci.* **28**, 459–462 (1991).
33. M. D. Spalding, C. Ravilious, E. P. Green, *World Atlas of Coral Reefs* (University of California Press, Berkeley, CA, 2001).
34. R. L. Moura, N. A. Secchin, G. M. Amado-Filho, R. B. Francini-Filho, M. O. Freitas, C. V. Minte-Vera, J. B. Teixeira, F. L. Thompson, G. F. Dutra, P. Y. G. Sumida, A. Z. Guth, R. M. Lopes, A. C. Bastos, Spatial patterns of benthic megahabitats and conservation planning in the Abrolhos Bank. *Cont. Shelf Res.* **70**, 109–117 (2013).
35. C. K. Sommerfield, C. A. Nittrouer, A. G. Figueiredo, Stratigraphic evidence of changes in Amazon shelf sedimentation during the late Holocene. *Mar. Geol.* **125**, 351–371 (1995).
36. C. T. Perry, S. G. Smithers, Evidence for the episodic "turn-on" and "turn-off" of turbid-zone coral reefs during the late Holocene sea-level highstand. *Geology* **38**, 119–122 (2010).
37. G. Olavo, P. C. S. Costa, A. S. Martins, B. P. Ferreira, Shelf-edge reefs as priority areas for conservation of reef fish diversity in the tropical Atlantic. *Aquat. Conserv.* **21**, 199–209 (2011).
38. H. T. Pinheiro, E. Mazzei, R. L. Moura, G. M. Amado-Filho, A. Carvalho-Filho, A. C. Braga; P. A. S. Costa, B. P. Ferreira, C. E. L. Ferreira, S. R. Floeter, R. B. Francini-Filho, J. L. Gasparini, R. M. Macieira, A. S. Martins, G. Olavo, C.R. Pimentel, L. A. Rocha, I. Sazima, T. Simon, J. B. Teixeira, L. B. Xavier, J.-C. Joyeaux, Fish biodiversity of the vitória-trindade seamount chain, Southwestern Atlantic: An updated database. *PLOS One* **10**, e0118180 (2015).
39. P. M. Meirelles, G. M. Amado-Filho, G. H. Pereira-Filho, H. T. Pinheiro, R. L. de Moura, J.-C. Joyeux, E. F. Mazzei, A. C. Bastos, R. A. Edwards, E. Dinsdale, R. Paranhos, E. O. Santos, T. Iida, K. Gotoh, S. Nakamura, T. Sawabe, C. E. Rezende, L. M. R. Gadelha Jr., R. B. Francini-Filho, C. Thompson, F. L. Thompson, Baseline assessment of mesophotic reefs of the Vitória-Trindade seamountchain based on water quality, microbial diversity, benthic cover and fish biomass data. *PLOS One* **10**, e0130084 (2015).
40. C. H. L. Schönberg, J. Fromont, Sponge gardens of Ningaloo Reef (Carnarvon Shelf, Western Australia) are biodiversity hotspots. *Hydrobiologia* **687**, 143–161 (2011).
41. J. J. Bell, S. K. Davy, T. Jones, M. W. Taylor, N. S. Webster, Could some coral reefs become sponge reefs as our climate changes? *Glob. Change Biol.* **19**, 2613–2624 (2013).
42. A. B. Klitgaard, O. S. Tendal, Distribution and species composition of mass occurrences of large-sized sponges in the northeast Atlantic. *Prog. Oceanogr.* **61**, 57–98 (2004).
43. L. I. Beazley, E. L. Kenchington, F. J. Murillo, M. del Mar Sacau, Deep-sea sponge grounds enhance diversity and abundance of epibenthic megafauna in the Northwest Atlantic. *ICES J. Mar. Sci.* **70**, 1471–1490 (2013).
44. L. A. Rocha, I. L. Rosa, Baseline assessment of reef fish assemblages of Parcel Manuel Luiz Marine State Park, Maranhão, north-east Brazil. *J. Fish Biol.* **58**, 985–998 (2001).
45. C. R. Wilkinson, Ed., *Status of Coral Reefs of the World: 2008* (Global Coral Reef Monitoring Network and Reef and Rainforest Research Centre, Townsville, Australia, 2008).
46. L. A. Pinheiro, F. L. Frédou, Caracterizaçãogeral de pesca industrial desembarcada no estado do Pará. *Rev. Cient. Universidade Federal doPará* **4**, 1–16 (2004).
47. K. C. Araujo-Silva, I. H. A. Cintra, M. Ramos-Porto, G. F. S. Viana, Lagostas capturadas na plataforma continental do estado do Amapá (Crustacea, Nephropoidea, Palinuroidea). *Bol. Téc. Cient. CEPNOR* **7**, 173–184 (2007).
48. A. A. Fonteles-Filho, Síntese sobre distribuição, abundância, potencial pesqueiro e biologia lagosta-vermelha *Panulirus argus* (Latreille) e a lagosta-verde *Panulirus laevicauda* (Latreille) do nordeste do Brasil (Ministério do Meio Ambiente/Recursos Vivos na Zona Econômica Exclusiva, Brasília, Brasil, 2008).
49. E. A. Chávez, Potential production of the Caribbean spiny lobster (Decapoda, Palinura) fisheries. *Crustaceana* **82**, 1393–1412 (2009).

50. G. Muricy, D. A. Lopes, E. Hajdu, M. S. Carvalho, F. C. Moraes, M. Klautau, C. Menegola, U. Pinheiro, *Catalogue of Brazilian Porifera* (Museu Nacional, Rio de Janeiro, 2011).
51. L. A. Rocha, B. W. Bowen, Speciation in coral reef fishes. *J. Fish Biol.* **72**, 1101–1121 (2008).
52. R. L. Moura, I. Sazima, Species richness and endemism levels of the Southwestern Atlantic reef fish fauna, *Ninth International Coral Reef Symposium*, Bali, Indonesia, 23–27 October 2000.
53. S. R. Floeter, , L. A. Rocha, D. R. Robertson, J. C. Joyeux, W. F. Smith-Vaniz, P. Wirtz, A. J. Edwards, J. P. Barreiros, C. E. L. Ferreira, J. L. Gasparini, A. Brito, J. M. Falcón, B. W. Bowen, G. Bernardi, Atlantic reef fish biogeography and evolution. *J. Biogeogr.* **35**, 22–47 (2008).
54. D. E. Canfield, F. J. Stewart, B. Thamdrup, L. De Brabandere, T. Dalsgaard, E. F. Delong, N. P. Revsbech, O. Ulloa, A cryptic sulfur cycle in oxygen-minimum–zone waters off the Chilean coast. *Science* **330**, 1375–1378 (2010).
55. R. B. Francini-Filho, E. O. C. Coni, P. M. Meirelles, G. M. Amado-Filho, F. L. Thompson, G. H. Pereira-Filho, A. C. Bastos, D. P. Abrantes, C. M. Ferreira, F. Z. Gibran, A. Z. Güth, P. Y. G. Sumida, N. L. Oliveira, L. Kaufman, C. V. Minte-Vera, R. L. Moura, Dynamics of coral reef benthic assemblages of the Abrolhos Bank, Eastern Brazil: Inferences on natural and anthropogenic drivers. *PLOS One* **8**, 54260 (2013).
56. G. Hendler, S. J. Brugneaux, New records of brittle stars from French Guiana: *Ophiactissa-vignyi* and the alien species *Ophiothela mirabilis* (Echinodermata: phiuroidea). *Mar. Biodiv. Rec.* **6**, 113 (2013).
57. O. J. Luiz, S. R. Floeter, L. A. Rocha, C. E. L. Ferreira, Perspectives for the lionfish invasion in the South Atlantic: Are Brazilian reefs protected by the currents? *Mar. Ecol. Prog. Ser.* **485**, 1–7 (2013).
58. T. Bruce, P. M. Meirelles, G. Garcia, R. Paranhos, C. E. Resende, R. L. de Moura, R.-F. Filho, E.O. C. Coni, A. T. Vasconcelos, G. A. Filho, M. Hatay, R. Schmieder, R. Edwards, E. Dinsdale, F. L. Thompson, Abrolhos bank reef health evaluated by means of water quality, microbial diversity, benthic cover, and fish biomassa data. *PLOS One* **7**, e36687 (2012).
59. D. B. Mills, L. M. Warda, C. Jones, B. Sweetena, M. Forth, A.H. Treusch, D. E. Canfield, Oxygen requirements of the earliest animals. *Proc. Natl. Acad. Sci. U.S.A.* **111**, 4168–4172 (2014).
60. V. Gloeckner, M. Wehrl, L. Moitinho-Silva, C. Gernert, P. Schupp, J. R. Pawlik, N. L. Lindquist, D. Erpenbeck, G. Wörheide, U. Hentschel, The HMA-LMA dichotomy revisited: An electron microscopical survey of 56 sponge species. *Biol. Bull.* **227**, 78–88 (2014).
61. J. M. de Goeij, D. van Ovelen, M. J. A. Vermeij, R. Osinga, J. J. Middelburg, A. F. P. M. Goeij, W. Admiraal, Surviving in a marine desert: The sponge loop retains resources within coral reefs. *Science* **342**, 108–110 (2013).
62. C. B. Silveira, A. W. Silva-Lima, R. B. Francini-Filho, J. S.M. Marques, M. G. Almeida, C. C. Thompson, C. E. Rezende, R. Paranhos, R. L. Moura, P. S. Salomon, F. L. Thompson, Microbial and sponge loops modify fish production in phase-shifting coral reefs. *Environ. Microbiol.* **17**, 3832–3846 (2015).
63. R. S. Robinson, M. Kienast, A. L. Albuquerque, M. Altabet, S. Contreras, R. De Pol Holz, N. Dubois, R. Francois, E. Galbraith, T.-C. Hsu, T. Ivanochko, S. Jaccard, S.-J. Kao, T. Kiefer, S. Kienast, M. Lehmann, P. Martinez, M. M. Carthy, J. Möbius, T. Pedersen, T. M. Quan, E. Ryabenko, A. Schmittner, R. Schneider, A. Schneider-Mor, M. Shigemitsu, D. Sinclair, C. Somes, A. Studer, R. Thunell, J.-Y. Yang, A review of nitrogen isotopic alteration in marine sediments. *Paleoceanography* **27**, PA4203 (2012).
64. T. Dittmar, R. J. Lara, G. Kattner, River or mangrove? Tracing major organic matter sources in tropical Brazilian coastal waters. *Mar. Chem.* **73**, 253–271 (2001).
65. T. Dittmar, N. Hertkorn, G. Kattner, R. J. Lara, Mangroves, a major source of dissolved organic carbon to the oceans. *Global Biogeoch. Cycles* **20**, GB1012 (2006).
66. O. Hoegh-Guldberg, P. J. Mumby, A. J. Hooten, R. S. Steneck, P. Greenfield, E. Gomez, C. D. Harvell, P. F. Sale, A. J. Edwards, K. Caldeira, N. Knowlton, C. M. Eakin, R. Iglesias-Prieto, N. Muthiga, R. H. Bradbury, A. Dubi, M. E. Hatziolos, Coral reefs under rapid climate change and ocean acidification. *Science* **318**, 1737–1742 (2007).
67. P. Descombes, M. S. Wisz, F. Leprieur, V. Parravicini, C. Heine, S. M. Olsen, D. Swingedouw, M. Kulbicki, D. Mouillot, L. Pellissier, Forecasted coral reef decline in marine biodiversity hotspots under climate change. *Glob. Change Biol.* **21**, 2479–2487 (2015).
68. J. M. Pandolfi, S. R. Connolly, D. J. Marshall, A. L. Cohen, Projecting coral reef futures under global warming and ocean acidification. *Science* **333**, 418–422 (2011).
69. A. J. Andersson, F. T. Mackenzie, A. Lerman, Coastal ocean and carbonate systems in the high CO_2 world of the anthropocene. *Am. J. Sci.* **305**, 875–918(2005).
70. B. W. Bowen, L. A. Rocha, R. J. Toonen, S. A. Karl; ToBo Laboratory, The origins of tropical marine biodiversity. *Trends Ecol. Evol.* **28**, 359–366(2013).
71. A. V. Norström, M. Nyström, J. Lokrantz, C. Folke, Alternative states on coral reefs: Beyond coral–macroalgal phase shifts. *Mar. Ecol. Prog. Ser.* **376**, 295–306 (2009).
72. P. M. Medeiros, M. Seidel, N. D. Ward, E. J. Carpenter, H. R. Gomes, J. Niggemann, A. V. Krusche, J. E. Richey, P. L. Yager, T. Dittmar, Fate of the Amazon River dissolved organic matter in the tropical Atlantic Ocean. *Global Biogeochem. Cy.* **29**, 677–690 (2015).
73. B. M. Satinsky, B. L. Zielinski, M. Doherty, C. B. Smith, S. Sharma, J. H. Paul, B.C. Crump, M. A. Moran, The Amazon continuum dataset: Quantitative metagenomic and metatranscriptomic inventories of the Amazon River plume, June 2010. *Microbiome* **2**, 17 (2014).
74. G. S. Cavalcanti, G. B. Gregoracci, E. O. dos Santos, C. B. Silveira, P. M. Meirelles, L. Longo, K. Gotoh, S. Nakamura, T. Iida, T. Sawabe, C. E. Rezende, R. B. Francini-Filho, R. L. Moura, G. M. Amado-Filho, F. L. Thompson, Physiologic and metagenomic attributes of the rhodoliths forming the largest $CaCO_3$ bed in the South Atlantic Ocean. *ISME J.* **8**, 52–62 (2014).
75. H. G. Greene, J. J. Bizzarro, V. M. O'Connell, C. K. Brylinsky, Mapp. *Seafloor Habitat Charact.* 141–155 (2007).
76. J. N. A. Hooper, R. W. M. van Soest, Eds., *Systema Porifera: A Guide to the Classification of Sponges* (Kluwer Academic/Plenum Press, New York, 2002).
77. G. D. Farquhar, J. R. Ehleringer, K. T. Hubick, Carbon isotope discrimination and photosynthesis. *Annu. Rev. Plant Phys.* **40**, 503–537 (1989).
78. R. Schmieder, Y. W. Lim, R. Edwards, Identification and removal of ribosomal RNA sequences from metatranscriptomes. *Bioinformatics* **28**, 433–435 (2012).
79. K. Katoh, K. Misawa, K.-i. Kuma, T. Miyata, MAFFT: A novel method for rapid multiple sequence alignment based on fast Fourier transform. *Nucleic Acids Res.* **30**, 3059–3066 (2002).
80. J. Salisbury, D. Vandemark, J. Campbell, C. Hunt, D. Wisser, N. Reul, B. Chapron, Spatial and temporal coherence between Amazon River discharge, salinity, and light absorption by colored organic carbon in western tropical Atlantic surface waters. *J. Geophys. Res.* **116**, C00H02 (2011).
81. R. W. Buddemeier, S. V. Smith, Coral adaptation and acclimatization: A most ingenious paradox. *AmerZool* **39**, 1–9 (1999).
82. P. S. Brasileiro, thesis, EscolaNacional de Botânica Tropical, Rio de Janeiro (2013).
83. R. G. Bahia, thesis, EscolaNacional de Botânica Tropical, Rio de Janeiro (2014).
84. R. K. Pang, The systematics of some Jamaican excavating sponges (Porifera). *Postilla* **161**, 1–75 (1973).
85. L. V. Barros, G. G. Santos, U. Pinheiro, *Clathria* (*Clathria*) Schmidt, 1862 from Brazil with description of a new species and a review of records (Poecilosclerida: Demospongiae: Porifera). *Zootaxa* **3640**, 284–295 (2013).

Acknowledgments: We thank J. C. Braga for the help with petrographic interpretations and J. Montoya, P. Medeiros, and V. Coles for providing oceanographic data. **Funding:** Conselho Nacional de Desenvolvimento Científico e Tecnológico (CNPq), Coordenadoria de Aperfeiçoamento de Pessoal de Nível Superior (CAPES), Fundação Carlos Chagas Filho de Amparo à Pesquisa do Estado do Rio de Janeiro (FAPERS), Fundação de Amparo à Pesquisa do Estado de São Paulo (FAPESP), and Brasoil provided essential funding. MCTI and the Brazilian Navy provided support with the NHo Cruzeiro do Sul in 2014. Expeditions in 2010 (R/V Knorr) and 2012 (R/V Atlantis) were funded by U.S. NSF (OCE-0934095 to P.L.Y.). Additional support was provided by the Gordon and Betty Moore Foundation (GBMF #2293 and #2928 to P.L.Y.). **Author contributions:** C.E.R. and F.L.T. coordinated the project. R..L.M., P.L.Y., C.E.R., and F.L.T. designed and coordinated the fieldwork. R.L.M., C.E.R., G.M.A.-F., A.C.B., F.C.M., P.L.Y., and F.L.T. wrote the paper. P.S.B., P.S.S., M.M.M., M.G.A., J.M.S., B.F.A., F.P.B., T.P.R., B.C.V.O., R.G.B., R.P.P., R.J.S.D., E.S., A.G.F., C.V.L., E.H., N.E.A., G.B.G., S.N.-L., P.L.Y., R.B.F.-F., A.F., M.C., B.S.S., A.P.B.M., L.O., A.C.S., R.C.P., L.A., N.L.O., J.B.T., C.C.T., and R.A.B.V. contributed with data and data analyses. **Competing interests:** The authors declare that they have no competing interests. **Data and materials availability:** All data used to obtain the conclusions in this paper are available online in the Brazilian Marine Biodiversity database (http://marinebiodiversity.lncc.br/files/index.php/s/TaLwiKC6QCiOvnY) and in the Biological and Chemical Oceanography Data Management Office (www.bco-dmo.org/project/2097).

Submitted 10 September 2015
Accepted 25 March 2016
Published 22 April 2016
10.1126/sciadv.1501252

Citation: R. L. Moura, G. M. Amado-Filho, F. C. Moraes, P. S. Brasileiro, P. S. Salomon, M. M. Mahiques, A. C. Bastos, M. G. Almeida, J. M. Silva Jr., B. F. Araujo, F. P. Brito, T. P. Rangel, B. C. V. Oliveira, R. G. Bahia, R. P. Paranhos, R. J. S. Dias, E. Siegle, A. G. Figueiredo Jr., R. C. Pereira, C. V. Leal, E. Hajdu, N. E. Asp, G. B. Gregoracci, S. Neumann-Leitão, P. L. Yager, R. B. Francini-Filho, A. Fróes, M. Campeão, B. S. Silva, A. P. B. Moreira, L. Oliveira, A. C. Soares, L. Araujo, N. L. Oliveira, J. B. Teixeira, R. A. B. Valle, C. C. Thompson, C. E. Rezende, F. L. Thompson, An extensive reef system at the Amazon River mouth. *Sci. Adv.* **2**, e1501252 (2016).

An extensive reef system at the Amazon River mouth

Rodrigo L. Moura, Gilberto M. Amado-Filho, Fernando C. Moraes, Poliana S. Brasileiro, Paulo S. Salomon, Michel M. Mahiques, Alex C. Bastos, Marcelo G. Almeida, Jomar M. Silva, Jr, Beatriz F. Araujo, Frederico P. Brito, Thiago P. Rangel, Braulio C. V. Oliveira, Ricardo G. Bahia, Rodolfo P. Paranhos, Rodolfo J. S. Dias, Eduardo Siegle, Alberto G. Figueiredo, Jr, Renato C. Pereira, Camille V. Leal, Eduardo Hajdu, Nils E. Asp, Gustavo B. Gregoracci, Sigrid Neumann-Leitão, Patricia L. Yager, Ronaldo B. Francini-Filho, Adriana Fróes, Mariana Campeão, Bruno S. Silva, Ana P. B. Moreira, Louisi Oliveira, Ana C. Soares, Lais Araujo, Nara L. Oliveira, João B. Teixeira, Rogerio A. B. Valle, Cristiane C. Thompson, Carlos E. Rezende and Fabiano L. Thompson (April 22, 2016)

Sci Adv 2016, 2:.
doi: 10.1126/sciadv.1501252

Science Advances

AAAS

advances.sciencemag.org/cgi/content/full/2/4/e1501252/DC1

Supplementary Materials for

An extensive reef system at the Amazon River mouth

Rodrigo L. Moura, Gilberto M. Amado-Filho, Fernando C. Moraes, Poliana S. Brasileiro, Paulo S. Salomon, Michel M. Mahiques, Alex C. Bastos, Marcelo G. Almeida, Jomar M. Silva Jr., Beatriz F. Araujo, Frederico P. Brito, Thiago P. Rangel, Braulio C. V. Oliveira, Ricardo G. Bahia, Rodolfo P. Paranhos, Rodolfo J. S. Dias, Eduardo Siegle, Alberto G. Figueiredo Jr., Renato C. Pereira, Camille V. Leal, Eduardo Hajdu, Nils E. Asp, Gustavo B. Gregoracci, Sigrid Neumann-Leitão, Patricia L. Yager, Ronaldo B. Francini-Filho, Adriana Fróes, Mariana Campeão, Bruno S. Silva, Ana P. B. Moreira, Louisi Oliveira, Ana C. Soares, Lais Araujo, Nara L. Oliveira, João B. Teixeira, Rogerio A. B. Valle, Cristiane C. Thompson, Carlos E. Rezende, Fabiano L. Thompson

Published 22 April 2016, *Sci. Adv.* **2**, e1501252 (2016)
DOI: 10.1126/sciadv.1501252

This PDF file includes:

- table S3. Corals, hydrocorals, and gorgonians recorded off the Amazon River mouth.
- table S4. Reef fish species recorded off the Amazon mouth [does not include species recorded at the Manuel Luis reefs; see de Moura *et al.* (*23*) and Rocha and Rosa (*44*)].
- table S5. Oceanographic stations (primary data sources).
- Legend for supplementary file
- References (*81–85*)

Other Supplementary Material for this manuscript includes the following:
(available at advances.sciencemag.org/cgi/content/full/2/4/e1501252/DC1)

- movie S1 (.mp4 format). Sampling the plume, subplume, and reefs off the Amazon river mouth during the NHo Cruzeiro do Sul cruise (2014).
- Supplementary file. Shape files.

Supplementary Figures

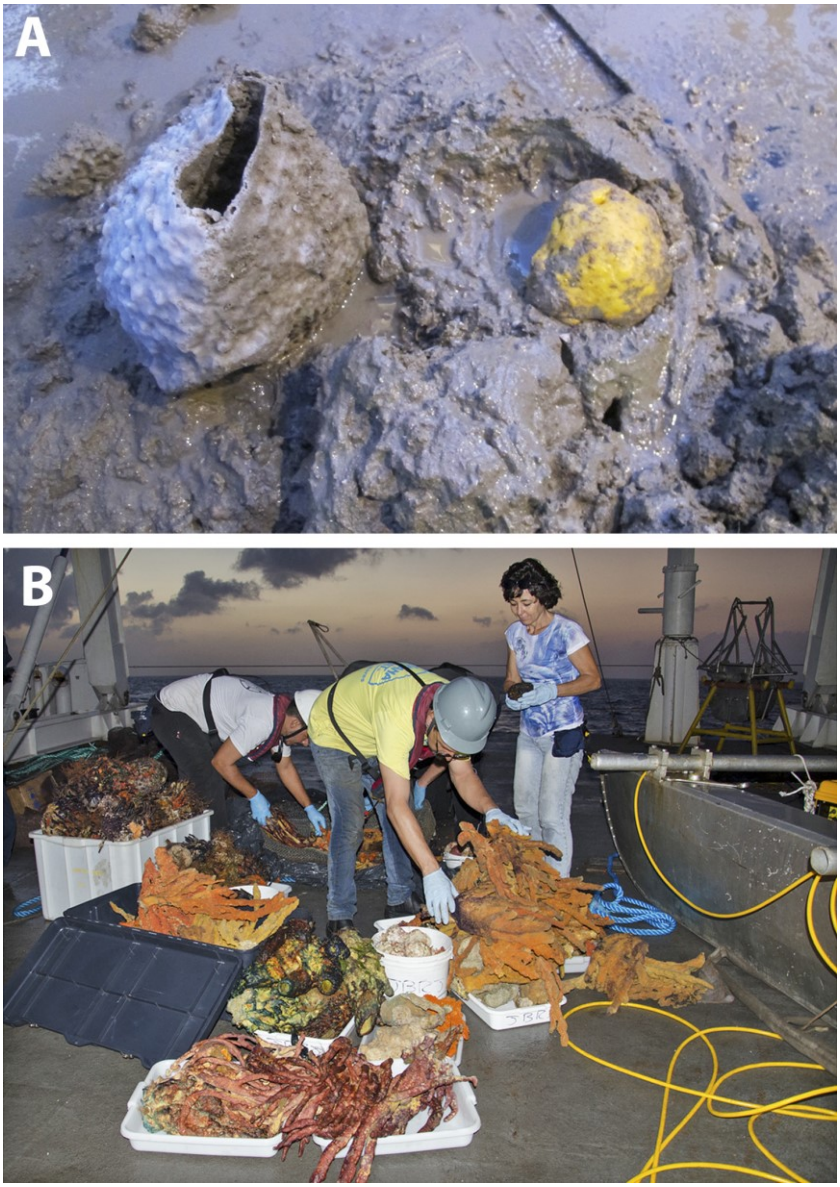

fig. S1. Trawl and dredge casts on ships' deck. (**A**) Northern Sector, mixed hard-muddy bottom [pale *Xestospongia muta* (left) and *Cinachyrella halientela* (right); (**B**) Central sector, rhodolith-covered bottom [from the left to the right: *Oceanapia bartschi* (largest white box), *Clathria nicoleae* (black box and large pile on the right), yellow and dark *Aplysina lacunosa* (tray) and rhodoliths (bucket), pinkish *Aplysina fulva* and pale *Callyspongia vaginalis* (lower tray), and orange *Clathria nicoleae* (larger pile on the right)]. [photo credit: F. Moraes, Instituto de Pesquisas Jardim Botânico do Rio de Janeiro]

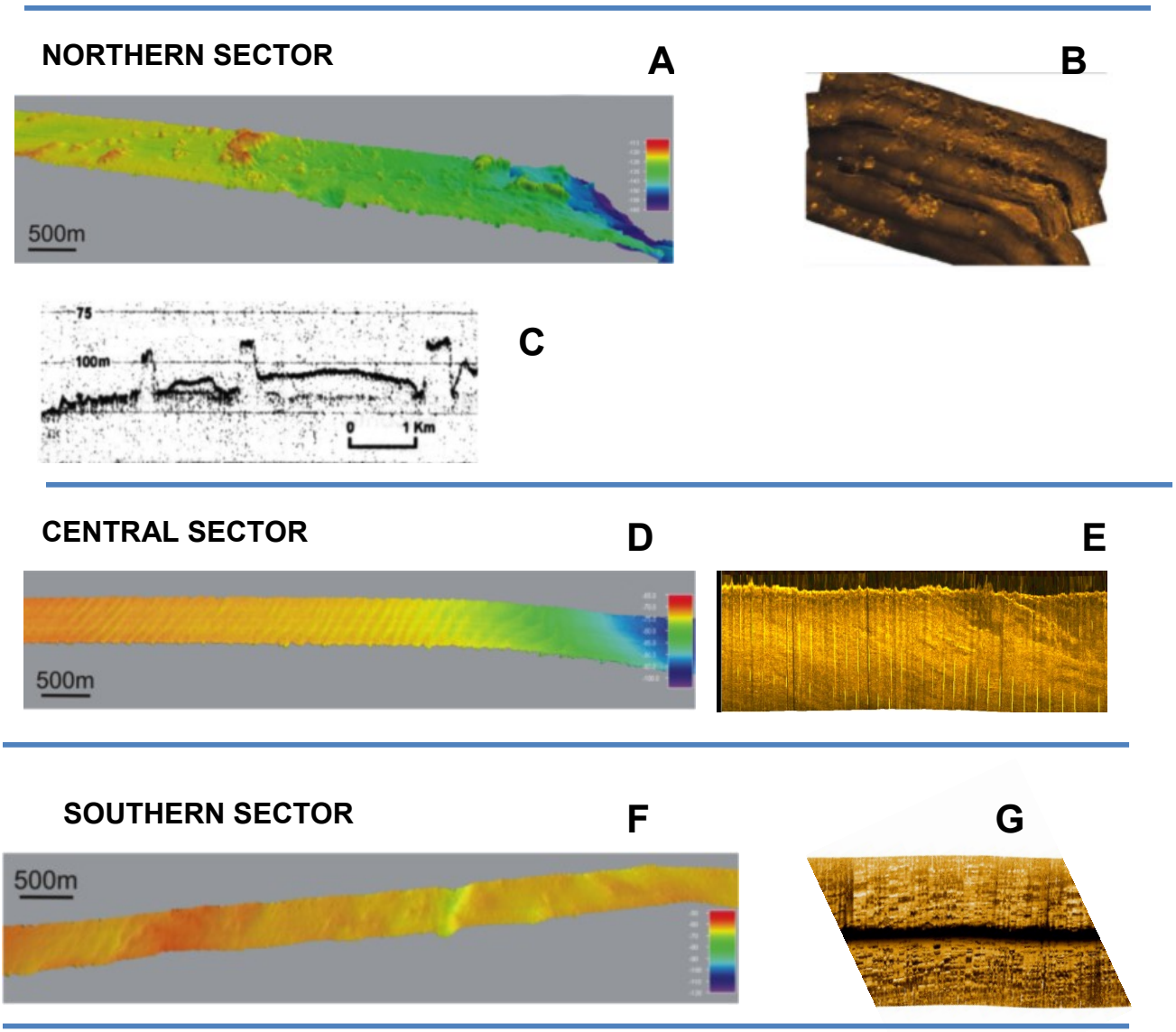

fig. S2. Sonographic images of the main reef megahabitats off the Amazon River mouth. **(A)** Cross-shelf multibeam transect evidencing high-relief erosive structures in the outer shelf; **(B)** Sidescan sonar images of structures among non-reflective (soft) sediments; **(C)** Echosounder profile (3 kHz) of outer shelf structures; **(D)** Cross-shelf multibeam transect evidencing the lower relief outer shelf in the Central Sector; **(E)** Sidescan sonar image evidencing the flat and highly reflective bottom typical of rhodolith beds (outer shelf); **(F)** Cross-shelf multibeam transect evidencing the rugose relief and higher density of structures; **(G)** Sidescan sonar image evidencing high density of structures among a reflective (rhodolith) bottom. Multibeam transects from the R/V Atlantis cruise (2012) and Sidescan sonar images from NhO Cruzeiro do Sul cruise.

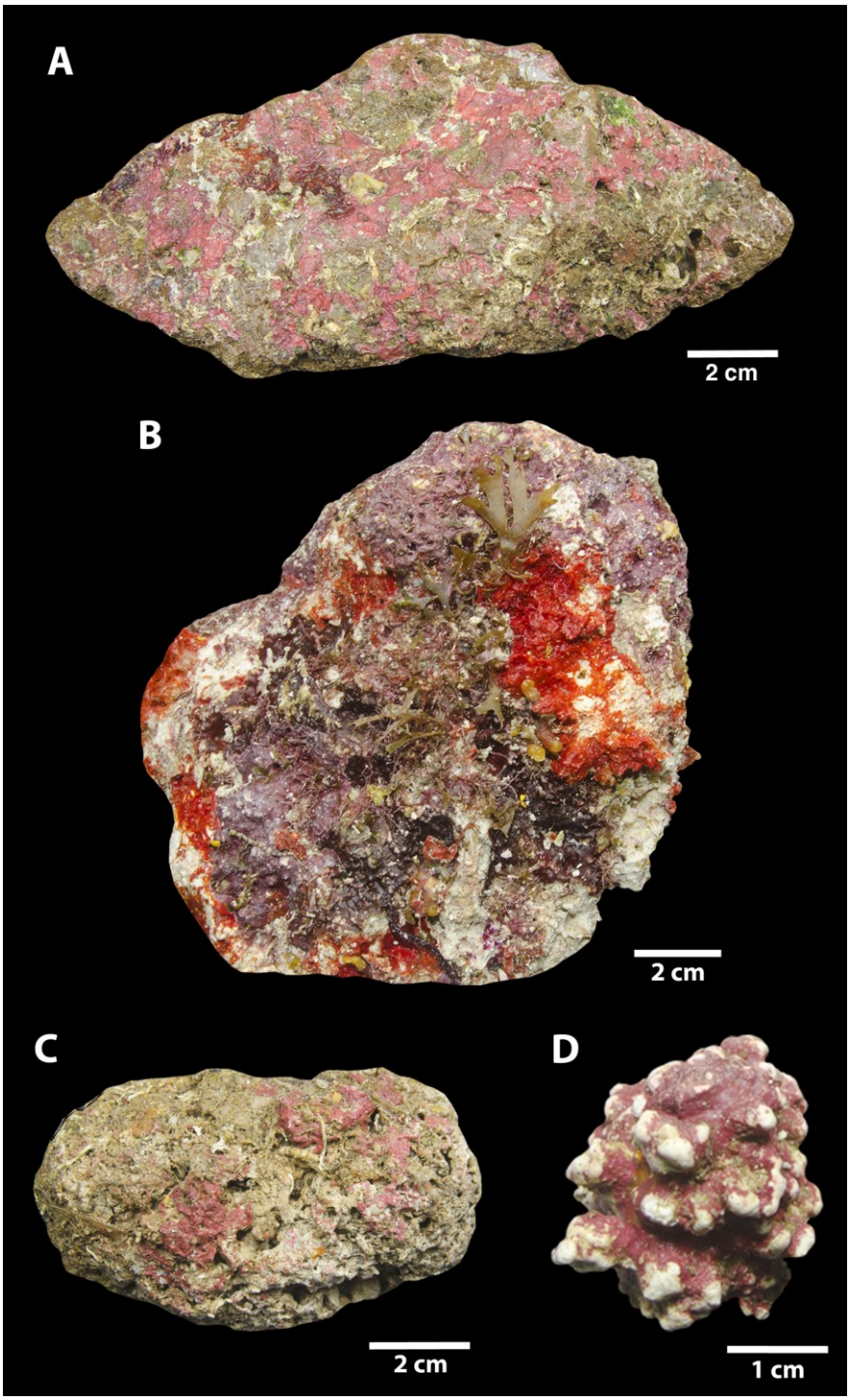

fig. S3. Carbonate fragments (A and B) and rhodoliths (C and D) sampled off the Amazon River mouth. Note pink patches indicating live crustose calcareous algae (pictures taken shortly after collection). **(A)** Northern Sector, 120 m; **(B)** Southern Sector, 23 m; **(C)** Central Sector, 95 m; **(D)** Southern Sector, 55m.

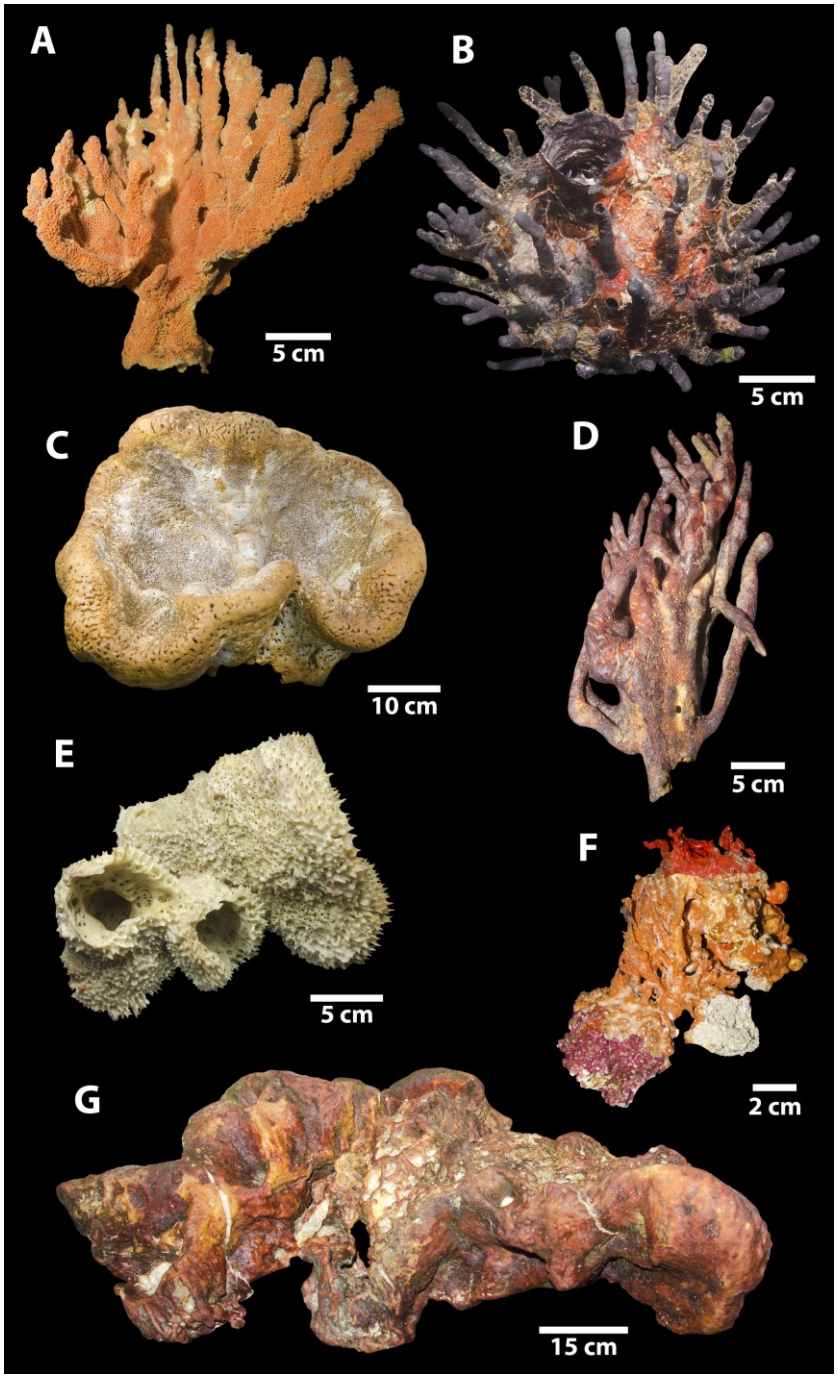

fig. S4. Representative species of sponges collected off the Amazon River mouth. (A) *Clathria nicoleae*; **(B)** *Oceanapia bartschi*; **(C)** *Agelas clathrodes*; **(D)** *Aplysina fulva*; **(E)** *Callyspongia vaginalis*; **(F)** *Monanchora arbuscula* (attached to live and dead rhodoliths); **(G)** *Geodia neptuni*.

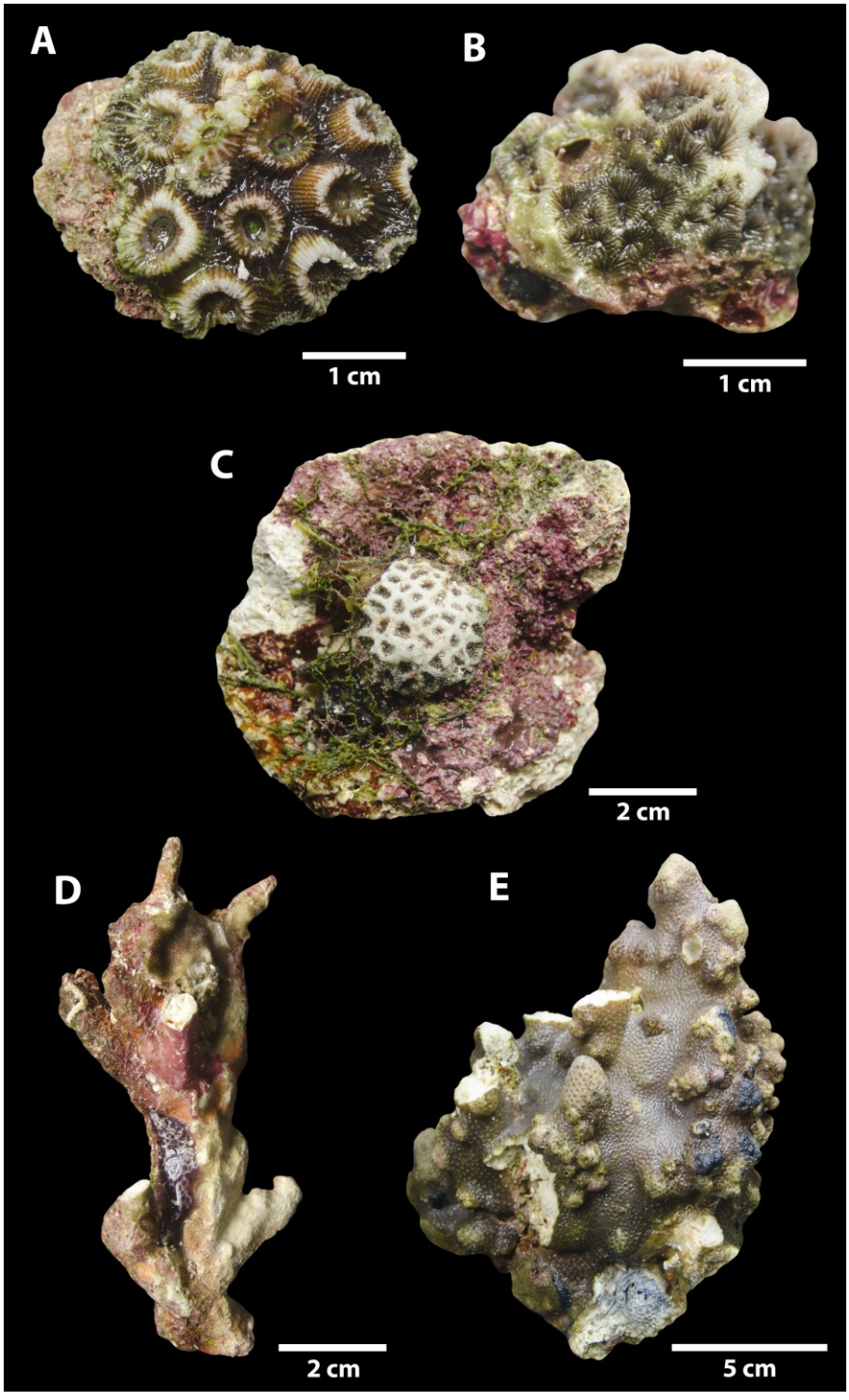

fig. S5. Representative species of corals and hydrocoral collected off the Amazon River mouth. (A) *Montastraea cavernosa*; **(B)** *Agaricia humilis*; **(C)** *Favia gravida*; **(D)** *Millepora* sp.; **(E)** *Madracis decactis*.

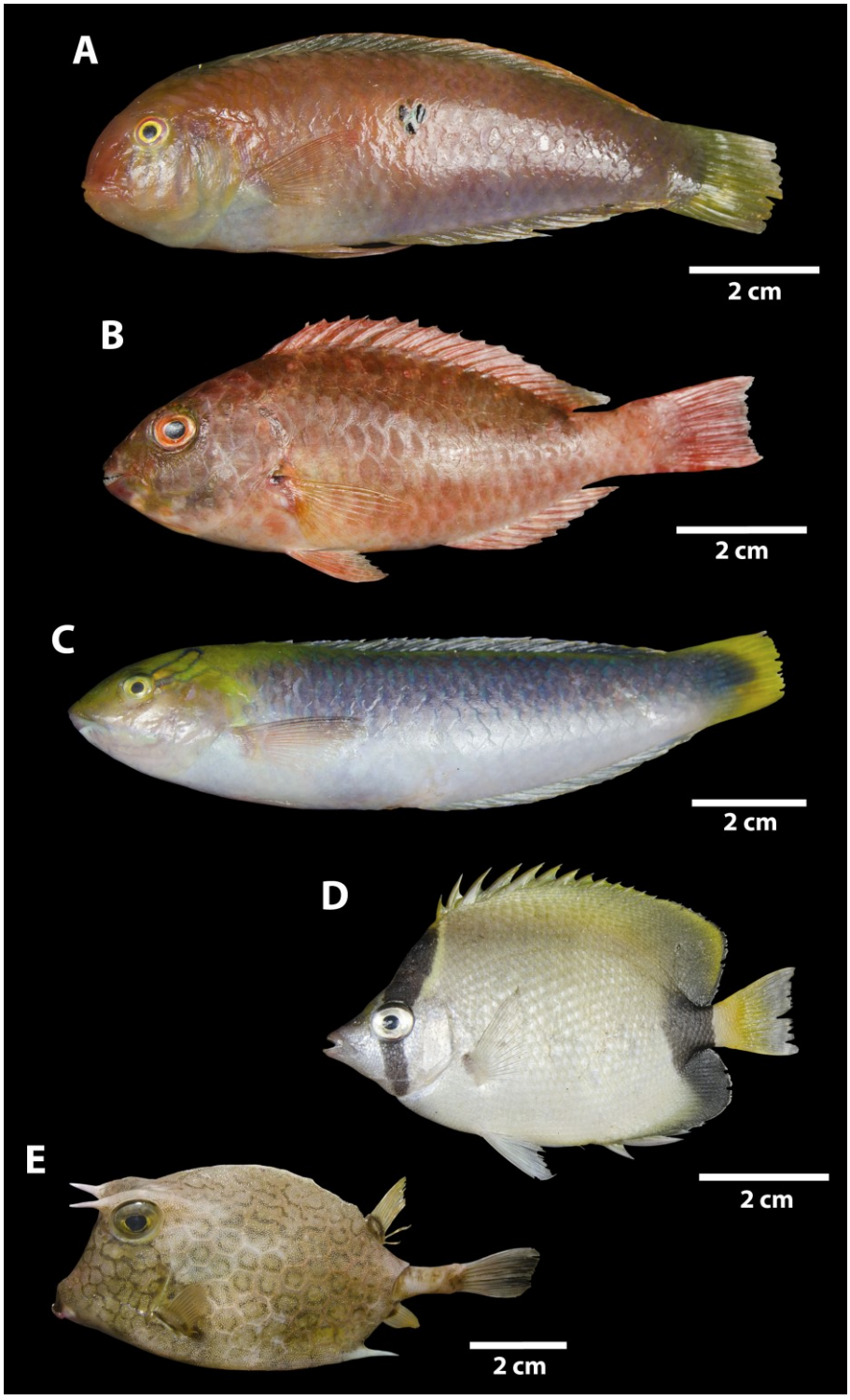

fig. S6. Representative reef fish species collected off the Amazon River mouth. (A) *Xyrichtys splendens*; **(B)** *Sparisoma frondosum*; **(C)** *Halichoeres dimidiatus*; **(D)** *Chaetodon ocellatus*; **(E)** *Acanthostracion polygonius*.

fig. S7. Fishing boat operating dinghies with hand lines and long lines near the shelf edge in the Northern Sector during the 2014 cruise. Reef fishes, mainly serranids and lutjanids (groupers and snappers), are the main targets of such operations [photo credit: F. Moraes, Instituto de Pesquisas Jardim Botânico do Rio de Janeiro].

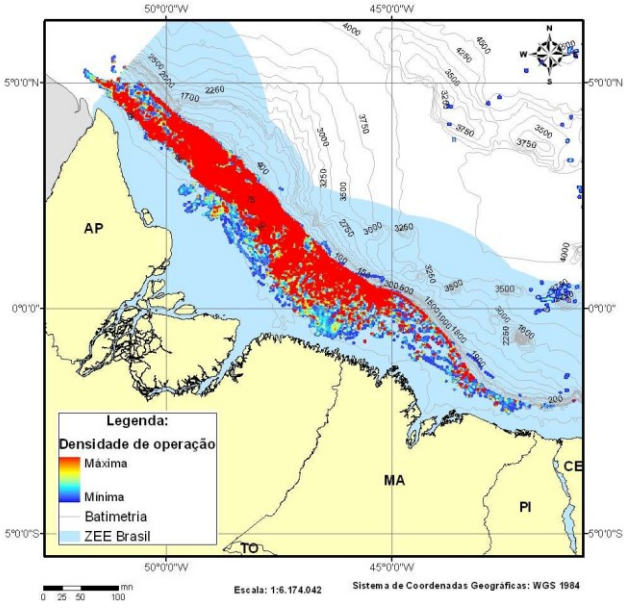

fig. S8. Density of fishing operations targeting red snapper (*L. purpureus*) in 2010 off the Amazon mouth. Notice concentration of operations in the outer shelf and slope across the entire region. Source: (*26*).

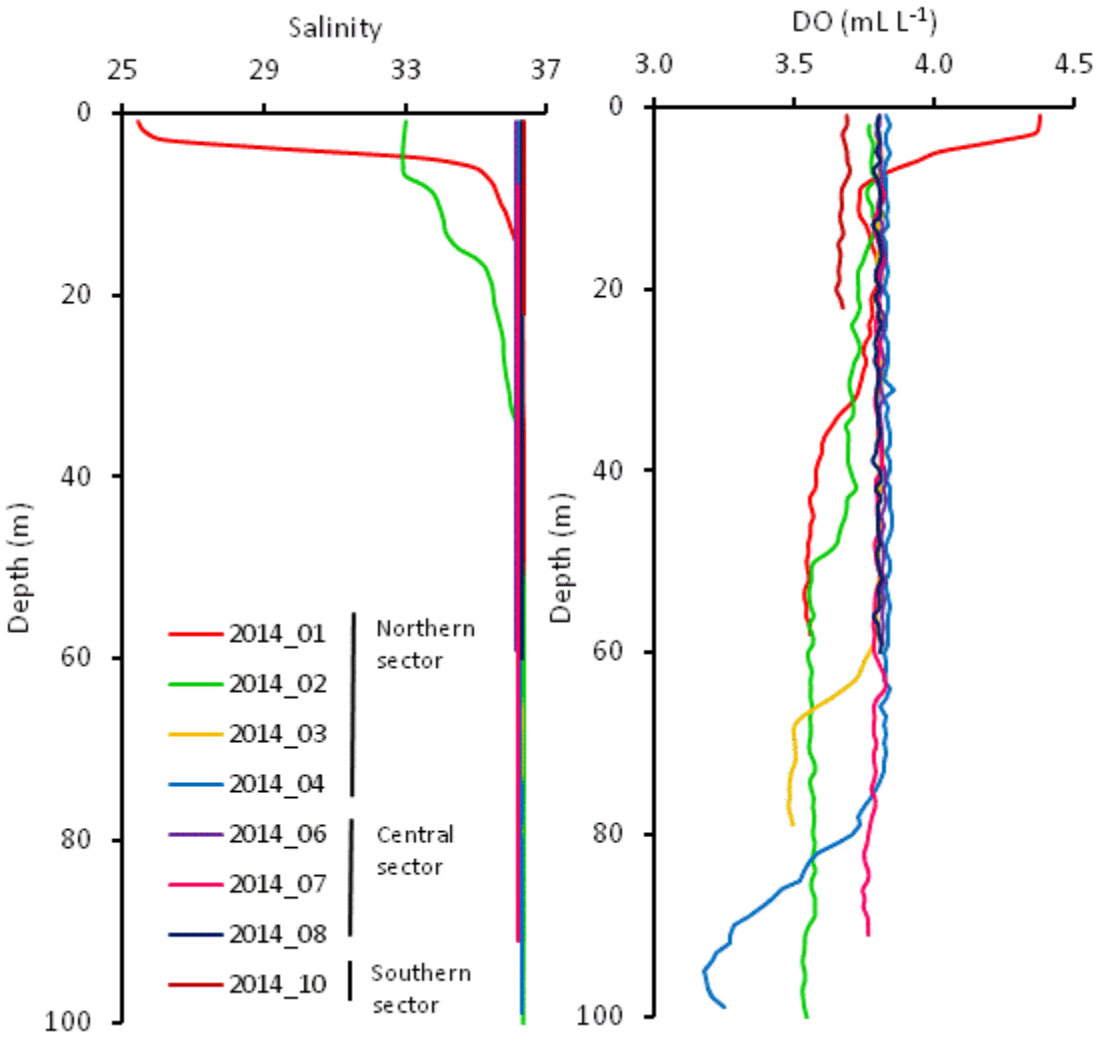

fig. S9. Depth profiles of salinity and DO measured during the R/V Cruzeiro do Sul cruise (September 2014). Station numbers are indicated in the salinity plot. The 5 m depth oxycline (red line), the 35-m oxycline (red line), and the 50-m oxycline (green line) in the right panel may be related to microbial activity.

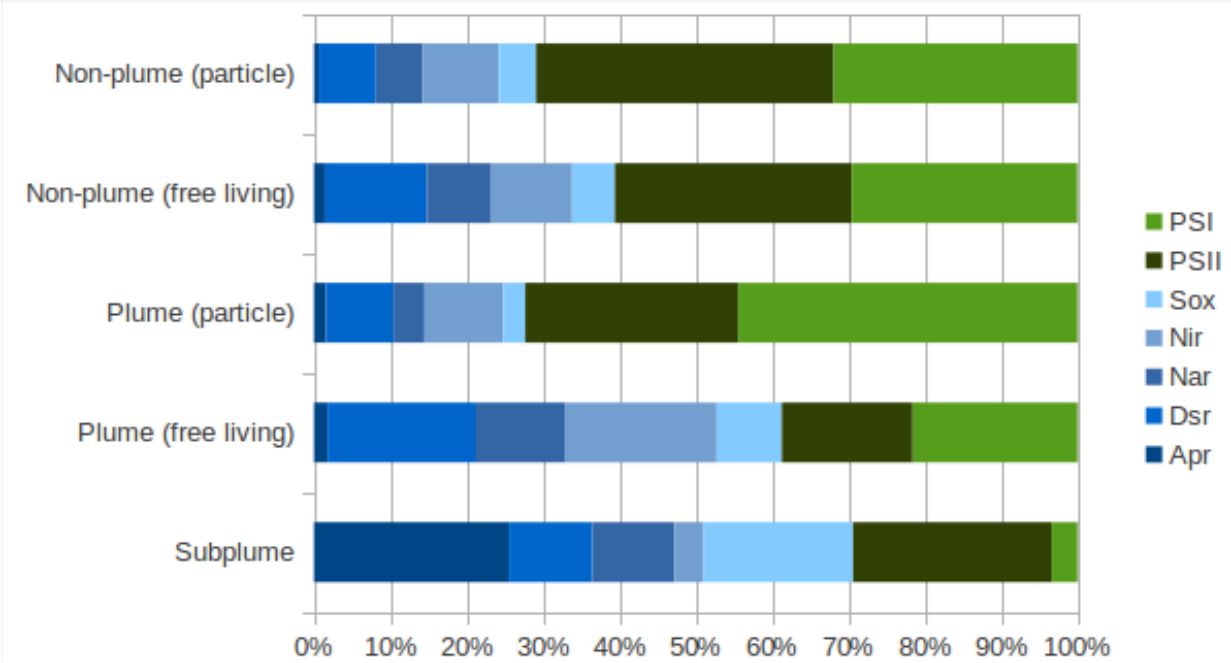

fig. S10. Relative contribution of functions related to chemosynthesis and photosynthesis recorded outside, within, and underneath the Amazon River plume. Average gene sequences associated with ammonia and sulfur metabolism (indicative of chemosynthesis) are shown in shades of blue. Average gene sequences associated with photosystems I and II are shown in shades of green. The relative contribution of photosynthesis is prominent in surface non-plume waters. Conversely, chemosynthesis reaches ~70% of the overall relative contribution in the Subplume (50 m depth). Samples were obtained during the 2010 cruise, except for sub-plume samples St3 and St5 obtained during the 2012 cruise. Samples ACM12 and ACM30 (Station 10), ACM13 (Sta. 23), ACM15 and ACM47 (Sta. 2), ACM17 (Sta. 27), ACM32 and ACM49 (Sta. 3) correspond to particle associated microbes (>2.0 µm). Samples ACM11 (Sta. 10), ACM14 and ACM46 (Sta. 2), ACM16 (Sta. 27), ACM29 (Sta. 10), ACM31 and ACM48 (Sta. 3,), ACM33 (Sta. 23) and ACM34 (Sta. 25) correspond to free living microbes (<2.0 and >0.2 µm).

table S1. Algae recorded off the Amazon River mouth. Geographic range codes: TStWA= Tropical and subtropical Western Atlantic; CtT= Circuntropical to temperate; TTAtl= Tropical to temperate Atlantic; CtAA= Circuntropical to Arctic and Antarctic. **Secondary data sources:** refs. 78, 79.

Group	Taxon	Functional group	Local distribution (Sectors)	Geographic range	Max. depth (m)
Rhodophyta					
	Acrochaetium antillarum W.R.Taylor	Filamentous uniseriate	S	TStWA	40
	Amphiroa fragilissima (L.) Lamouroux	Small sized articulated corallines	C/S	CtT	60
	Amphiroa rigida Lamouroux	Small sized articulated corallines	C/S	CtT	30
	Ceramium sp.	Filamentous uniseriate	S		
	Chondria sp.	Corticated w/ hollow thallus	S		
	Chrysymenia sp.	Larger-sized corticated	S		
	Erythrotrichia carnea (Dillwyn) J.Agardh	Epiphyte	C/S	CtT	60
	Gelidiopsis sp.	Larger-sized corticated	C/S		
	Gelidium pusillum (Stackhouse) Le Jolis	Larger-sized corticated	S	CtT	60
	Gelidium sp.	Larger-sized corticated	N/C/S		
	Gracilaria sp.	Larger-sized corticated	S		
	Halymenia floresii (Clemente) C.Agardh	Flattened macrophytes w/cortication	S	CtT	55
	Herposiphonia secunda (C.Agardh) Ambronn	Filamentous uniseriate w/ ext. prostrate filaments	S	CtT	70
	Hydrolithon rupestre (Foslie) Penrose	Encrusting calcified	C/S	CtT	65
	Hypoglossum tenuifolium (Harvey) J.Agardh	Blade-like w/ one or few cell layers	S	TTAtl	83
	Jania adhaerens Lamouroux	Small sized artic. corallines	C/S	CtT	106
	Kallymenia sp.	Flattened macroph. w/cortication	S		
	Lithothamnion crispatum Hauck	Encrusting calcified	N/C/S	CtT	60
	Mesophyllum erubescens (Foslie) Lemoine	Encrusting calcified	S	CtT	28
	Nitophyllum sp.	Blade-like w/ one or few cell layers	S		

Peyssonnelia sp.	Encrusting calcified	C/S		
Polysiphonia sp.	Filamentous unis. w/ erect thallus	S		
Rhodymenia sp.	Flattened macroph. w/cortication	S		
Sahlingia subintegra (Rosenvinge) Kornmann	Epiphyte	S	CtT	109
Sporolithon ptychoides Heydrich	Encrusting calcified	N/C/S	CtT	60
Chlorophya				
Anadyomene sp.	Blade-like	N		120
Caulerpa racemosa (Forsskål) J.Agardh	Single-celled macrophytes with creeping axes from which distinct erect fronds arise	?	CtT	85
Cladophora sp. 1	Filamentous uniseriate	S		
Cladophora sp. 2	Filamentous uniseriate	S		
Halimeda sp.	Siphonous with thin compacted filaments	S		
Ulva sp.	Blade-like	S		
Ulvella viridis (Reinke) R.Nielsen, C.J.O'Kelly & B.Wysor	Epiphyte	S	CtAA	25
Ochrophyta				
Dictyota sp. 1	Compressed w/ branched or divided thallus	S		
Dictyota sp. 2	Same as above	S		
Lobophora variegata (Lamouroux) Womersley ex E.C.Oliveira	Compressed w/ blade-like habit	S	CtT	125
Sargassum sp.	Thick leathery macrophytes	S		

table S2. Sponges recorded off the Amazon River mouth. **Geographic range codes**: **CAR**= Caribbean; **TWA**= Tropical West Africa; **BRA**= Brazil. **Functional group assignment** (cf. *37*, cf. *38*): **CUP(t)** = Cup-like (Tube); **CUP(g)**= Cup-like (Globet); **CUP(b)**= Cup-like (Barrel); **CUP(i)**= Cup-like (Incomplete Cup, Curly Fan and Tube); **ENC(tk)**= Encrusting (Thick); **ENC(tn)**= Encrusting (Thin); **ENC(b)**= Encrusting (Bioeroder); **MAS(b)**= Massive (Ball); **MAS(s)**= Massive (Simple); **ERE(s)**= Erect (Simple); **ERE(b)**= Erect (Branching); **ERE(p)**= Erect (Palmate); **ERE(l)**= Erect (Laminar). *****= new record for Brazil; ****** New record for the Amazon mouth region. Depths in parenthesis are new depth records.

Group	Taxon	Functional Group	Local distribution (Sectors)	Geographic Range	Depth range in meters	Source Ref. #	Voucher (MNRJ)
CLASS CALCAREA							
Unidentified Family, Order Leucosolenida	unidentified species	CUP(t)	N				18748
CLASS HOMOSCLEROMORPHA							
Plakiniidae	*Plakinastrella globularis* Domingos, Moraes & Muricy, 2013	ENC(tk)	C	BRA, from Bahia to Rio de Janeiro **	70-270 (55)	*24*	16581
	Plakinastrella sp.	ENC(tk)	S				18751
CLASS DEMOSPONGIAE							
Tetillidae	*Cinachyrella kuekenthali* (Uliczka, 1929)	MAS(b)	N	CAR, TWA and BRA, from Amapá to R. Janeiro	10-270	*24*	18776
Ancorinidae	*Stelletta* sp. 1	MAS(b)	N				16667
	Stelletta sp. 2	MAS(s)	C				16555
	Ecionemia sp.	ERE(s)	C				16575
	Melophlus sp.	MAS(s)	C				16580
	Asteropus sp.	ENC(tk)	C				18752
	Tribrachium schmidtii Weltner, 1882	CUP(t)	N	CAR and BRA, from Bahia to R.	7-91	*24*	16607

				Janeiro **			
Geodiidae	*Geodia corticostylifera* Hajdu, Muricy, Cust., Rus. & Pei., 1992	MAS(b)	C	CAR and BRA, from Ceará to São Paulo **	2-72	*24*	18807
	Geodia gibberosa Lamarck, 1815	MAS(s)	N	CAR and BRA, from Ceará to S. Paulo **	0-77	*24*	16672
	Geodia neptuni (Sollas, 1886)	MAS(s)	C	CAR and BRA, from Amapá to Alagoas	13-640	*24*	18792
	Geodia sp.	MAS(b)	C				18811
Clionaidae	*Cliona schmidtii* (Ridley, 1881)	ENC(b)	S	CAR, Adriatic Sea and BRA (Pernambuco) **	15-75	*24, 83*	18804
	Cliona sp.	ENC(b)	S				18735c
Suberitidae	*Aaptos* sp.	MAS(b)	N				16678
	Prosuberites sp.	ENC(tn)	C				16559
	Pseudosuberites sp.	MAS(s)	C				18802
Chondriliidae	*Chondrosia* sp.	ENC(tk)	C	CAR and BRA, from Rio Grande do Norte to Alagoas **	0.5-40	*24*	16554
Unidentified Family of Order Lithistida	unidentified species	MAS(s)	N				18753
Theonellidae	*Theonella atlantica* van Soest & Stentoft, 1988	ERE(b)	C	CAR *	120-153 (100)	*24*	18756
Desmanthidae	*Petromica* sp.	MAS(s)	N				18774
Acarnidae	*Acarnus* sp.	ENC(tn)	N				16523
Microcionidae	*Clathria* cf. *calla* (de Laubenfels, 1934)	ENC(tn)	l	CAR, TWA and BRA (Pernambuco and St Paul`s Rocks) **	3-51	*24, 84*	16501
	Clathria echinata (Alcolado, 1984)	ENC(tn)	C	CAR *	10-13 (80)	*24, 84*	16513

	Clathria nicoleae Barros, Garcia & Pinheiro, 2013	ERE(b)	C	BRA, from Rio Grande do Norte to Paraíba **	17-31 (55)	*24, 81*	18813
	Clathria (*Microciona*) sp.	ENC(tn)	C				16569
Raspailiidae	*Echinodictyum dendroides* Hechtel, 1983	ERE(b)	C	BRA, from Ceará to Alagoas **	6-75	*24*	18781
Coelosphaeridae	*Lissodendoryx* (*Anomodoryx*) sp.	MAS(s)	N/C				18803
Crambeidae	*Monanchora arbuscula* (Duchassaing & Michellotti, 1864)	ERE(b)	C/S	CAR and BRA, from Amapá to St Catarina	15-160	*24*	18799
Crellidae	Unidentified species	ENC(tn)	C				16603
Tedaniidae	*Tedania ignis* (Duchassaing & Michelotti, 1864)	ENC(tk)	C	CAR and BRA, from Maranhão to St Catarina **	0-36 (80)	*24*	16548
Axinellidae	Unidentified species	ERE(s)	N				18739
	Dragmacidon reticulatum (Ridley & Dendy, 1886)	MAS(s)	N/C	CAR and BRA, from Amapá to Rio Grande do Sul	5-80	*24*	16631
Desmoxyidae	*Didiscus verdensis* Hiemstra & van Soest, 1991	ENC(tk)	N	Cape Verde Islands *	6-15 (95)	*85*	18731
Dictyonellidae	*Myrmekioderma* sp.	MAS(s)	N				18743
	Acanthella sp.	ERE(p)	N				16646
	Topsentia ophiraphidites	ERE(b)	N				16635
Halichondriidae	*Halichondria* sp.	MAS(s)	C				16577
	Topsentia ophiraphidites (de Laubenfels, 1934)	MAS(s)	C/S	CAR and BRA, from Maranhão to Espírito Santo**	1-370	*24*	16594
Agelasidae	*Agelas clathrodes* (Schmidt, 1870)	CUP(g)	C	CAR and BRA, from Amapá to R. Jan.	1,5-110	*24*	18790
	Agelas dispar Duchassaing & Michelotti, 1864	MAS(s)	C	CAR and BRA, from Pará to R. Janeiro	2-270	*24*	16596
	Agelas sventres Lehnert & van Soest, 1996	ERE(s)	C	CAR and BRA (Rio Gde do Norte) **	62-79 (55)	*24*	16597

Callyspongiidae	*Callyspongia vaginalis* (Lamarck, 1814)	CUP(i)	C	CAR and BRA, from Maranhão to Bahia **	5-160	*24*	16499
	Callyspongia sp.	ERE(s)	C				16498
	Arenosclera sp.	ERE(l)	C				18778
Niphatidae	*Amphimedon* aff. *compressa* Duchassaing & Michelotti, 1864	MAS(s)	S	CAR and BRA, from Ceará to Alagoas **	1-75	*24*	18771
	Amphimedon sp.	MAS(s)	N				16664
	Niphates erecta Duchassaing & Michelotti, 1864	ERE(s)	C	CAR and BRA, from Amapá to Pernam.	1-95	*24*	16511
	Niphates sp.	MAS(s)	S				18783
Phloeodictyidae	*Oceanapia bartschi* (de Laubenfels, 1934)	MAS(b)	N/C	CAR and BRA, from Amapá to Rio Grande do Norte	13-160	*24*	18816
Petrosiidae	*Petrosia* sp.	MAS(s)	N				18729
	Xestospongia muta (Schmidt, 1870)	CUP(b)	N/C	CAR and BRA, from Amapá to Bahia	12-160	*24*	16585
	Xestospongia sp.	MAS(s)	N				16661
Irciniidae	*Ircinia strobilina* (Lamarck, 1816)	MAS(s)	N/C	CAR and BRA, from Amapá to E. Santo	1-730	*24*	18818
Spongiidae	*Hyattella cavernosa* (Pallas, 1766)	ERE(s)	N/C	CAR and BRA, from Ceará to R. Jan.**	20-90	*24*	18777
Dysideidae	*Dysidea* sp.	MAS(s)	N				16649
Aplysinidae	*Aiolochroia crassa* (Hyatt, 1875)	MAS(s)	C	CAR and BRA, from Amapá to R. Jan.	2-125	*24*	16589
	Aplysina cauliformis (Carter, 1882)	ERE(s)	C	CAR and BRA, from Amapá to S. Paulo	5-270	*24*	16591
	Aplysina fulva (Pallas, 1766)	ERE(b)	C	CAR and BRA, from Amapá to S. Paulo	1-78	*24*	18815
	Aplysina lacunosa (Lamarck, 1814)	CUP(t)	C	CAR and BRA, from Ceará to E. Santo**	20-730	*24*	16560

table S3. Corals, hydrocorals, and gorgonians recorded off the Amazon River mouth. Geographic range codes: CAR= Caribbean**; BRA=** Brazil**; ATL=** Atlantic**; WATL**= Western Atlantic (tropical and subtropical); **CIRC**= Circuntropical**. Records with * from (*13*)**

Group	**Taxon**	**Local distribution** (Sectors)	**Geographic range**	**Max. depth** (m)
Octocorallia				
	* *Acanthogorgia aspera* Pourtalès, 1867	N/A	CAR, BRA	122
	* *A. schrammi* (Duchassaing & Michellotti, 1864)	N/A	CAR, BRA	360
	* *Bebryce parastellatta* Deichmann, 1936	N/A	CAR, BRA	497
	* *Carijoa riisei* (Duchassaing & Michellotti, 1860)	N/A	CIRC	103
	* *Diodogorgia nodulifera* (Hargitt, 1901)	N/A	WATL	180
	* *Ellisella elongata* (Pallas, 1766)	N	WATL	480
	* *Heterogorgia uatumani* Castro, 1990	N/A	CAR, BRA	200
	* *Iciligorgia schrammi* Duchassaing, 1870	N/A	CAR, BRA	1,130
	* *Leptogorgia euryale* (Bayer, 1952)	N/A	WATL	77
	L. miniata (Milne-Edwards & Haime, 1857)	N	CAR, BRA	125
	* *L. punicea* (Milne-Edwards & Haime, 1857)	N/A	WATL	117
	* *L. setacea* (Pallas, 1766)	N/A	WATL	60
	* *L. stheno* (Bayer, 1952)	N/A	WATL	66
	* *Muriceopsis cf. petila* Bayer, 1961	N/A	CAR, BRA	90
	* *Muriceopsis sp.*	N/A	BRA	90
	* *Nicella guadalupensis* (Duchassaing & Michellotti, 1860)	N	CAR, BRA	395
	* *Nidalia occidentalis* Gray, 1835	N/A	WATL	118
	* *Nidalia sp.*	N/A	BRA	90
	* *Olindagorgia gracilis* (Verril, 1868)	N/A	BRA	100
	* *Pacifigorgia sp.*	N/A		30
	* *Primnoella delicatissima* Kukenthal, 1908	N/A	BRA	160
	* *Scleracis exserta* (Ellis & Solander, 1786)	N	WATL	100
	* *Thelogorgia studeri* Bayer, 1992	N/A	CAR, BRA	117
	* *Thesea bicolor* Deichmann, 1936	N/A	BRA	497

* *T. gracilis* (Gray, 1868)	N/A	BRA	118
* *Trichogorgia brasiliensis* Castro, Medeiros & Loiola, 2010	N/A	BRA	32
Antipatharia	N		
Antipathes furcata Gray, 1857	N	WATL	2,480
* *Cirrhipathes* sp.	N/A	BRA (?)	
Tanacetipathes tanacetum (Pourtalès, 1880)	N	CAR, BRA	1,300
Scleractinia			
Agaricia agaricites (Linnaeus 1758)	C/S	CAR, tropical BRA	75
* *Agaricia fragilis* (Dana, 1846)	N/A	CAR, tropical BRA	102
Astrangia rathbuni Vaughan, 1906	N	Tropical and subtropical ATL	60
* *Astrangia solitaria* (Lesueur, 1817)	N/A	WATL	50
Favia gravida Verril, 1868	S	tropical ATL	30
Madracis decactis (Lyman, 1859)	C/S	Tropical and subtropical ATL	300
Meandrina braziliensis (Milne-Edwards & Haime, 1849)	C/S	CAR, tropical BRA	247
Montastraea cavernosa Linnaeus, 1767	C/S	tropical ATL	180
* *Mussismilia hispida* (Verrill, 1901)	N/A	BRA	60
* *Phyllangia americana Milne-Edwards & Haime, 1849*	N/A	WATL	53
* *Rhizosmilia maculata (Poutalés, 1874)*	N/A	WATL	73
* *Scolymia wellsii* Laborel, 1967	N/A	WATL	45
Hydrozoa			

Millepora cf. alcicornis Linnaeus, 1758	S	West ATL and Cape Verde	108

table S4. Reef fish species recorded off the Amazon river mouth [does not include species recorded at the Manuel Luis reefs; see Moura *et al*. (*23*) and Rocha and Rosa (*44*)]. Geographic range codes: **WEA**= Western and Eastern Atlantic; **TEP**= Tropical Eastern Pacific; **WA**= Western Atlantic; **CG**= circunglobal. **Trophic level codes**: **INV**= invertivore; **PLK**= planktivore; **PIS**= piscivore; **SPO**= spongivore; **OMN**= omnivore; **HER**= herbivore; **DET**= detrivore. **Reproductive mode codes**: **LB**= livebearer; **PS**= pelagic spawner; **OB**= oral brooder; **DS**= demersal spawner; **BT**= balistid-type spawner. **Primary source of the record**: **i**: fishing market observation by RLM (Belém, Pará, Brasil)

Family	Species	Geographic range	Trophic level	Max depth (m)	Reproduct. mode	Primary source of record
Ginglymostomatidae	*Ginglymostoma cirratum* (Bonnaterre, 1788)	WEA, TEP	INV	130	LB	i
Dasyatidae	*Dasyatis americana* Hildebrand & Schroeder, 1928	WA	INV-PIS	53	LB	*23*
Muraenidae	*Gymnothorax ocellatus* Agassiz, 1831	WA	INV-PIS	160	PS	*23*
	G. vicinus (Castelnau, 1855)	WEA	INV	186	PS	*12*
Synodontidae	*Synodus foetens* (Linnaeus, 1766)					*23*
	S. intermedius (Spix & Agassiz, 1829)	WA	PIS	320	PS	*23*
Holocentridae	*Holocentrus adscensionis* (Osbeck, 1765)	WEA	INV	200	PS	*12*
	Myripristis jacobus Cuvier, 1829				PS	*23*
Apogonidae	*Apogon pseudomaculatus* Longley, 1932	WA	PLK	100	OB	*12*
Aulostomidae	*Aulostomus strigosus* Wheeler, 1955	CG	PIS-INV	100	PS	*12*
Syngnathidae	*Hippocampus reidi* Ginsburg, 1933					*23*
Dactylopteridae	*Dactylopterus volitans* (Linnaeus, 1758)					*23*
Mullidae	*Mulloidichthys martinicus* (Cuvier, 1829)	WA, rare in the EA	INV	66	PS	*12*
	Pseudupeneus maculatus (Bloch, 1793)	WA	INV	90	PS	*12*
Sphyraenidae	*Sphyraena picudilla* Poey, 1860					*23*
Carangidae	*Caranx latus* Agassiz, 1831	WA, rare in the EA	PIS-INV	140	PS	i

	Seriola rivoliana Valenciennes, 1833					*23*
Bothidae	*Bothus ocellatus* (Agassiz, 1831)	WA	INV	120	PS	*12*
	B. lunatus (Linnaeus, 1758)	WEA	INV	120	PS	*12*
Pomacentridae	*Chromis multilineata* (Guichenot, 1853)	WEA	PLK	84	DS	*12*
	C. scotti Emery, 1968					*23*
	Stegastes pictus (Castelnau, 1855)	Brazil**	PLK	85	DS	n. record
Chaetodontidae	*Chaetodon sedentarius* Poey, 1860	WA	INV	92	PS	*12*
	C. ocellatus Bloch, 1787	WA	INV	30	PS	*12*
Haemulidae	*Haemulon aurolineatum* Cuvier, 1830	WA	INV	70	PS	*12*
	H. plumierii (Lacepède, 1801)	WA	INV	45	PS	*12*
	H. steindachneri (Jordan & Gilbert, 1882)	WA, TEP	INV	50	PS	*12*
	Orthopristis ruber (Cuvier, 1830)				PS	*23*
Lutjanidae	*Lutjanus purpureus* (Poey, 1866)	WA	PIS-INV	340	PS	*12*
	L. synagris (Linnaeus, 1758)	WA	INV	400	PS	i
	Ocyurus chrysurus (Bloch, 1791)	WA	INV	180	PS	*12*
	Pristipomoides aquilonaris (Goode & Bean, 1896)	WA	INV	370	PS	*12*
	Rhomboplites aurorubens (Cuvier, 1829)	WA	PLK	300	PS	*12*
Pomacanthidae	*Pomacanthus arcuatus* (Linnaeus, 1758)	WA	SPO-OMN	30	PS	*12*
	P. paru (Bloch, 1787)	WA, St. Pauls' Rocks and Ascension	SPO-OMN	100	PS	*12*
	Holacanthus ciliaris (Linnaeus, 1758)	WA	SPO-INV	120	PS	*12*
	H. tricolor (Bloch, 1795)				PS	*23*

Priacanthidae	*Priacanthus arenatus* Cuvier, 1829	WEA	INV	200	PS	*12*
Sciaenidae	*Equetus lanceolatus* (Linnaeus, 1758)	WA	INV	60	PS	*12*
Labridae	*Decodon puellaris* (Poey, 1860)				PS	*23*
	Halichoeres dimidiatus (Agassiz, 1831)	Brazil and French Guiana	INV	71	PS	n. record
	Xyrichtys splendens Castelnau, 1855,	WA	INV	90	PS	n. record
Labridae, Scarinae	*Cryptotomus roseus* Cope, 1871	WA	HER-DET	66	PS	n. record
	Nicholsina usta (Valenciennes, 1840)				PS	*23*
	Sparisoma frondosum (Agassiz, 1831)	Brazil**	HER-DET	45	PS	n. record
Antennariidae	*Antennarius striatus* (Shaw, 1794)				DS	*23*
Diodontidae	*Chilomycterus antillarum* Jordan & Rutter, 1897	WA	OMN	50	PS	*12*
	C. reticulatus (Linnaeus, 1758)	CS	OMN	100	PS	*12*
	C. antennatus (Cuvier, 1816)	WEA	OMN	13	PS	*12*
	Diodon hystrix Linnaeus, 1758				PS	*23*
Balistidae	*Balistes vetula* Linnaeus, 1758	WEA	OMN	110	BT	*12*
Monacanthidae	*Aluterus monoceros* (Linnaeus, 1758)	CG	OMN	72	BT	*12*
	Cantherhines pullus (Ranzani, 1842)	WEA	OMN	57	BT	*12*
	Stephanolepis hispidus (Linnaeus, 1766)	WEA	OMN	293	BT	*12*
Ostraciidae	*Acanthostracion quadricornis* (Linnaeus, 1758)				BT	*23*
	A. polygonius Poey, 1876	WA	OMN	80	BT	n. record
Acanthuridae	*Acanthurus chirurgus* (Bloch, 1787)	WEA	HER-DET	70	PS	*12*
Serranidae	*Cephalopholis fulva* (Linnaeus, 1758)	WA	PIS-INV	220	PS	*12*

	Dermatolepis inermis (Valenciennes, 1833)				PS	*23*
	Diplectrum bivittatum (Valenciennes, 1828)	WA	PIS-INV	140	PS	*12*
	D. formosum (Linnaeus, 1766)				PS	*23*
	D. radiale (Quoy & Gaimard, 1824)				PS	*23*
	Epinephelus itajara (Lichtenstein, 1822)	WEA	PIS-INV	100	PS	i
	E. morio (Valenciennes, 1828)	WA	PIS-INV	300	PS	*12*
	Hyporthodus niveatus (Valenciennes, 1828)	WA	INV	400	PS	i
	H. nigritus (Holbrook, 1855)	WA	INV	525	PS	i
	Paranthias furcifer (Valenciennes, 1828)	WEA	INV	70	PS	*12*
	Pseudogramma gregoryi (Breder, 1927)	WA	INV	85	PS	n. record
	Rypticus randalli Courtenay, 1967				PS	*23*
	R. bistrispinus (Mitchill, 1818)				PS	*23*
	Serranus atrobranchus (Cuvier, 1829)	WA	INV	220	PS	*12*
	S. phoebe Poey, 1851	WA	INV	400	PS	*12*
Scorpaenidae	*Scorpaena ishtmensis* Meek & Hildebrand, 1928				PS	*23*

table S5. Oceanographic stations (primary data sources). Gear codes: CTD= a; **Water sampling (w/rosette or surface pump)**= b; **multibeam**= c; **benthic dredges/van Veen**= d; **sidescan sonar**= e.

Station	Latitude (degrees)	Longitude (degrees)	Date GMT (yyyymmdd)	Water depth (m)	Sampling
2010_02	10.29	-54.50	20100525	4370	a, b
2010_03	7.29	-53.00	20100526	580	a, b
2010_04	5.94	-51.50	20100527	1050	a, b
2010_08	4.35	-46.85	20100601	3140	a, b
2010_10	4.88	-51.36	20100605	60	a, b
2010_23	10.64	-54.40	20100616	4520	a, b
2010_25	11.31	-56.49	20100618	4450	a, b
2010_27	12.42	-52.21	20100621	5025	a, b
2012_03	8.03	-50.98	20120717	4465	a,b
2012_05	4.82	-50.01	20120719	1803	a,b
2012_16b	0.76	-46.64	20120724	32	c, d
2012_17	1.08	-46.36	20120725	90	c, d
2012_18	1.32	-46.83	20120725	65	c, d
2012_19	3.16	-49.34	20120725	45	c, d
2012_20	4.38	-50.45	20120726	80	c, d
2012_21	4.39	-50.7	20120726	75	c, d
2014_01	4.4	-50.7	20140924	64	a, b, d, e
2014_02	4.37	-49.92	20140925	120	a, b, d, e
2014_03	3.6	-49.14	20140926	91	a, b, d, e
2014_04	2.95	-48.49	20140926	90	a, b, d, e
2014_05	1.32	-46.84	20140927	53	a, b, d, e
2014_06	1.3	-46.78	20140927	53	a, b, d, e
2014_07	1.1	-46.5	20140928	103	a, b, d, e
2014_08	0.76	-46.64	20140928	51	a, b, d, e
2014_09	0.11	-45.56	20140929	60	a, b, d, e
2014_10	-0.27	-44.81	20140929	23	a, b, d, e

Captions for additional file type that cannot be embedded into the Word file.

movie S1. Sampling the plume, subplume, and reefs off the Amazon river mouth during the NHo Cruzeiro do Sul cruise (2014).

Supplementary file. Shape files (*shp) containing all the spatially explicit data used in Figure 1 (benthic megahabitats and fisheries) and all sidescan and multibean tracks (these files may also be uploaded on datadryad or other open data-sharing platform)